The role of the ubiquitin-proteasome system in Gcn4 target gene transcription

By

Gregory C. Howard

Dissertation
Submitted to the Faculty of the
Graduate School of Vanderbilt University
in partial fulfillment of the requirements
for the degree of

DOCTOR OF PHILOSOPHY
in

Cell and Developmental Biology
December, 2016
Nashville, Tennessee

Approved:

David M. Miller, III, Ph.D.

Ryoma Ohi, Ph.D.

Roland W. Stein, Ph.D.

William P. Tansey, Ph.D.

P. Anthony Weil, Ph.D.

ACKNOWLEDGEMENTS

I would like to thank Bill Tansey whose guidance and training have pushed me to be both a better scientist and a communicator. I would also like to thank the members of the Tansey laboratory, both past and present, for creating not only a collaborative but also an enjoyable work environment. The smooth operation of the lab is in large part thanks to Shelly Lorey. I would like to thank my committee members David Miller, Puck Ohi, Roland Stein, and Tony Weil who have invested their valuable time into my guidance and training through my graduate career.

I would also like to thank my parents whose support, not only over the past few years but throughout my entire academic career, has enabled me to reach this academic milestone. I would also like to thank Scott and Sarah Collier who have become like family over the past few years in Nashville and have provided support through the graduate school experience.

TABLE OF CONTENTS

LIST OF TABLES

LIST OF FIGURES

CHAPTER I

INTRODUCTION

Abstract

The ubiquitin–proteasome system (UPS) influences gene transcription in multiple ways. One way in which the UPS impacts transcription centers on transcriptional activators, the function of which can be stimulated by components of the UPS that also trigger their destruction. Activation of transcription by the yeast activator Gcn4, for example, is attenuated by mutations in the ubiquitin-ligase that mediates Gcn4 ubiquitylation or by inhibition of the proteasome, leading to the idea that ubiquitin-mediated proteolysis of Gcn4 is required for its activity. Here, I probe the steps in Gcn4 activity that are perturbed by disruption of the UPS. I show that the ubiquitylation machinery and the proteasome control different steps in Gcn4 function, and that proteasome activity is required for the ability of Gcn4 to bind to its target genes in the context of chromatin. Curiously, the impact of proteasome inhibition on Gcn4 activity is suppressed by mutations in the ubiquitin-selective chaperone Cdc48, revealing that proteolysis per se is not required for Gcn4 activity. My data highlights the role of Cdc48 in controlling promoter occupancy by Gcn4 and support a model in which ubiquitylation of activators—not their destruction—is important for function.

Overview

A cell's genome can contain thousands of genes which are converted into RNA through the process of transcription, during which a DNA sequence is used as a template to synthesize a complementary RNA strand. Because of the sheer number of biological processes that involve transcription and the diseases that arise from transcriptional misregulation, a solid understanding of transcription regulatory mechanisms will go far in uncovering both normal and abnormal cellular processes. Some of these diseases include cancer, diabetes, and developmental disorders, among others (Lee and Young, 2013). In this thesis, I present my study of a

mechanism of transcriptional regulation in which cellular machinery that targets a protein for degradation is actually *required* for that proteins ability to stimulate transcription. In this Chapter, I give an overview of transcriptional activation by this protein, termed a transcriptional activator, and an overview of the cellular degradation machinery, collectively referred to as the ubiquitin-proteasome system (UPS). Finally, I discuss the nexus of these two processes and the studies that support a model for transcriptional regulation that reconciles the requirement of the UPS machinery for transcriptional activation.

Transcriptional Activators

Transcriptional activators stimulate transcription by recruiting RNA polymerase along with general transcription factors and coactivators to gene promoters. Therefore, transcription of specific genes can be regulated by controlling corresponding transcriptional activators. A prototypical transcriptional activator contains an activation domain that interacts with transcriptional machinery and a DNA binding domain that recognizes specific DNA sequences in the genome. The specific type of RNA polymerase recruited to a promoter is dependent on the type of RNA strand being produced. In the case of protein-coding messenger RNA (mRNA), RNA polymerase II is recruited along with general transcription factors (GTFs) that function in bending DNA at the TATA box to allow for protein assembly (TFIID), positioning RNA polymerase II at the start site (TFIIB), unwinding DNA at the transcription start site (TFIIH), stabilizing protein-protein interactions within the complex (TFIIF) and recruiting other GTFs (TFIIE) (Hahn and Young, 2011). Two examples of coactivators are Mediator and the SAGA complex. Mediator is a large, twenty-five subunit complex that acts as an intermediate between the transcriptional activator and RNA polymerase II (Conaway and Conaway, 2011). Mediator also contains enzymatic activity as evident by Mediator's multiple kinase subunits including the cyclin-dependent kinase (Cdk) Srb10.

Coactivators, such as the SAGA complex, can stimulate transcription by converting chromatin into an "active" state (Rodriguez-Navarro, 2009). In its most basic form, chromatin is made up of nucleosomes. One nucleosome is one hundred and forty-seven nucleotides wrapped around an

octamer of histones. One nucleosome contains two each of the histones H2A, H2B, H3, and H4. Between nucleosomes is the linker histone H1. For transcription to occur, nucleosomes may be removed or rearranged along the DNA strand, a process stimulated by coactivators. Nucleosomes may also be chemically modified through the addition of histone marks at the histone tails that extend from the globular histone proteins. These marks can alter the strength of histone-DNA interactions and stimulate recruitment of other proteins to DNA.

A cell can tightly regulate transcription by regulating the ability of a transcriptional activator to interact with DNA, often through post-translational modifications. One method of transcriptional control is through controlling the sub-cellular localization of a transcriptional activator. This is illustrated well with the transcriptional activator STAT1 which is activated by tyrosine phosphorylation in response to stimulation of extracellular receptors (Shuai et al., 1993). Phosphorylation triggers homo-dimerization of STAT1, leading to a conformational change to expose the nuclear localization sequence (NLS) and signal nuclear import to facilitate interaction with DNA (Wenta et al., 2008). Phosphorylation can also repress transcription by stimulating nuclear export of a transcriptional activator. Pho4 is a transcriptional activator that stimulates transcription when cellular phosphate levels are low. To inhibit transcription of Pho4 target genes, Pho85 phosphorylates Pho4 at two specific residues (Komeili and O'Shea, 1999). Phosphorylation at these two residues stimulates export to the cytoplasm via the nuclear export shuttling protein Msn5 (Kaffman et al., 1998). Additional post-translational modifications, including ubiquitylation, can also modify transcriptional activators and regulate transcription.

Ubiquitin-Proteasome System

Ubiquitylation entails the covalent attachment of one or more ubiquitin moieties often at the epsilon amino group of a lysine residue in a target protein (Finley et al., 2012). Covalent attachment of ubiquitin occurs through an enzymatic cascade involving an E1 ubiquitin-activating enzyme, an E2 ubiquitin-conjugating enzyme, and an E3 ubiquitin-ligating enzyme (Figure 1A). The enzymatic cascade begins with the attachment of ubiquitin to the E1 enzyme through an

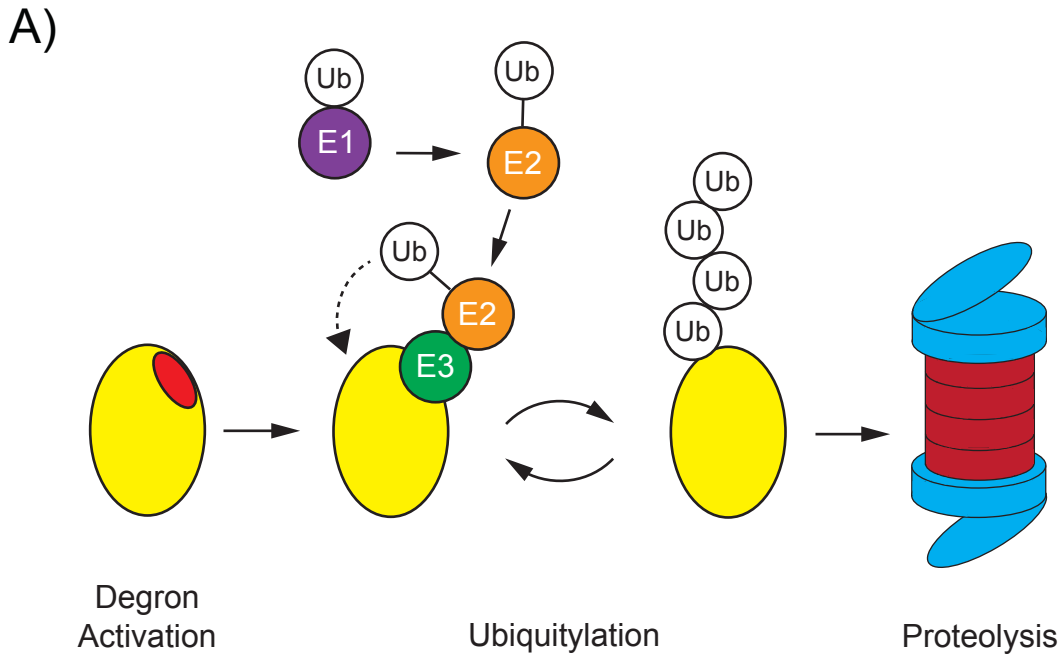

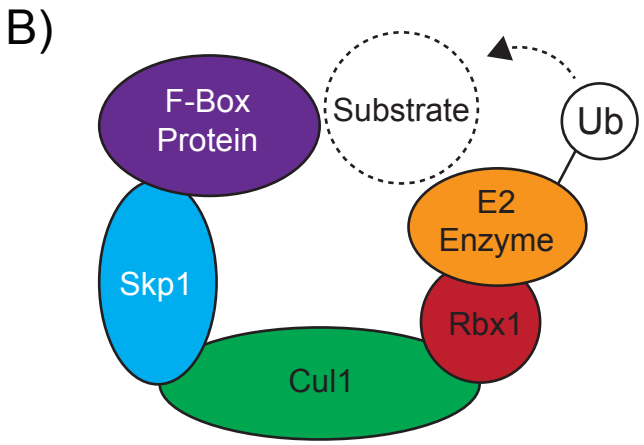

Figure 1. Ubiquitin-proteasome system (UPS). (A) Ubiquitylation and degradation by the UPS. (B) Skp1-Cullin-F-box protein (SCF) complex E3 enzyme.

ATP-dependent linkage between the carboxyl group at the C-terminus of ubiquitin to a cysteine residue in the E1 enzyme. This “activated” ubiquitin is then transferred to a cysteine residue within the E2 ubiquitin conjugating enzyme. The subsequent transfer of ubiquitin from the E2 enzyme to the target protein is mediated by the E3 enzyme whose recognition of a target protein provides specificity for ubiquitylation. One type of E3 enzyme that is most relevant to the work presented in this thesis is the Skp1—Cullin—F-box protein (SCF) complex (Figure 1B). SCF complexes facilitate ubiquitylation by recognizing target proteins by an F-box protein, thereby orienting the target protein for ubiquitylation by an E2 enzymes associated with the SCF complex. By changing the associated F-box protein, an SCF complex can recognize different substrates.

Additional cycles of ubiquitylation by the same E3 enzyme creates a ubiquitin chain through linkages at one of seven lysine residues of the target-bound ubiquitin. In some cases, chain elongation occurs in cooperation with an additional ubiquitylation enzyme termed an E4 enzyme. By selectively targeting different lysine residues in ubiquitin, ubiquitin chain linkages provide an additional layer of regulation within the UPS. For example, ubiquitin chain extension from the K48 residue of ubiquitin canonically stimulates interaction with the proteasome to signal degradation. Alternatively, ubiquitin linkages can signal non-proteolytic processes as is the case with K63 linkages in vesicular trafficking.

Recognition of targets by the ubiquitylation machinery is stimulated by a region of the targeted protein referred to as the degron (Figure 1A) (Ravid and Hochstrasser, 2008). For some substrates, the degron stimulates constitutive ubiquitylation and degradation which keeps proteins at low steady-state levels. In other cases, the degron stimulates ubiquitylation only after the degron is “activated”, often through phosphorylation. Another method of degron activation occurs when protein structures change in such a way as to expose a previously hidden degron. An example of this method is the degradation of misfolded proteins during protein quality control processes. This misfolding of proteins exposes hydrophobic regions that are normally hidden within the protein structure (Fredrickson et al., 2011).

The 26S proteasome contains a 20S core particle and a 19S regulatory particle located at either one or both ends of the 20S core particle. The core particle is arranged in a barrel shape containing four stacks of heptameric rings which create a central pore. It is within this pore that proteolysis occurs by six proteolytic proteasome subunits. The two outer rings of the structure contain alpha subunits while the two central rings contain beta subunits. For proteolysis to occur, a substrate enters the central pore through the regulatory particle. The regulatory particle serves multiple functions including recognition of ubiquitylated substrates via its Rpn10 and Rpn13 subunits and cleavage of the ubiquitin chain for recycling via the Rpn11 deubiquitylating enzyme. Translocation of the polypeptide chain into the core's central pore occurs in an ATP-dependent manner through action by the regulatory particle. Each beta-ring contains a tryptic, chymotryptic, and caspase-like proteolytic subunit. Once inside the pore, a polypeptide is cleaved into smaller fragment through these proteolytic sites.

For many proteins, attachment of a ubiquitin chain containing at least four ubiquitin moieties can be sufficient to stimulate recognition by the proteasome for degradation. However, chaperones can act between the steps of ubiquitylation and proteolysis to present ubiquitylated substrates to the proteasome. One well-characterized chaperone is the Cdc48 complex, a homo-hexameric ATPase that generates mechanical force through ATP hydrolysis to remove ubiquitylated proteins from their interacting partners. Each Cdc48 monomer contains an N-terminal domain, two AAA domains, and an unstructured C-terminal domain. It is at the N-terminal and C-terminal domains that Cdc48 recruiting cofactors and substrate processing cofactors bind, respectively. Cdc48 cofactors can edit ubiquitin chains through E4 enzymes which extend chain length and deubiquitylase enzymes which shorten chain length. It is because of the multiple potential outcomes resulting from the Cdc48 complex and its associated cofactors that the complex has been referred to as a "gear-box" by which a protein can be directed to one of several outcomes (Jentsch and Rumpf, 2007).

The UPS has been shown to regulate transcription both positively and negatively, depending on the context. In many of these examples, the role of the UPS is straightforward such as degrading transcriptional activators to prevent transcription or degrading transcriptional repressors to stimulate transcription. However, for several transcriptional activators, the role of the UPS is not so clear. For one such group of transcriptional activators, which is the focus of this thesis, components of the UPS that target a transcriptional activator are actually required for the transcriptional activator's ability to stimulate transcription. In the following sections, I will overview several examples of how the UPS can regulate transcription, either proteolytically or non-proteolytically, and provide multiple examples of when targeting a transcriptional activator for degradation is apparently required for its function.

Proteolytic regulatory mechanisms

The most straight-forward method by which the UPS can regulate transcription is by degrading transcription factors during times in which transcription is not required. This has been well-characterized for beta-catenin, a key component of the Wnt signaling pathway whose constitutive phosphorylation, ubiquitylation, and degradation by the proteasome suppresses beta-catenin protein levels in the absence of Wnt signaling (Aberle et al., 1997; Polakis, 2000). To allow for transcription in the presence of Wnt, phosphorylation of beta-catenin is downregulated, thereby inhibiting its degradation and allowing beta-catenin levels to increase and bind DNA.

The UPS can proteolytically stimulate transcription by degrading an inhibitory protein. In one such case, nuclear factor (NF)-kappa B associates with the inhibitor I-kappa B in the cytoplasm, preventing import into the nucleus. Upon inflammation, I-kappa B is phosphorylated, ubiquitylated, and degraded by the proteasome, thereby allowing NF-kappa B to enter the nucleus and act at chromatin (Palombella et al., 1994). In another case, the endoplasmic reticulum (ER)-anchored transcriptional activator Spt23 is activated by cleavage of an ER anchor region through limited proteasomal proteolysis of Spt23. Following cleavage, Spt23 remains associated with the ER through dimerization with unprocessed, ER-bound Spt23. Extraction of

activated Spt23 occurs through the Cdc48 complex, thereby allowing Spt23 to enter the nucleus and stimulate transcription (Hoppe et al., 2000; Rape et al., 2001).

Non-proteolytic regulatory mechanisms

Regulation of transcription factors by the UPS can occur independently of proteolysis via transcription factor ubiquitylation. In one such case, mono-ubiquitylation of FOXO4 occurs in response to oxidative stress to signal nuclear import of FOXO4 and allow its interaction with chromatin. Nuclear localization is reversed by removal of ubiquitin from FOXO4 via the deubiquitylase enzyme Usp7, also stimulated by oxidative stress (van der Horst et al., 2006). Another transcription factor regulated by ubiquitylation is the transcriptional coactivator SRC-3 whose function requires mono-ubiquitylation (Wu et al., 2007). Based on this work, it is proposed that ubiquitylation provides temporal control of transcriptional output as successive rounds of ubiquitylation would stimulate recognition by the proteasome and trigger degradation of SRC-3. This mechanism of self-limiting transcription has been termed the “molecular clock” model in which sequential additions of ubiquitin to the ubiquitin chain temporally limits SRC-3 function to the time between mono-ubiquitylation and proteolysis.

Ubiquitylation can regulate transcription independently of proteolysis by stimulating recognition by the Cdc48 complex as is the case with the transcriptional repressor alpha-2. The UPS can regulate alpha-2 protein levels within the cell through UPS-dependent degradation. However, loss of alpha-2 from promoters occurs through a process independent of alpha-2 degradation (Laney and Hochstrasser, 2003; Wilcox and Laney, 2009). Instead of proteolysis, alpha-2 ubiquitylation stimulates extraction from chromatin through a Cdc48-dependent mechanism. The Cdc48 complex has also been implicated in disrupting chromatin interaction with other proteins including the RNA pol II subunit Rpb1 and the synthetic transcriptional activator LexA-VP16 fused to non-cleavable ubiquitin (Ndoja et al., 2014; Verma et al., 2011).

Transcription factor degradation and activation

A more intriguing role of the UPS for transcription has emerged in which the UPS targets a transcriptional activator to facilitate transcriptional activation. This paradoxical relationship

between destruction and activity has been observed with many transcription factors. A survey of several of these transcriptional activators uncovers a common theme including the requirement of the E3 enzyme that targets the transcriptional activator for transcription. Work with many of these activators has also shown that the ubiquitylation machinery can be detected at chromatin, suggesting that ubiquitylation may occur while the activator is on DNA. Furthermore, ubiquitylation of several of these activators is stimulated by phosphorylation. However, a model that accounts for why an activator must be destroyed for function has yet to emerge.

The first indication that transcriptional activation and degradation can overlap emerged with the discovery that the transcriptional activation domains and degrons of many transcriptional activators overlap with one another. This work also demonstrated the functional overlap between these two processes using the Gal4-VN8 transcriptional activator in which the Gal4 DNA binding domain was fused to an increasing copy number of the VN8 activation domains (derived from the VP16 activation domain). As the number of VN8 activation domains fused to the Gal4 DNA binding domain increased, so too did the strength of transcriptional activation. Correspondingly, the half-life of these Gal4-VN8 constructs decreased as the strength of transcriptional activation increased (Geng et al., 2012; Molinari et al., 1999; Salghetti et al., 2000).

Following the work with Gal4-VN8, our lab examined the role of ubiquitin in transcriptional activation by studying another synthetic transcriptional activator containing the LexA DNA binding domain and VP16 transcriptional activation domain (Salghetti et al., 2001). The VP16 activation is destabilized through recognition by the E3 enzyme SCF^{Met30}. Interestingly, transcriptional activation is dependent on Met30 as deletion resulted in a defect in transcriptional activation. Fusion of ubiquitin to the N-terminus of LexA-VP16 rescued its ability to stimulate transcription in the absence of Met30. Although these data suggest that a single ubiquitin fusion is sufficient to rescue transcription in the absence of Met30, work from the Yao laboratory demonstrates that the ubiquitin fused to LexA-VP16 is cleaved, thereby triggering polyubiquitylation through the N-end ubiquitylation pathway (Ndoja et al., 2014). Cleavage of ubiquitin from LexA-VP16 most likely occurs via a deubiquitinase enzyme that processes precursor forms of ubiquitin. Cleavage can be inhibited through mutation of amino acid 76 from alanine to valine (Ndoja et al., 2014). These

data suggest that not only can the UPS recognize a transcriptional activator during transcription but it can also be *required* for its function.

The requirement for ubiquitylation machinery to stimulate transcription is further demonstrated with the endogenous transcriptional activator c-Myc which contains an overlapping transcriptional activation domain and degron (Salghetti et al., 2000). The E3 enzyme SCF^{Skp2} ubiquitylates and destabilizes c-Myc in mammalian cells and is required for transcription of c-Myc target genes (Kim et al., 2003). In addition, c-Myc and Skp2 appear to interact at chromatin as Skp2 and proteasomal subunits recruit to the c-Myc target gene promoter Cyclin D2 in a c-Myc-dependent manner (von der Lehr et al., 2003). More recent work reveals that c-Myc ubiquitylation is required for elongation by RNA pol II of target genes. When ubiquitylation is blocked, c-Myc fails to recruit P-TEFb, which phosphorylates the RNA pol II CTD to stimulate transcription elongation, and TRAPP, a scaffold for multiple histone deacetylase complexes (Jaenicke et al., 2016).

Another transcriptional activator that requires ubiquitylation for proper cofactor recruitment is Gal4. Gal4 is targeted for ubiquitylation by two E3 enzymes: SCF^{Grr1} which down-regulates Gal4 protein levels in non-inducing conditions and SCF^{Met30} which targets transcriptionally active Gal4 (Muratani et al., 2005). In the absence of the Met30 F-box protein, Gal4 stimulates the production of transcripts but these transcripts are not translated. Presumably, this is due to defects in post transcriptional processing as the RNA pol II CTD has reduced levels of Ser5 phosphorylation in the absence of Met30 and a decrease in recruitment of the Bur1 kinase and the Cet1 mRNA capping enzyme to chromatin (Muratani et al., 2005). Transcription of Gal4 target genes also requires the proteasome. Gal4 dynamically interacts with chromatin during transcriptional activation, and proteasome inhibition increases Gal4 levels at the *GAL10* promoter (Collins et al., 2009; Geng and Tansey, 2012; Lipford et al., 2005).

Transcriptional activation by estrogen receptor alpha (ERα) best illustrates a dynamic interaction between a transcriptional activator and DNA through a UPS-dependent mechanism. In response to transcriptional induction by estradiol treatment in synchronized cells, ERα associates cyclically with DNA response elements with a periodicity of 45 minutes. Both transcriptional activation by

ERα and the cyclical association with DNA occur in a proteasome-dependent manner as proteasome inhibition increased the periodicity of ERα binding to 2 hours while RNA pol II failed to be recruited to the promoter of the pS2 gene (Lonard et al., 2000; Reid et al., 2003). Furthermore, the MDM2 and E6AP E3 enzymes that target ERα for ubiquitylation also cyclically associate with response elements and enhance transcriptional activation of target genes (Nawaz et al., 1999; Saji et al., 2001).

For several transcriptional activators, ubiquitylation is stimulated by phosphorylation. Sterol regulatory element-binding proteins (SREBP) translocate to the nucleus in response to low cellular sterol levels and interact with transcription cofactors to bind regulatory elements on DNA and stimulate transcription of target genes. Binding of SREBP1a to DNA stimulates hypo-phosphorylation of the SREBP1a phospho-degron by glycogen synthase kinase (GSK) (Bengoechea-Alonso et al., 2005; Punga et al., 2006). Once phosphorylated, SREBP1a is ubiquitylated by the E3 enzyme SCF^{Fbw7}. Fbw7 interacts with SREBP1a in response to SREBP1a phosphorylation stimulated by DNA binding which suggests that SREBP1a ubiquitylation may occur at chromatin. Furthermore, proteasome inhibition triggers an accumulation of phosphorylated SREBP1a on DNA and an increase in target gene transcript levels (Sundqvist and Ericsson, 2003) (Punga et al., 2006) (Bengoechea-Alonso and Ericsson, 2009).

Transcriptional activation by the transcription factors Smad2/3 also demonstrates the coupling between transcriptional activation and ubiquitylation stimulated by phosphorylation. In response to TGF-beta signaling, Smad 2 and 3 are phosphorylated, forming P-Smad2/3 which translocates into the nucleus with Smad4 (Mavrakis et al., 2007). Once in the nucleus, P-Smad2/3 associates with DNA binding partners and stimulates transcription. Not only does phosphorylation stimulate P-Smad2/3 activity on chromatin but triggers ubiquitylation by the E3 enzyme Arkadia and proteasome-dependent degradation. Arkadia is required for transcription of Smad2/3 target genes, suggesting that ubiquitylation is not just a result of transcriptional activation but is also a requisite step in the process.

The transcriptional activators presented above provide multiple examples in which transcriptional activation and recognition by the UPS occur concomitantly. However, it is still unknown as to why a transcriptional activator would require recognition by the UPS for its function. In light of work with the transcriptional activator Gcn4 (Figure 2A), a new model has emerged that can mechanistically explain the requirement for the UPS. Gcn4 is synthesized in response to cellular stresses including amino acid starvation. Gcn4 is ubiquitylated through the E2 enzyme Cdc34 and the E3 enzyme SCF^{Cdc4} (Figure 2B). Work from the Deshaies laboratory demonstrates that transcription of Gcn4 target genes requires both the E2 enzyme Cdc34 and the F-box protein Cdc4 (Lipford et al., 2005). Additionally, transcription of Gcn4 target genes also requires the proteasome. When Cdc34, Cdc4, or the proteasome are disrupted, Gcn4 remains present on chromatin despite a loss of target gene transcripts and a loss of RNA pol II at target genes.

Most importantly, this work revealed an intriguing connection between Gcn4 phosphorylation and the requirement of the UPS for transcriptional activation. Gcn4 is phosphorylated by two different cyclin dependent kinases, Pho85 and Srb10, to stimulate ubiquitylation and degradation (Chi et al., 2001; Meimoun et al., 2000). Pho85 is responsible for stimulating Gcn4 degradation when Gcn4 is no longer required while Srb10 is a component of the Mediator complex that associates with RNA pol II. To block phosphorylation, the Deshaies laboratory utilized a mutant in which five predicted Cdk target residues are mutated to generate the 3T2S-Gcn4 mutant (Figure 2A). Interestingly, 3T2S-Gcn4 was capable of stimulating transcription during proteasome inhibition (Lipford et al., 2005). These data suggest that Gcn4 phosphorylation converts Gcn4 into a state that requires recognition by the UPS in order to function, but this requirement can be bypassed when Cdk-dependent phosphorylation is blocked.

In light of the work with Gcn4, along with work on other transcriptional activators requiring the UPS for function, we propose a model that mechanistically explains how a transcriptional activator can require ubiquitylation and degradation for its function. In this model, referred to as the “Spent/Stuck” model, a transcriptional activator binds DNA and stimulates transcription by recruiting the transcriptional machinery (Figure 3). Following the first few rounds of transcription, the transcriptional activator converts from an active to an inactive “spent” state through

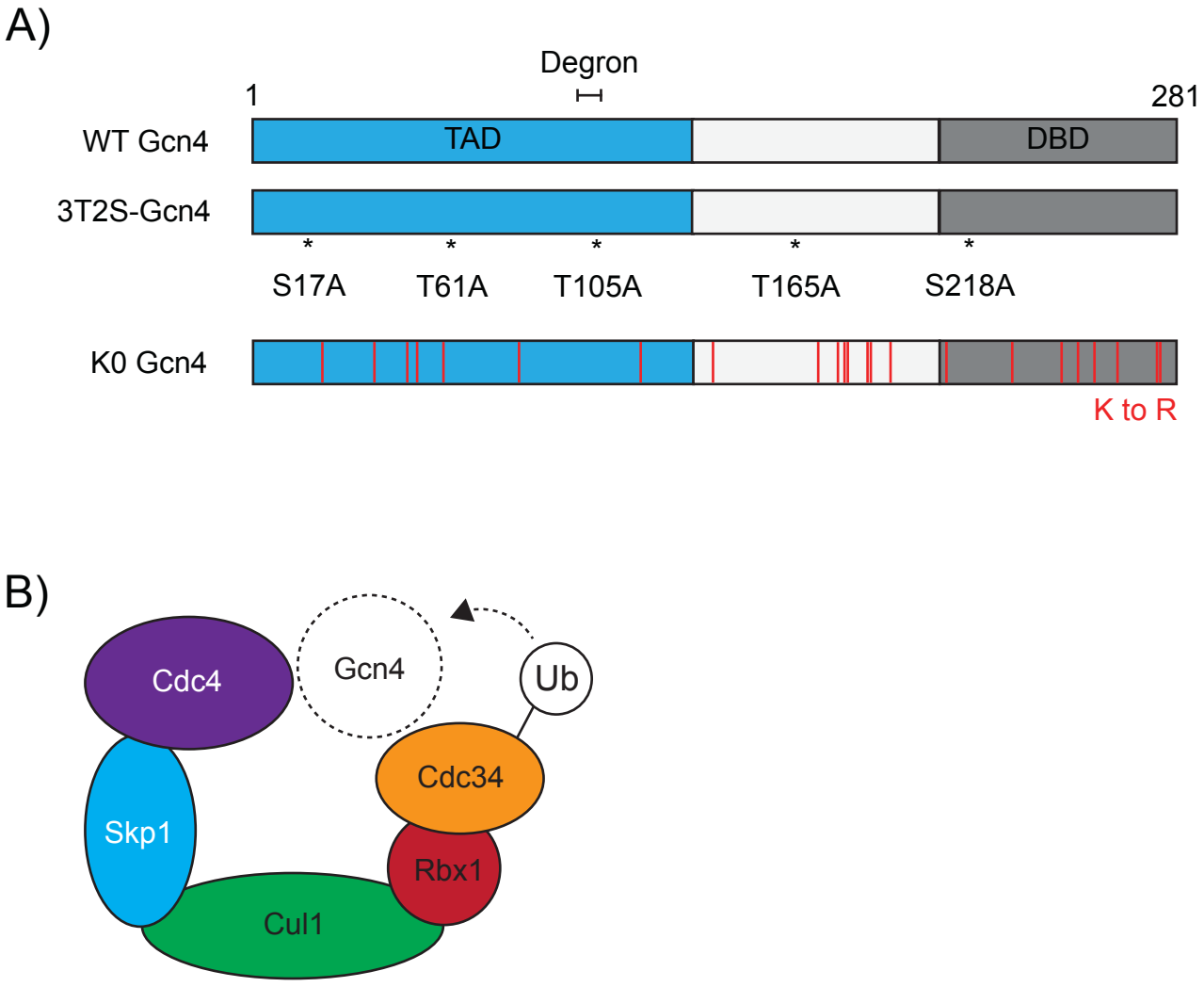

Figure 2. Gcn4 is a transcriptional activator targeted by the ubiquitin-proteasome system. (A) Graphical representation of Gcn4 showing the functional domains of the protein (TAD, transcriptional activation domain, blue; DBD, DNA-binding domain, gray). The wild-type (WT) Gcn4 protein is represented on top, the 3T2S mutant (showing the location of five alanine substitution mutations) in the middle, and the lysine free, K0, mutant at the bottom. (B) Gcn4 is ubiquitylated through the Cdc34 E2 enzyme and SCF^{Cdc4} E3 enzyme.

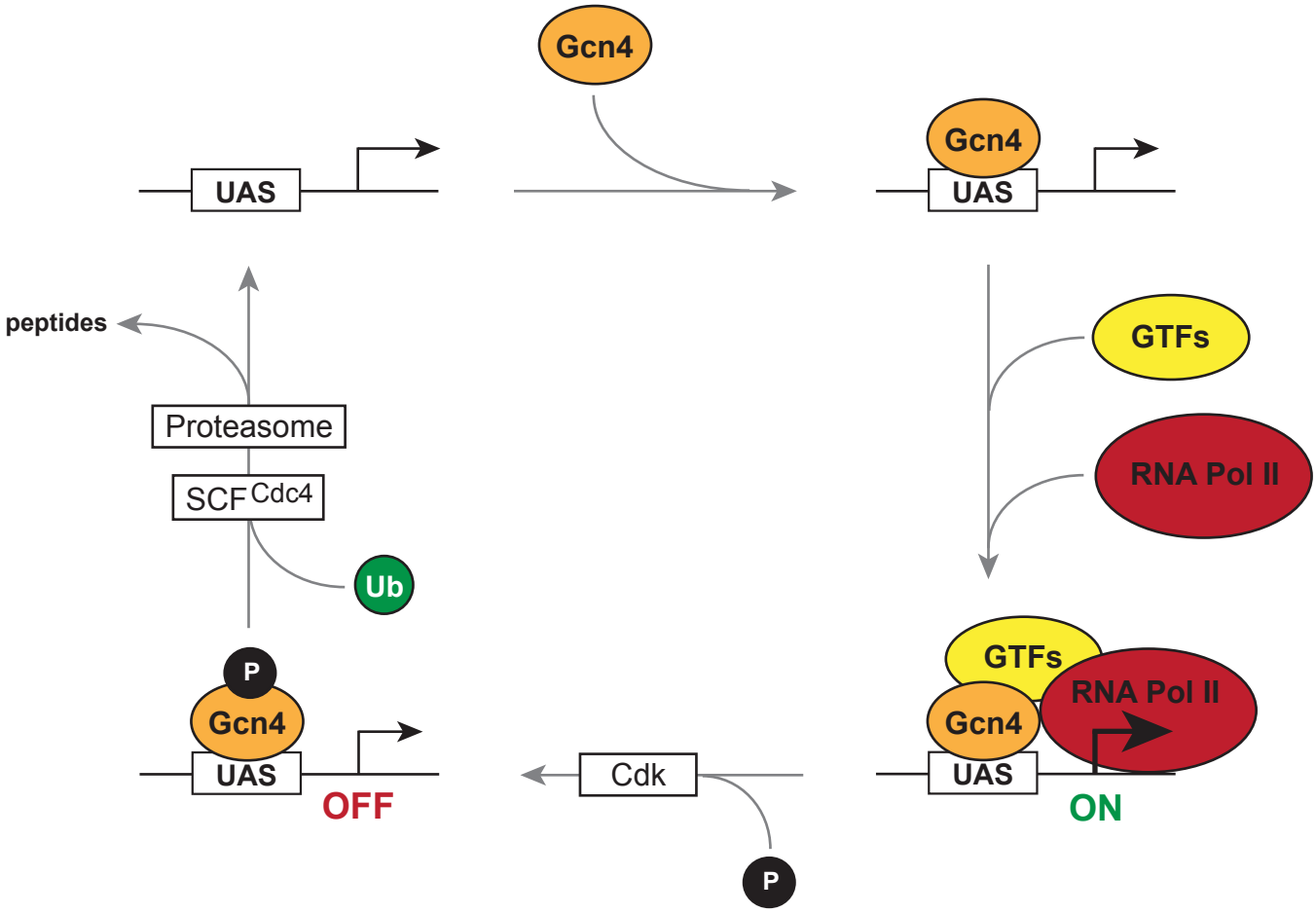

Figure 3. Spent/Stuck model for transcriptional activation.

phosphorylation and remains bound to chromatin (“stuck”). In order to stimulate subsequent rounds of transcription, the UPS clears the “spent” transcriptional activator from DNA and allows fresh activator to bind its recognition sequences. In this thesis, I will challenge this model using the transcriptional activator Gcn4 as a model

Summary of Thesis

The work presented in this thesis challenges the Spent/Stuck stuck model using the budding yeast transcriptional activator Gcn4. I began by examining the role the ubiquitylation machinery targeting Gcn4 plays in transcription of Gcn4 target genes. I found that disruption of Gcn4 ubiquitylation with temperature sensitive alleles of the E2 enzyme Cdc34 and the F-box protein Cdc4 resulted in a decrease in Gcn4 target gene transcript levels. I also discovered that disruption of the F-box protein Cdc4 did not affect the level of Gcn4 found at a representative target gene. To study the role of the proteasome in transcription of Gcn4 target genes, I modified a method of comprehensive proteasome inhibition in which all three types of proteolytic sites within the proteasome are disrupted through a combined chemical-genetic approach. Using this method, I discovered that transcript levels of representative Gcn4 target genes following proteasome inhibition decreased to levels comparable to uninduced levels while Gcn4 remained present in the cell, although accumulating in a highly ubiquitylated state. The decrease in Gcn4 target gene transcript levels corresponded to a decrease in Gcn4 levels found at the UAS of representative target genes, demonstrating that the Spent/Stuck model is not correct in its current form. The decrease in Gcn4 DNA binding did not correspond to a loss of Gcn4 nuclear localization or changes in nucleosome location at Gcn4 recognition sites. Also, the decrease in Gcn4 transcript levels following proteasome inhibition was not due to the arginine repression complex. Interestingly, I found that Gcn4 interacted with the Cdc48 complex, and disruption of the Cdc48 complex restored DNA binding of Gcn4 and target gene transcript levels following proteasome inhibition. In sum, these data support a new model of Gcn4-mediated transcription in which ubiquitylation could function as a method of self-limiting transcriptional activation in which ubiquitylation both promotes Gcn4 activity while also negatively regulating the levels of Gcn4 on

chromatin. This model also demonstrates that Cdc48, not the proteasome, plays the critical role of regulating Gcn4 binding to chromatin.

CHAPTER II

MATERIALS AND METHODS

Yeast strains and manipulations

Yeast strains are described in Table 1. Gene deletions were performed via homologous recombination using PCR-amplified auxotrophic markers or antibiotic resistance genes from plasmids, as indicated. Primers sequences are listed in Table 2. Plasmids are listed in Table 3. Epitope-tagging of endogenous loci was performed similarly (Knop et al., 1999; Sheff and Thorn, 2004). mCherry-tagging of endogenous Htb2 was performed as described above except using an mCherry-tagging cassette amplified from SWY5678 genomic DNA (Lord et al., 2015). Strains carrying the *3T2S-GCN4* allele were generated through deletion of endogenous *GCN4* with the *URA3* cassette followed by insertion of PCR-amplified *3T2S-GCN4* through homologous recombination. PCR genotyping was used to confirm all genomic manipulations. Replacement of the *cdc48-3* allele for wild-type *CDC48* was performed through homologous recombination of a PCR fragment encoding wild-type *CDC48* and spanning the sites of the two mutations in *cdc48-3* (P257L, R387K). Colonies were selected for ability to grow at the restrictive temperature of 37°C, and restoration of the wild-type *CDC48* sequence confirmed by PCR-amplification of the locus and Sanger DNA-sequencing. For anchor away strains, epitope tagging of *GCN4* and deletion of *PDR5* were performed as described above. *CDC34* and *GCN4* were tagged with FRB as described above for epitope-tagging except using an FRB tagging construct (Haruki et al., 2008). For genomic manipulations, and introduction of plasmids, a high-efficiency yeast transformation protocol was used (Gietz and Schiestl, 2007).

Transcriptional induction

Overnight liquid yeast cultures grown at 30°C in YPAD (1% Yeast Extract, 2% Peptone, 20 mg/L Adenine, 2% Dextrose) were washed once with sterile water and diluted to an OD_{600} of 0.3 and grown for 5 hours in minimal media (0.67% Yeast Nitrogen Base w/o Amino Acids, 2% Dextrose) supplemented with only amino acids required for auxotrophy. Sulfometuron methyl (Cat #

Table 1. Yeast strains		
Strain	Genotype	Origin
W303-1a	MATa l*eu2-3,112 trp1-1 can1-100 ura3-1 ade2-1 his3-11,15*	Patton et al., 1998
GHY106	W303-1a *GCN4-HA::KAN*	This study
MT670	W303-1a *cdc34-2*	Patton et al., 1998
GHY109	MT670 *GCN4-HA::KAN*	This study
MT668	W303-1a *cdc4-1*	Patton et al., 1998
GHY107	MT668 *GCN4-HA::KAN*	This study
GHY243	W303-1A *GCN4-HA::KAN* [pRS316]	This study
GHY244	W303-1A *GCN4-HA::KAN* [pUB221]	This study
GHY245	MT668 *GCN4-HA::KAN* [pRS316]	This study
GHY246	MT668 *GCN4-HA::KAN* [pUB221]	This study
HHY168	MATα *tor1-1 can1-100 leu2-3,112 ura3-1 ade2-1 his3-11,15 fpr1::NAT RPL13A-2×FKBP12::TRP1*	Haruki et al., 2008
GHY139	HHY168 *pdr5::LEU2 GCN4-HA::KAN*	This study
GHY149	HHY168 *pdr5::LEU2 GCN4-HA::KAN CDC34-FRB::HIS*	This study
GHY151	HHY168 *pdr5::LEU2 GCN4-HA::KAN CDC4-FRB::HIS*	This study
GHY147	HHY168 *pdr5::LEU2 GCN4-HA::KAN TBP-FRB::HIS*	This study
GHY145	HHY168 *pdr5::LEU2 GCN4-FRB::HIS*	This study
Y80	MATa *can1-100 ade2-1 his3-11,15 leu2-3,112 trp1-1 ura3-1*	S. Elledge
Y552	Y80 *skp1-11*	S. Elledge
Y554	Y80 *skp1-12*	S. Elledge
WCG4a	MATa *leu2-3,112 ura3 his3-11,15 CanS GAL2*	Heinemeyer et al., 1997
YUS5	WCG4a *pup1-T30A pre3-T20A*	Heinemeyer et al., 1997
GHY010	YUS5 *GCN4*	This study
GHY025	YUS5 *GCN4-HA::KAN*	This study
GHY021	YUS5 *GCN4-9xMYC::HIS*	This study
RJD3037	MATa *his3-1, leu2-0, met15-0, ura3-0 pdr5::KAN GCN4-9xMYC::HIS3*	Lipford et al., 2005
GHY004	YUS5 *gcn4::URA3*	This study
GHY356	YUS5 *GCN4-HA::KAN* [pUB221]	This study
GHY360	YUS5 *3T2S-GCN4-HA::KAN* [pUB221]	This study
GHY014	YUS5 *3T2S-GCN4*	This study
GHY339	YUS5 *GCN4-GFP::KAN HTB2-mCherry::HIS3*	This study
RHY2455	MATα *ura3–52 leu2–3,112*	Sato and Hampton, 2006
RHY2457	MATα *ura3–52 leu2–3,112 cdc48–3*	Sato and Hampton, 2006
GHY116	RHY2455 *GCN4-HA::KAN*	This study
GHY118	RHY2457 *GCN4-HA::KAN*	This study
GHY279	RHY2457 *cdc48-3::CDC48*	This study
GHY285	YUS5 *GCN4 CDC48-3xMYC::HIS3*	This study
GHY287	YUS5 *GCN4-3xHA::KAN CDC48-3xMYC::HIS3*	This study
GHY124	YUS5 *K0 GCN4-3xHA::KAN CDC48*	This study
GHY293	YUS5 *K0 GCN4-3xHA::KAN CDC48-3xMYC::HIS3*	This study
GHY161	YUS5 *GCN4 ubx1::NAT*	This study
GHY189	YUS5 *GCN4 ubx2::NAT*	This study
GHY165	YUS5 *GCN4 ubx3::NAT*	This study
GHY185	YUS5 *GCN4 ubx4::NAT*	This study
GHY168	YUS5 *GCN4 ubx5::NAT*	This study
GHY170	YUS5 *GCN4 ubx6::NAT*	This study
GHY171	YUS5 *GCN4 ubx7::NAT*	This study
GHY081	YUS5 *GCN4 arg80::NAT*	This study
GHY079	YUS5 *gcn4::URA3 arg80::NAT*	This study

Table 2. Primers for strain generation	
Primer	Sequence
gcn4::URA3 F	TTAAAATGTCCGAATATCAGCCAAGTTTATTTGCTTTAAAT CCAATGGGTTagtgcaccacgcttttcaat
gcn4::URA3 R	TTTCTAGCACGTTTTAGAGCAGCAGGATCACTGGATTCG GGCACAATTGGttgaagctctaatttgtgagtttagt
S3 GCN4	TTGGAAAATGAGGTTGCCAGATTAAAGAAATTAGTTGGC GAACGCCGTACGCTGCAGGTCGAC
S2 GCN4	TACACGAGAATGAAATAAAAAATATAAAATAAAAGGTAAAT GAAAATCGATGAATTCGAGCTCG
GCN4 F5	ATCACTTGGAAAATGAGGTTGCCAGATTAAAGAAATTAGT TGGCGAACGCggtgacggtgctggttta
GCN4 R3	TATACACGAGAATGAAATAAAAAATATAAAATAAAAGGTAA ATGAAATCAtcgatgaattcgagctcg
CDC48 S3	CAGGTGCTGCATTTGGTTCTAATGCGGAGGAAGATGATG ATTTGTATAGTcgtacgctgcaggtcgac
CDC48 S2	AGAAATGACTTGAATTTACGATTTAAAATAAAAATATACCT GGCATATAAatcgatgaattcgagctcg
arg80::NAT F	TTTTTTTTCCCACATTAGTTACATACACTCTCTAAAGAATAT TGCTAAATcgccagatctgtttagcttg
arg80::NAT R	CTATATGGATCTGCCTATGCCTTCGTGGGGCATCTCTTAC TCTCGCATGTcgttagtatcgaatcgacag
full-length gcn4-HA::URA3 F	TTTTGTTTACCAATTTGTCTGCTCAAGAAAATAAATTAAAT ACAAATAAAagtgcaccacgcttttcaat
full-length gcn4-HA::URA3 R	GGAACATCGTATGGGTAAAAGATTCCGGATCCGTCGACC TGCAGCGTACGttgaagctctaatttgtgagtttagt
gcn4::NAT F	TTAAAATGTCCGAATATCAGCCAAGTTTATTTGCTTTAAAT CCAATGGGTTcgccagatctgtttagcttg
gcn4::NAT R	TTTCTAGCACGTTTTAGAGCAGCAGGATCACTGGATTCG GGCACAATTGGcgttagtatcgaatcgacag

Table 3. Plasmids		
Plasmid	Genotype	Origin
GHE001	pCR2.1 GCN4-HA::KAN	This study
GHE003	pCR2.1 3T2S-GCN4	This study
pRS306	pBluescript-URA3	Sikorski et al. 1989
pRS316	pBluescript-URA3, CEN6, ARSH4	Sikorski et al. 1989
pYM1	pFA6a-3xHA-KANMX6	Knop et al. 1999
pYM5	pFA6a-3xMyc-HIS3	Knop et al. 1999
pYM19	pFA6a-9xMyc-HIS3	Janke et al. 2004
pAG25	pFA6a-NATMX4	Goldstein et al. 1999
pUB221	P_{CUP1}-Hisx6-Myc-Ubiquitin, URA3	Yaglom et al. 1995
pKT127	pFA6a-yEGFP-KAN (Add Gene #8728)	Sheff and Thorn 2004

sc-251091 from Santa Cruz Biotechnology) dissolved in water was then added to liquid cultures to a final concentration of 0.5 µM and allowed to grow for 90 minutes to induce Gcn4.

Proteasome inhibition

Liquid cultures were treated with 50 µM MG132 (Cat # 81-5-15 from American Peptide Company dissolved in DMSO for 50 mM stock) and 0.004% SDS (Liu et al., 2007) and grown for 60 minutes at 30°C before transcriptional induction with SM treatment.

RNA Isolation

Cell pellets were resuspended in 400 µl RNA Extraction Buffer (50 mM NaAc, pH 4.8; 0.5% SDS; 10 mM EDTA) and 400 µl phenol (pH 4.5) and vortexed 5 seconds. Samples were incubated on 65°C heat block for 1 hour, with brief vortexing after 30 minutes. Samples were then incubated on ice for 5 minutes and spun at 14 k g for 5 minutes at 4°C. The aqueous layer was transferred to a new tube and 400 µl phenol, pH 4.5, added, vortexed briefly, and placed on ice for 5 minutes. Samples were spun at 14 k g for 5 minutes at 4°C. The aqueous layer was transferred to a new tube and 400 µl Phenol:Chloroform:Isoamyl alcohol and 100 µl RNA extraction buffer was added. Samples were vortexed and spun at 14 k g for 5 minutes at room temperature. The aqueous layer was transferred to a new tube and RNA precipitated for at least 1 hour at -20°C with 1 ml 100% EtOH and 40 µl 3 M NaAc, pH 4.8. RNA was pelleted by spinning at 14 k g at 4°C for 10 minutes. Supernatant was removed and RNA pellet washed once with 70% EtOH. Pellets were then air-dried at room temperature. RNA was resuspended in 25 µl H_2O. Contaminating DNA was removed by adding 1.5 µl 10x DNase Buffer and 1 µl DNase to 12.5 µl of sample and incubated at 37°C for 10 minutes. DNase was inactivated by adding 1 µl 25 mM EDTA to each sample and incubation at 65°C for 15 minutes.

cDNA Synthesis

One µg of DNase-treated RNA was brought up to 10 µl with H_2O and 1 µl dNTPs (10 mM) and 1 µl Random Hexamers added. Samples were incubated at 65°C for 5 min and cooled on the benchtop. 1 µl H_2O, 2 µl 0.1 M DTT, and 4 µl 5x First Strand Buffer were added to each tube and incubated at 25°C for 2 minutes before added 0.5 µl SuperScript II Reverse Transcriptase

(Invitrogen). Samples were then incubated in a thermocycler at 25°C for 10 minutes, 42°C for 50 minutes, and 70°C for 20 minutes. Each sample was then diluted with 20 µl H_2O to prepare for qPCR.

qPCR

Reactions were performed in duplicate and contained 6.25 µl KAPA SYBR Fast qPCR Master Mix (2x), 0.75 µl F/R Primer Mixture (10 mM), 4.25 µl H_2O, and 1.25 µl cDNA reaction. RT-qPCR primer sets used are in Table 4. Data was normalized to *ACT1* and analyzed using the ΔΔCT Method.

Protein Isolation

Yeast cell pellets were resuspended in Buffer A (6 M Guanidine-HCl; 0.1 M Na_2HPO_4/NaH_2PO_4, pH 8.0; 10 mM Imidazole) to an OD_{600} ~150 and glass beads added until 2 mm of liquid remained above beads in 2 mL screw-top bead beating tubes. Samples were vortexed at maximum setting for 20 seconds followed by 30 seconds in ice slurry a total of six times. 100 µl Buffer A was added, samples vortexed briefly and spun at 14 k g for 5 minutes at 4°C. Supernatant was transferred to fresh tube and protein concentration measured by Bradford Assay.

Western blotting

Twenty µg of protein was precipitated in ice-cold 100% ethanol for 15 minutes and washed with 70% ethanol. Pellets were air dried for 5 minutes and resuspended in 20 µl urea loading buffer (200 mM Tris-HCl, pH 6.8; 5% glycerol, 8 M Urea, 143 mM beta-mercaptoethanol, 8% SDS). Samples were heated for 5 minutes at 65°C before loading onto 10% polyacrylamide gels. Protein was transferred to 0.2 µm pore size nitrocellulose membrane using the semi-dry transfer method for 90 minutes at 25V and 400 mA. Nitrocellulose was blocked with 5% milk solution in Tris-buffered saline (15 mM Tris-HCl, 137 mM NaCl, pH 7.6) with 0.1% Tween 20 and probed using appropriate antibody: anti-HA-Peroxidase (Roche, Product #12013819001), anti-c-Myc-Peroxidase (Roche, Product #11814150001), or anti-beta-actin (Abcam, Product #ab8224).

Table 4. qPCR Primers	
ACT1 F	AGCCGTTTTGTCCTTGTACTCTTCC
ACT1 R	AGCGTAAATTGGAACGACGTGAGTA
ARG1 F	GCCAACGGTGTTGGTAGAAT
ARG1 R	AGTCAATGGAGCCTGTTCGT
ARG4 F	GTCATCCAAACGACGAGGAT
ARG4 R	ACCGGTGTGGACTTTACCAG
HIS4 F	ACAACTGCCACGTGTGGATA
HIS4 R	TTGGACATTTCAAGGGCTTC
CPA2 F	CTTGCCCGTTACACCAGAAT
CPA2 R	CTGTTTGACCACCGAAGGTT
ADH3 F	GTGACTGGGTTGCCATCTCT
ADH3 R	TAACCCATCGCAGTTGCATA

Western blot membranes were imaged through enhanced chemiluminescence (ECL) by X-ray film exposure.

His-Myc-Ubiquitin Pull-down

Strains containing either pRS316 or the His-Myc-Ub expression plasmid pUB221 (Yaglom et al., 1995) were grown in 200 ml liquid cultures under SM induction media conditions. 1 hr prior to SM treatment, 400 µl of 250 mM $CuSO_4$ was added to induce His-Myc-Ub expression. Protein was collected as described above using Buffer A. Equivalent protein amounts (as determined by Bradford Assay) were incubated 2 hrs at 4°C with Ni-NTA agarose beads (Qiagen, Product #30210). Beads were washed three times with Buffer A, three times with Buffer A / TI (1 Volume Buffer A: 3 Volumes TI), and once with TI (25 mM Tris, 20 mM Imidazole, pH 6.8). Pull-downs were eluted by incubating with 40 µl elution buffer (0.5 M Imidazole, 0.15 M Tris HCl, pH 6.8, 30% glycerol, 0.72 M beta-mercaptoethanol, 5% SDS) and rotated for 20 minutes at 25°C. Liquid was transferred to new 1.5 ml microcentrifuge tube and boiled before running on polyacrylamide gels.

Chromatin-Immunoprecipitation

Formaldehyde was made by dissolving 9.2 g paraformaldehyde in 30 mL water and 4 mL 10x phosphate buffered saline on a hot plate at medium setting for 5 minutes. 5 µl 10 N KOH was added and stirred for 30 minutes. Solution was cooled on ice for 5 minutes and filter sterilized with 0.45 µm vacuum filter. Solution was brought up to 40 mL with water. 100 ml cultures were cross-linked with 1% final concentration of formaldehyde for 15 minutes while shaking at 25°C. Cross-linking was stopped by adding 1/10 culture volume of 2.5 M glycine and shaking for 5 minutes at 25°C. Cells were spun down for 10 minutes at 1100 g at 4°C and supernatant removed. Pellets were washed with 20 ml ice-cold PBS and centrifuged for 10 minutes at 1300 g at 4°C. Supernatant was removed, resuspended in 1 ml ice-cold PBS, transferred to 1.5 ml microcentrifuge tube, spun, and supernatant removed. Pellets were flash-frozen in liquid nitrogen and stored at -80°C.

Cell pellets were resuspended in 800 µl Chromatin FA Buffer (50 mM HEPES, pH 7.5; 150 mM NaCl; 1 mM EDTA; 1 % Triton X-100; 0.5 % SDS; 0.1 % DOC) w/ 1 mM DTT, 5 mM NaF, 2x

Roche Protease Inhibitor Cocktail, EDTA-free (Roche, Product #11873580001), 0.4 mg/ml Pefabloc SC and transferred to 2.0 ml screw-cap tubes containing 1.5 ml pre-chilled glass beads. Cells were lysed by bead-beating at 4°C for 40 seconds and in ice-bath for 2 minutes, for a total of 5 times. Cell lysate was collected by puncturing the bottom of screw-cap tubes and centrifugation. Supernatant of the flow-through was transferred to a new 1.5 ml microcentrifuge tube and 8 µl Pefabloc and 8 µl Roche cocktail added. Samples were sonicated with Ultra-Sonic Processor (GE130PB-1) at 40 (Pulse Mode) for 10 seconds, 12 times, incubating 1 minute on ice between each sonication. Samples were centrifuged at 14 k g for 15 minutes at 4°C, supernatant transferred to new 1.5 ml microcentrifuge tube, and stored at -80°C.

Immunoprecipitation was performed by bringing sample up to 1 ml with FA Buffer (50 mM HEPES, pH 7.5; 150 mM NaCl; 1 mM EDTA; 1 % Triton X-100; 0.1 % SDS; 0.1 % DOC) w/ 10 µl Roche Cocktail and 10 µl Pefabloc and appropriate amount of lysate per targeted protein. Antibody was added and incubated on rotator at 4°C overnight. Thirty-five µl Roche Protein A Agarose Beads (50% bed volume) were blocked in 1 ml FA Buffer w/ 10 µl Roche Inhibitor, 10 µl Pefabloc, and 10 µl BSA (10 mg/ml) and rotated for 30 minutes at room temperature. Blocking solution was removed and beads resuspended with FA Buffer to create 50% bead slurry. 35 µl bead slurry was added to each pull-down and rotated at room temperature for 1 hour. Beads were pelleted by spinning at 625 g at room-temperature for 1 minute and supernatant removed. Beads were washed by adding 1 ml FA Buffer, rotated for 5 minutes at 25°C, spun at 1300 g, and supernatant removed. Washing was then repeated using FA Buffer w/ 0.5 M NaCl (50 mM HEPES, pH 7.5; 500 mM NaCl; 1 mM EDTA; 1 % Triton X-100; 0.5 % SDS; 0.1 % DOC), LiCl-NP-40 (250 mM LiCl; 0.5 % NP-40; 0.5 % DOC; 1 mM EDTA; 10 mM Tris-HCl, pH 8.0), and then using TE. After final wash, 200 µl ChIP Elution Buffer (1 % SDS; 0.1 $NaHCO_3$; 0.2 M NaCl) was added and samples rotated for 20 minutes at 25°C. Cells were pelleted and eluted samples were transferred to new 1.5 ml microcentrifuge tube. Cross-linking was reversed by incubating in a 65°C water bath overnight.

Following overnight incubation, 8 µl 1 M Tris-HCl (pH 7.0), 4 µl EDTA, and 1 µl Proteinase K (10 mg/ml in water) were added and incubated at 37°C for 2 hours. 200 µl TE was then added and

protein extracted with 400 µl Phenol:Chloroform:Isoamyl Alcohol. 360 µl aqueous layer was transferred to a new 1.5 ml microcentrifuge tube and DNA precipitated overnight with 1 ml 100% EtOH, 36 µl 3 M NaAc (pH 4.8), and 1 µl glycogen (10 mg/ml). DNA was pelleted by centrifugation at 12 k g for 15 minutes at 4°C and supernatant removed. Pellets were washed with 70% EtOH and pellets air-dried at room temperature until EtOH evaporated. Samples were resuspended in 100 µl TE. qPCR was performed with reactions containing 2 µl of resuspended DNA pellet as described above. qPCR primers for ChIP samples are listed in Table 5.

Fluorescent Microscopy

Images were acquired with a standard microscope (BX50, Olympus) equipped with a motorized stage (model 999000, Ludl), UPlanF1 ×100, numerical aperture 1.30 oil immersion objective, and digital charge-coupled device camera (Orca-R2, Hamamatsu).

Nucleosome Mapping via MNase Protection Assay

185 ml yeast cultures grown to 2 x 10^7 cells/ml (OD_{600} ~.670) were cross-linked with a final concentration of 2% formaldehyde while shaking at 30°C for 30 minutes. Cross-linking was stopped by adding 10.3 ml 2.5 M glycine (made fresh in water) while shaking at 25°C for 10 minutes. 1.2 x 10^9 cells were pelleted at 1300 g for 5 minutes at 4°C and resuspended with 13 ml Tris-Buffered Saline (TBS). Cells were pelleted again at 1300 g for 3 minutes at 4°C and supernatant removed. Pellets were flash frozen in liquid nitrogen and stored at -80°C. Frozen pellets were resuspended in 5.7 ml Zymolyase Digestion Buffer (50 mM Tris, pH 7.5; 1 M Sorbitol; 10 mM Beta-Mercaptoethanol and 0.5 mM Spermidine, both added fresh) and treated with 300 µl Zymolyase 20T (MP Biomedicals, Cat # ICN320921, 5 mg/ml in ZDB) for 30 minutes at 30°C on a nutator to generate spheroplasts. Spheroplasts were pelleted at 1300 g for 10 minutes at 4°C. Supernatant was removed and washed with 2 ml NP Buffer (1 M Sorbitol; 50 mM NaCl; 10 mM Tris, pH 7.5; 5 mM $MgCl_2$; 1 mM $CaCl_2$; 0.075% NP-40) by inverting tube. Spheroplasts were pelleted again at 1300 g for 10 minutes at 4°C and supernatant removed. Spheroplasts were resuspended thoroughly in 1.8 ml NP Buffer for subsequent S7 Micrococcal nuclease (MNase, Roche, Cat # 10107921001) digestion. 300 µl of resuspended spheroplasts were digested with either 0, 1.0, 2.5, 5.0, 10, or 20 U MNase at 37°C for 45 minutes while on nutator. Reactions were

Table 5. ChIP Primers	
ARG1 GCN4 BS2 F	GCTGTCGCAACCTATTTCCA
ARG1 GCN4 BS2 R	TCAATCTGATCCAATGAAGATGA
ARG1 TATA F	ATCTGAGCAGTTGCGAGACC
ARG1 TATA R	AACTGTGGGCAAGAACAAGG
ARG1 ORF3 F	CAAGCCCACATTTCTTACGAG
ARG1 ORF3 R	ATCGACGATCAATTTCCACA
ARG4 Gcn4 BS F	GGTTACTCATTGGCAGAATCC
ARG4 Gcn4 BS R	TTCAATTTGCGCCAGCTTAT
ARG5 Gcn4 BS F	TCCGAATGACTCAGTCTACATCA
ARG5 Gcn4 BS R	GCGCGCAAGCTCTTTATATG
ARO4 Gcn4 BS F	CACCCTGTGCATTTTGTACG
ARO4 Gcn4 BS R	CGTCCCGCACATCTTTTT
CPA2 Gcn4 BS F	GAGATAGGAACCTCCATGTCG
CPA2 Gcn4 BS R	TGGCAGAAATGCTTATGACG
HIS4 Gcn4 BS F	TGCACAGTGACTCACGTTTTT
HIS4 Gcn4 BS R	TCGGAGGTGAATATAACGTTCC
HIS7 Gcn4 BS F	GGCTAATTAGGTGATCATGAAAAA
HIS7 Gcn4 BS R	AACCTGATTGAGTAGTCGTCGAT
LEU3 Gcn4 BS F	TCTAGCTATTCTAAATCATCTGCATGT
LEU3 Gcn4 BS R	CCTCCGATCGAAGAGAGGTT
LYS1 Gcn4 BS F	TTTGGAATTCCGCTCTCAAC
LYS1 Gcn4 BS R	ATCGTGGTTTCTCGAGGATG
SNZ1 Gcn4 BS F	AGCCGGGCTTTTTCACTACT
SNZ1 Gcn4 BS R	GTAACTAACGGTGCGGCAGA
THR4 Gcn4 BS F	CAACGAGGAAATAGAAGAAAATGAA
THR4 Gcn4 BS R	CCAAATGGAAAAATATAAGATACACAA

stopped by adding 75 µl Stop Buffer (5% SDS; 50 mM EDTA) and brief vortexing. 5 µl Proteinase K (20 mg/ml, Roche, made fresh in water) was added to each sample and incubated at 65°C overnight. DNA was purified by adding 400 µl phenol:chloroform:isoamyl alcohol (PCI, 25:24:1), vortexing, and spinning at 14 k g. Supernatant was saved and treated with 5 µl RNase (10 mg/ml) at 37°C for 1 hour. Samples were treated again with 400 PCI and supernatant was saved. DNA was precipitated by adding 70 µl 7.5 M ammonium acetate and 450 µl isopropanol and spun at 14 k g for 10 min at 4°C. Supernatant was removed and DNA pellet washed with 500 µl 80% EtOH. DNA pellet was air-dried and resuspended in 100 µl TE. Efficiency of each MNase digestion was determined by qPCR using NB primers (amplifying site of previously mapped nucleosome in the *GAL1-10* promoter) and NUB primers (amplifying site of previously mapped nucleosome-free region in the *GAL1-10* promoter) (ΔΔCT Method, using the 0 U MNase sample as reference). Samples with MNase digestion efficiency of ~0.95 were then used for subsequent qPCR as previously described using overlapping scanning primers (Table 6). Enrichment for each primer set was calculated using the formula: $[2^{(0\text{ U MNase CT - Optimum U Mnase CT})}]_{\text{Target Primer}}$ / $[2^{(0\text{ U MNase CT - Optimum U Mnase CT})}]_{\text{NB Primer}}$

Co-Immunoprecipitation

Cell pellets from 100 ml cultures were resuspended in 800 µl Yeast Lysis Buffer (YLB) (10 mM Na_2HPO_4/NaH_2PO_4, pH 8.0; 150 mM NaCl; 2 mM EDTA; 0.1% NP-40; 50 mM NaF; 0.1 mM Na_3VO_4; 1x Roche Protease Inhibitor; 0.4 mg/ml Pefabloc; 50 µM MG132; 2 mg/ml Iodoacetamide; 200 µM 1,10-Phenanthroline). Cells were lysed by bead-beating at 4°C for 40 seconds and in ice-bath for 2 minutes, for a total of 5 times. Cell lysate was collected by puncturing the bottom of screw-cap tubes and centrifugation. Cell lysates were cleared by centrifugation at 14 k g for 5 minutes at 4°C and supernatant transferred to new 1.5 ml microcentrifuge tube.

Immunoprecipitation was performed by adding 12CA5 primary antibody to 600 µl of cell lysate and samples incubated on rotator at 4°C for 2 hrs. Roche Protein A Agarose Beads were blocked in 1 ml YLB w/ 10 µl Roche Proteinase Inhibitor, EDTA-free, 10 µl Pefabloc, and 10 µl BSA (10 mg/ml) and rotated for 30 minutes at 4°C. Blocking solution was removed and beads

Table 6. Nucleosome mapping primers	
GAL1 NB F	CCCCACAAACCTTCAAATTAACG
GAL1 NB R	CGCTTCGCTGATTAATTACCC
GAL1 NUB F	CGGATTAGAAGCCGCCGA
GAL1 NUB R	ATCTTTATTGTTCGGAGCAGTG
ARG1 -820 F1	ACGTCCGCATGGAAGACCTA
ARG1 -716 R1	AAAGAGGCAACAGGAAAGATCAGA
ARG1 -740 F2	CTCTGATCTTTCCTGTTGCCTCTT
ARG1 -653 R2	CTGTAGTAATGTTACTAGTAGTAGTTGTAGAACTTGTG
ARG1 -690 F3	CACAAGTTCTACAACTACTACTAGTAACATTACTACAGTT
ARG1 -541 R3	CGGTGATGTGATATGTAAACGATAATAG
ARG1 -580 F4	CCATTATACACGCTATTATCGTTTACATATC
ARG1 -471 R4	ATAGATAACAGAAAAGGTTATGGCGATTA
ARG1 -557 F5	TACATATCACATCACCGTTAATGAAAGA
ARG1 -448 R5	TCGAAGAAACAGCTTTAAGGGCTAT
ARG1 -510 F6	ACACAATTAAATAATCGCCATAACCTT
ARG1 -415 R6	GGCCCATGTGGAGAATTACTG
ARG1 -492 F7	CATAACCTTTTCTGTTATCTATAGCCCTTA
ARG1 -382 R7	GTGACTAACATAGCGCTCTTATCTCAGT
ARG1 -469 F8	GCCCTTAAAGCTGTTTCTTCGAG
ARG1 -361 R8	ATGACTGGAGAGCCGTCAGTAGT
ARG1 -444 F9	TTTTCACTGCAGTAATTCTCCACAT
ARG1 -326 R9	CCAAATGCGACATGAGTCACTAA
ARG1 -410 F10	CACTGAGATAAGAGCGCTATGTTAGTC
ARG1 -297 R10	AATAGGTTGCGACAGCGGAA
ARG1 -383 F11	ACTACTGACGGCTCTCCAGTCAT
ARG1 -281 R11	CGGCACCGTTAATGGAAATAG
ARG1 -348 F12	TTAGTGACTCATGTCGCATTTGG
ARG1 -256 R12	CCTGCCTTTAAATGACTCTTCCATAC
ARG1 -312 F13	GCTGTCGCAACCTATTTCCATTA
ARG1 -211 R13	ACGCAGTCATCAATCTGATCCA
ARG1 -290 F14	AACGGTGCCGTATGGAAGAG
ARG1 -179 R14	TCGCAACTGCTCAGATTACACTATCT
ARG1 -231 F15	GGATCAGATTGATGACTGCGTA
ARG1 -141 R15	CCCATTAATATACTATTGAGACAGTGC
ARG1 -207 F16	GGCAGATAGTGTAATCTGAGCAGTTG
ARG1 -114 R16	GCAAGAACAAGGGAGTACGAATGT
ARG1 -170 F17	CTGGCACTGTCTCAATAGTATATTAATGG
ARG1 -76 R17	AGACAAGATACAAGAAGTAAAGAGAGAGAGAA
ARG1 -142 F18	GGCATACATTCGTACTCCCTTGT
ARG1 -51 R18	TGTTCCTTATCGCTGCACAATG
ARG1 -109 F19	AGTTCTCTCTCTCTTTACTTCTTGTATCTTGTC
ARG1 -15 R19	TGTGTATTTCTTTTGTATCCGTGTATATTAGA
ARG1 -43 F20	GCAGCGATAAGGAACATTGTTCTA
ARG1 +20 R20	CAAACTTTTCCCTTAGACATTATTTTATGC
ARG1 -35 F21	CGGATACAAAAGAAATACACATAATTGC
ARG1 +60 R21	CAAAATGACGGAGGTATCTAAACCA
ARG1 -10 F22	TGCATAAAATAATGTCTAAGGGAAAAGTT
ARG1 +79 R22	CTTGGTCTAGTAGCCAAGCCAAA
ARG1 +21 F23	TTTGGCTTATTCTGGTGGTTTAGAT
ARG1 +111 R23	TACATTAGCCATGAAAGCTACAACTTC
ARG1 +33 F24	TGGTGGTTTAGATACCTCCGTCAT
ARG1 +137 R24	GCGGCATCGAAATCTTCTTCT

Table 6—Contd. Nucleosome mapping primers	
ARG1 +84 F25	CGAAGTTGTAGCTTTCATGGCTAAT
ARG1 +170 R25	TTGCAGGCACCGATCTTCA
ARG1 +102 F26	GGCTAATGTAGGGCAAGAAGAAGAT
ARG1 +197 R26	TCTTCACGACAATCCACACAAAC
ARG1 +153 F27	GAAGATCGGTGCCTGCAAGT
ARG1 +235 R27	TGACCTGTACAGCTGGGAATAGAAT
ARG1 +175 F28	GTTTGTGTGGATTGTCGTGAAGA
ARG1 +269 R28	GTACCCAACAGATAAACGTCTTCGT
AGR1 +190 F29	CGTGAAGATTTTGTCAAGGATATTCTATT
ARG1 +291 R29	AATAACAGGTCTTGCCAAAGAGGTA
ARG1 +213 F30	TCTATTCCCAGCTGTACAGGTCAA
ARG1 +312 R30	GACGTCAATTTGGGCTTTGG
ARG1 +234 F31	GTACGAAGACGTTTATCTGTTGGGTA
ARG1 +349 R31	AACCATGAGAGACCGCGAAA
ARG1 +279 F32	AAGACCTGTTATTGCCAAAGCC
ARG1 +383 R32	TCGAATCTGATTTGATCATTACCTTT
ARG1 +325 F33	GGCTGTTTCGCGGTCTCTC
ARG1 +426 R33	TGTAATACACTTAACGTCTGGCTTCA
ARG1 +341 F34	CTCATGGTTGTACCGGTAAAGGTAA
ARG1 +444 R34	TTCAGGCATTCTCCATGGTGTA
ARG1 +381 F35	CGAATTGTCATTTTACGCTCTGAA
ARG1 +471 R35	CTTTCTGCCAGCAAATCTTTCG
ARG1 +411 F36	CGTTAAGTGTATTACACCATGGAGAATG
ARG1 +506 R36	GGAATACCCTTTTGTGCAGCATAG
HIS4 -757 F1	TGTCGTAAGCCAACTACACGA
HIS4 -679 R1	TCAGGAGTTCGACATCTTCG
HIS4 -707 F2	TTTCTCATAATCAACCCACTGGT
HIS4 -618 R2	CAAATTGGTCTTCTATGTTGCGTA
HIS4 -679 F3	CGAAGATGTCGAACTCCTGA
HIS4 -586 R3	GCGTTCTTTAGCCCACTTTG
HIS4 -640 F4	ACGCAACATAGAAGACCAATTT
HIS4 -550 R4	TTTACTGAGCGAATCGTTATGC
HIS4 -598 F5	GGCTAAAGAACGCGAACAAT
HIS4 -493 R5	CGATGAGGAATCTTGTGGTTT
HIS4 -557 F6	TCAGTAAAGAATACCAAAATTTGAGC
HIS4 -470 R6	TCAGTAAAGAATACCAAAATTTGAGC
HIS4 -509 F7	CACAAGATTCCTCATCGGAAG
HIS4 -412 R7	TGTTTGTGCTTGAGCCTGTT
HIS4 -469 F8	AAAACTTGAAGAGGCTAATGAAAAA
HIS4 -385 R8	GTCGAAAATTGGCAACGATT
HIS4 -419 F9	CACAAACAGCCGTGGAATC
HIS4 -328 R9	ATCGCAATGCTCACACCACT
HIS4 -381 F10	CCTGCACCAGTCGATACCAC
HIS4 -297 R10	GGGGGCATTCTGCTGTATTA
HIS4 -342 F11	TGTGAGCATTGCGATACGAT
HIS4 -257 R11	TCGACTGCCTAGAAGAACTGC
HIS4 -299 F12	CCCATCACAATCCTGACAAC
HIS4 -196 R12	TCACTGTGCATGGGTTTAGC
HIS4 -257 F13	AACTGACTCTAATAGTGACTCCGGTAA
HIS4 -161 R13	CCTTCTATATCGAATGACTGATAAAA
HIS4 -205 F14	TGCACAGTGACTCACGTTTTT
HIS4 -88 R14	CGGAGGTGAATATAACGTTCC
HIS4 -176 F15	CATTCGATATAGAAGGTAAGAAAAGGA
HIS4 -78 R15	CAACACACATCGGAGGTGAA

Table 6—Contd. Nucleosome mapping primers	
HIS4 -96 F16	TCACCTCCGATGTGTGTTGT
HIS4+23 R16	GGTAGAATCGGCAAAACCATT
HIS4 -56 F17	GCACAACTGCGCTGTGTAAT
HIS4 +44 R17	CATGAGGCCAGATCATCAAT
HIS4 -6 F18	CTGAATAATGGTTTTGCCGATT
HIS4 +83 R18	ACCTGACCAACAAGTGAAACG
HIS4 +31 F19	GATCTGGCCTCATGGAATAG
HIS4 +140 R19	TCCTCTTTGGAGAACTGGAGA
HIS4 +71 F20	TTGTTGGTCAGGTACTTTTGGA
HIS4 +162 R20	CAAAGCCACCAATGGAACTT
HIS4 +120 F21	TCTCCAGTTCTCCAAAGAGGA
HIS4 +218 R21	CCGTTGTTCAAGAAGGCAAT
HIS4 +158 F22	CTTTGTCCTTGCCAAGTGGT
HIS4 +266 R22	TGTTCGGCTGTTTTAGCATC
HIS4 +202 F23	GCCTTCTTGAACAACGGAGT
HIS4 +299 R23	CGCTCCTTTGGTACATTCAA
HIS4 +246 F24	AGATGCTAAAACAGCCGAACA
HIS4 +335 R24	TGATTGGAGAAAACACCGTTC
HIS4 +285 F25	TGTACCAAAGGAGCGTGTTG
HIS4 +375 R25	CACAATTTTATCTTGCGAGAATTT
HIS4 +328 F26	TCCAATCAATTCATGGTAAAACA
HIS4 +422 R26	CCAAGCACTTCTTTGGTCAAC
HIS4 +390 F27	AAGCAAGGATATGTTGACCAAAG
HIS4 +476 R27	TGGTCGACAACTAGGGTGGT
HIS4 +444 F28	TGACGGTTTATATACCACCCTAGTT
HIS4 +536 R28	TCGATGGCCTTTGCTATAGATT
ADH3 -183 F1	CTTTTCGCCAGCTCCTAAAC
ADH3 -92 R1	GATAAAGCGAGTGTTCCTTTCTAA
ADH3 -143 F2	CGTCTTATAAAATTAAACAAACCCTTT
ADH3 -68 R2	CATGTATAGTAAATTCGGTCGAAGA
ADH3 -99 F3	CTTTATCTCTTCGACCGAATTTAC
ADH3 -24 R3	TATTCCTAGTTTTAACTGTGAACAGAA
ADH3 +16 F4	ACATTGTTCACCAGGCGTGT
ADH3 +94 R4	TAGGGATTGCAGCTGTGGAT
ADH3 +31 F5	CGTGTCCAACCAAGCCTATT
ADH3 +113 R5	ATGACACCTTTTTGAGTCTTAGGG
ADH3 +72 F6	GCAATCCACAGCTGCAATC
ADH3 +146 R6	TTGTAATGCAGCTTCCCCTTA
ADH3 +91 F7	CCTAAGACTCAAAAAGGTGTCATC
ADH3 +165 R7	CTCGGGGACAGGGATATCTT
ADH3 +121 F8	GAGAATAAGGGGAAGCTGCAT
ADH3 +195 R8	AACGTTGATTAAAATTTCATTTGG
ADH3 +154 F9	CCTGTCCCCGAGCCTAAG
ADH3 +233 R9	CAAGCATGTAAATCGGTGTGA
ADH3 +162 F10	CGAGCCTAAGCCAAATGAAA
ADH3 +260 R10	TTAACAGGTAATGGCCAATCG

resuspended with Yeast Lysis Buffer to create 50% bead slurry. 35 µl bead slurry was added to each pull-down and rotated at 4°C for 3 hours. Beads were pelleted by spinning at 700 g at 4°C for minute and supernatant removed. Beads were washed by adding 1 ml YLB, rotated for 5 minutes at 4°C, spun at 700 g, and supernatant removed. Washing was repeated for a total of 3 washes. Following final wash all YLB was removed using a 27 gauge needle. Protein was eluted from beads by adding 100 µl 2x Laemmli Buffer and boiling. Protein elutions were then used for western blotting as described above.

CHAPTER III

CDC34- and CDC4-DEPENDENT TRANSCRIPTION OF GCN4 TARGET GENES

Introduction

Multiple transcriptional activators, including Gcn4, require components of the UPS that target them for degradation in order to activate transcription (Lipford et al., 2005). A mechanistic understanding as to why the UPS is required for the function of these transcriptional activators remains to be determined. Although a model has emerged from our lab that reconciles the published data, the model has yet to be challenged. In this model referred to as the “Spent/Stuck” model, a transcriptional activator transitions from an active to an inactive (“spent”) state after stimulating the first rounds of transcription (Figure 3). Once inactivated, the transcriptional activator remains bound (“stuck”) to promoters, thereby inhibiting recruitment of fresh, active, transcriptional activators. As a result of the activator remaining bound, the UPS functions to ubiquitylate and degrade the activator to clear the promoter for subsequent rounds of transcription.

A fundamental prediction based on this model is that the E2 and E3 enzymes and the proteasome function at the same step in transcription. Using the budding yeast transcriptional activator Gcn4, I sought to challenge this prediction, and thus the model. I chose this prototypical transcriptional activator for several reasons: (i) Gcn4 has an overlapping activation domain and degron (ii) Gcn4 has a well-characterized degradation pathway in which the E2 enzyme Cdc34 and the E3 enzyme SCF^{Cdc4} ubiquitylate Gcn4 (Figure 2B) (Chi et al., 2001; Kornitzer et al., 1994; Meimoun et al., 2000), (iii) Gcn4 is published to require Cdc34, SCF^{Cdc4}, and the proteasome for transcription of representative Gcn4 target genes (Lipford et al., 2005), and (iv) the use of budding yeast as a model system allows for straight-forward genetic manipulations and experimentation.

In the studies presented in this chapter, I first looked at the roles of the E2 and E3 enzymes that target Gcn4 in transcription of Gcn4 target genes. Gcn4 target gene transcript levels decreased following inhibition of the E2 enzyme Cdc34, the Skp1 subunit of the SCF complex, and the F-box protein Cdc4 of the SCF^{Cdc4} complex through the use of corresponding conditional alleles. I also demonstrated that excluding Cdc34 from the nucleus decreased Gcn4 target gene transcript levels. Lastly, these studies demonstrated that Gcn4 remained localized at chromatin during Cdc4 disruption. In sum, these data are congruent with the "Spent/Stuck" model as representative Gcn4 target gene transcript levels decreased and Gcn4 remained bound to chromatin when disrupting ubiquitylation.

Results

Effects of Cdc34 and Cdc4 disruption on Gcn4 ubiquitylation and ARG1 *transcript levels*

Ubiquitylation of Gcn4 occurs via the E2 enzyme Cdc34 and the E3 enzyme SCF^{Cdc4} (Kornitzer et al., 1994; Meimoun et al., 2000). As these genes are essential for cell viability in budding yeast, experimentation required conditional disruption of these proteins. In my studies I utilized the temperature sensitive alleles *cdc34-2* and *cdc4-1* (Patton et al., 1998), both of which have been used in previous Gcn4 studies (Chi et al., 2001; Lipford et al., 2005; Meimoun et al., 2000). Strains containing either *cdc34-2* (Figure 4) or *cdc4-1* (Figure 5) exhibited a growth defect at the restrictive temperature 37°C, but not at the permissive temperature 25°C, when compared to congenic wild-type strains. Both *cdc34-2* and *cdc4-1* strains also exhibited a slight growth defect at the semi-permissive temperature 30°C. I disrupted Cdc34 or Cdc4 in subsequent experiments by shifting wild-type and *cdc34-2* or *cdc4-1* strains to the non-permissive temperature 37°C in order to replicate the experimental conditions in the study by the Deshaies laboratory.

To determine the effect of either Cdc34 or Cdc4 disruption on Gcn4 ubiquitylation in my experimental conditions, I performed an *in vivo* ubiquitylation assay to visualize ubiquitylated species of Gcn4. To do this, I expressed His-Myc-Ub in wild-type and *cdc34-2* (Figure 6) or *cdc4-1* (Figure 7) strains at 37°C and induced Gcn4 synthesis via treatment with sulfometuron

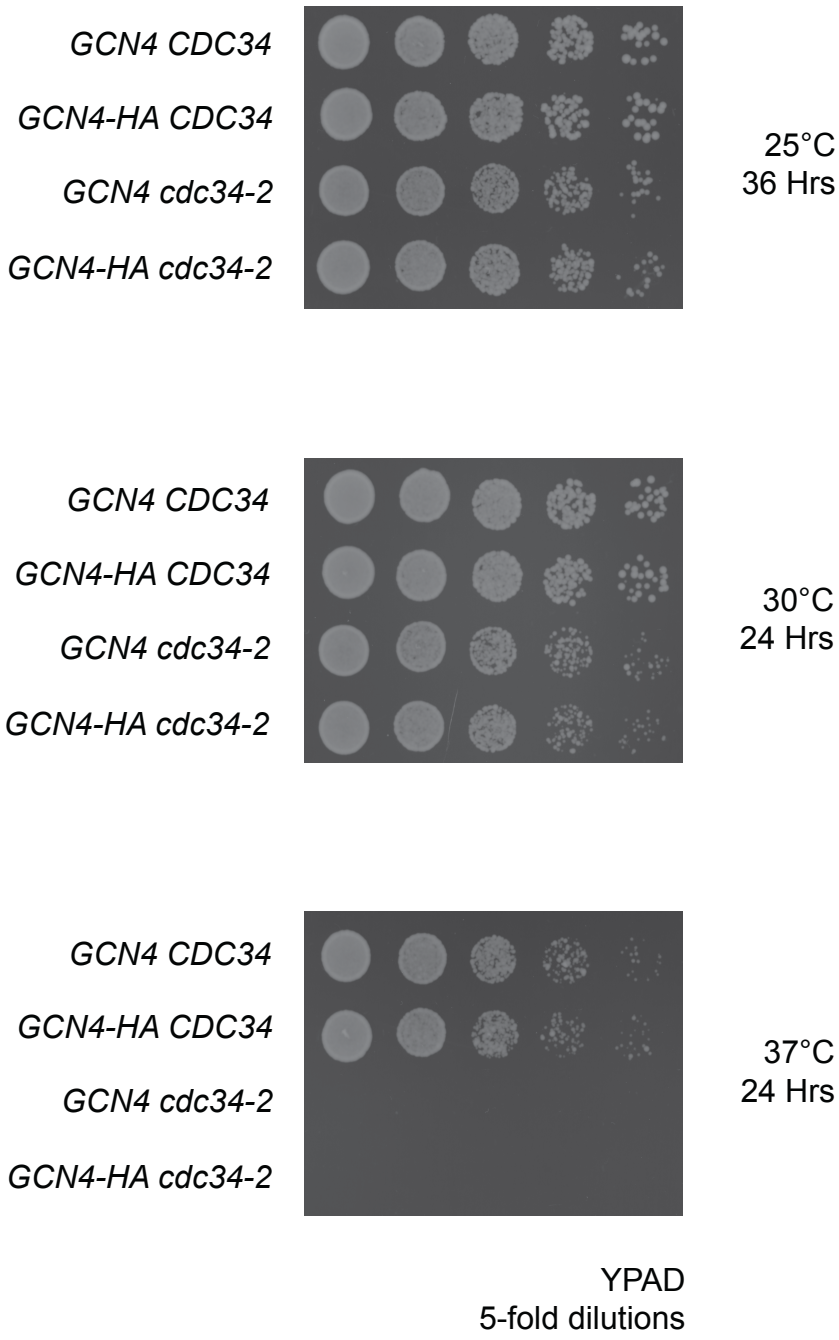

Figure 4. *cdc34-2* confers a growth defect at 37°C. *GCN4 CDC34* (W303-1a), *GCN4-HA CDC34* (GHY106), *GCN4 cdc34-2* (MT670), and *GCN4-HA cdc34-2* (GHY109) yeast were spotted on YPAD agar plates at 5-fold dilution per spot and grown at the indicated temperatures for the indicated time before imaging.

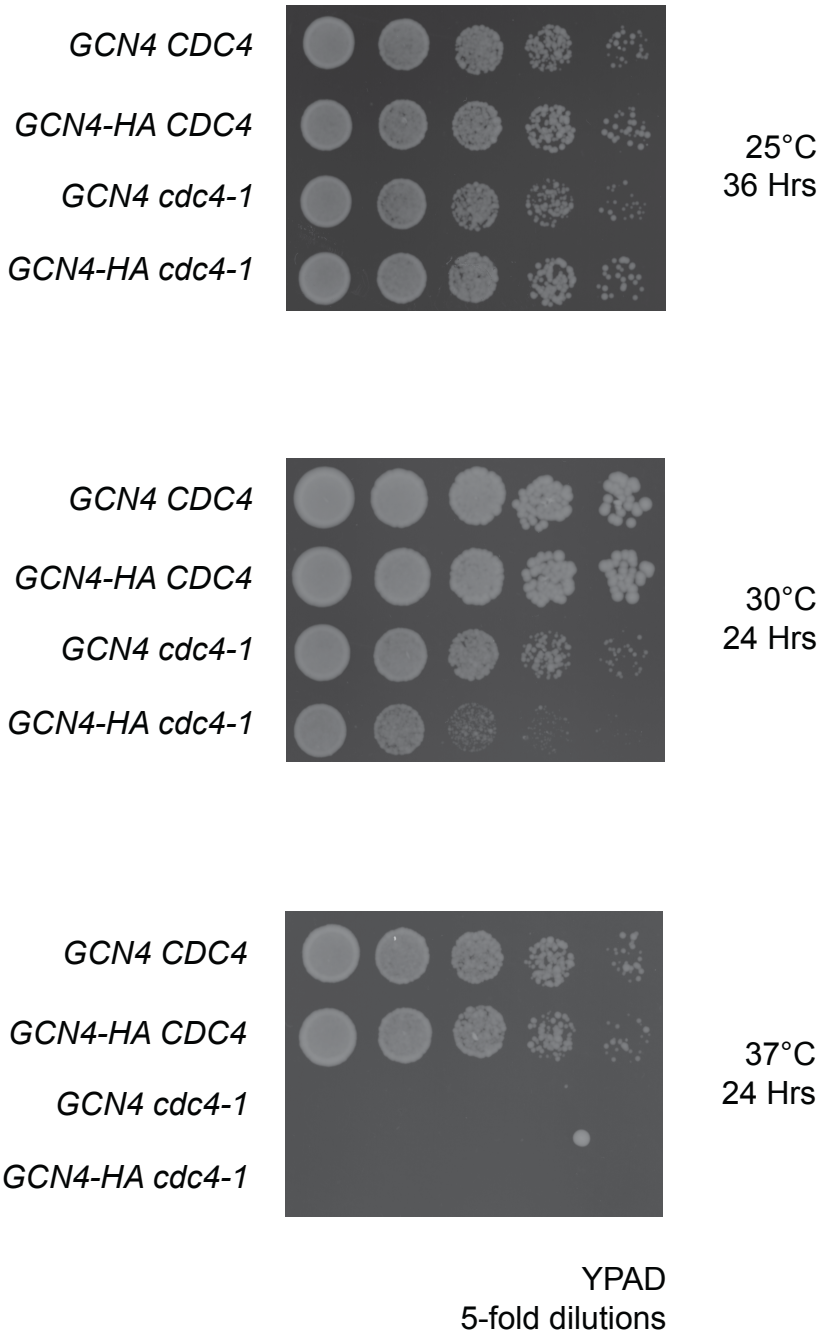

Figure 5. *cdc4-1* confers a growth defect at 37°C. *GCN4 CDC4* (W303-1a), *GCN4-HA CDC4* (GHY106), *GCN4 cdc4-1* (MT668), and *GCN4-HA cdc4-1* (GHY107) yeast were spotted on YPAD agar plates at 5-fold dilution per spot and grown at the indicated temperatures for the indicated time before imaging.

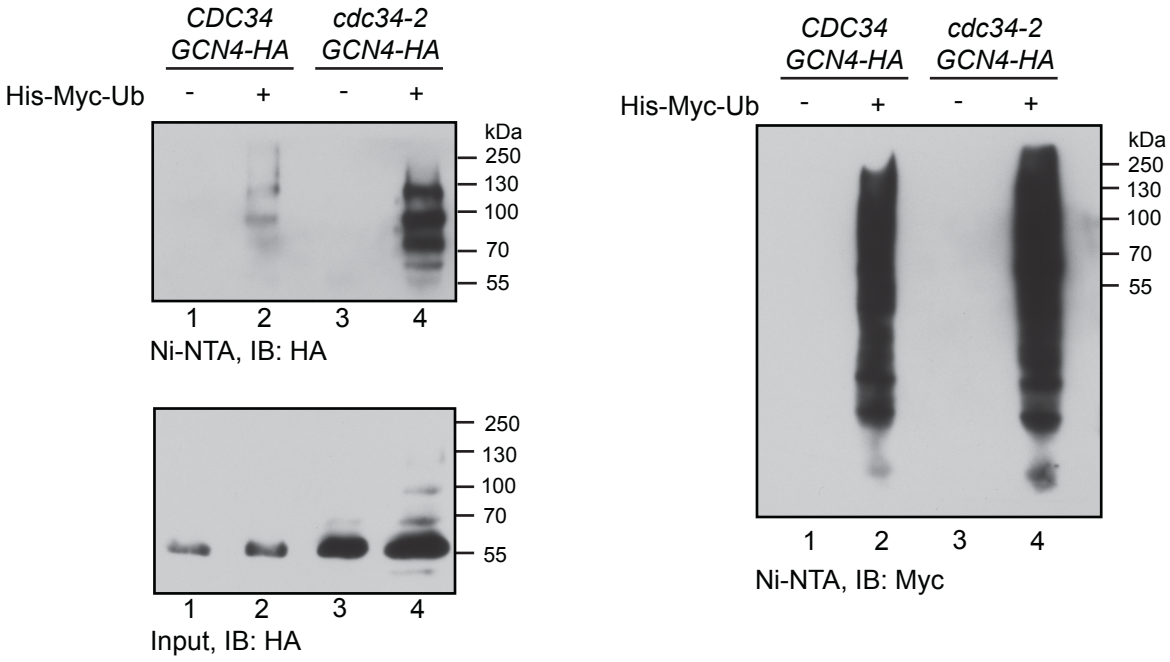

Figure 6. *cdc34-2* confers a decrease in high-molecular weight species of Ub-Gcn4 conjugates. *CDC34 GCN4-HA* (GHY243) and *cdc34-2 GCN4-HA* (GHY245) yeast carrying an empty vector and *CDC34 GCN4-HA* (GHY244) and *cdc34-2 GCN4-HA* (GHY246) yeast carrying a copper-inducible His-Ub expression plasmid (pUB221) were grown to log phase in minimal media and treated with CuSO4 and either DMSO or MG132 for one hour. Yeast were induced with SM, or DMSO, for an additional 1.5 hours, at which time protein lysates were collected under denaturing conditions. Ubiquitin-conjugates were captured by nickel-resin (Ni-NTA) chromatography, resolved by SDS-PAGE, and probed for HA-tagged Gcn4 protein by western blotting. A sample of the input material to the nickel resin was also probed for HA-tagged Gcn4. IB, immunoblot.

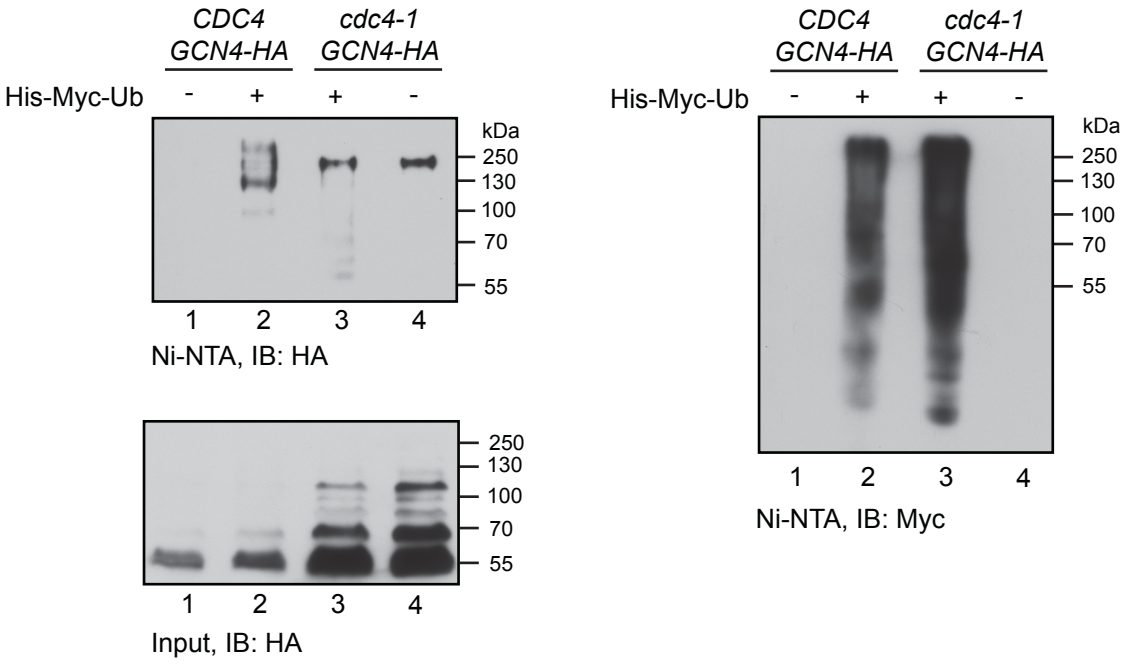

Figure 7. *cdc4-1* confers a decrease in Ub-Gcn4 conjugates. *CDC4 GCN4-HA* (GHY243) and *cdc4-1 GCN4-HA* (GHY109) yeast carrying an empty vector and *CDC4 GCN4-HA* (GHY106) and *cdc4-1 GCN4-HA* (GHY109) yeast carrying a copper-inducible His-Ub expression plasmid (pUB221) were grown to log phase in minimal media and treated with CuSO4 and either DMSO or MG132 for one hour. Yeast were induced with SM, or DMSO, for an additional 1.5 hours, at which time protein lysates were collected under denaturing conditions. Ubiquitin-conjugates were captured by nickel-resin (Ni-NTA) chromatography, resolved by SDS-PAGE, and probed for HA-tagged Gcn4 protein by western blotting. A sample of the input material to the nickel resin was also probed for HA-tagged Gcn4. IB, immunoblot.

methyl (SM), an inhibitor of branched amino acid synthesis (Falco and Dumas, 1985). I then isolated protein under denaturing conditions to preserve ubiquitin modifications, precipitated ubiquitylated proteins using nickel-affinity chromatography, and western blotted for Gcn4 in the precipitated material. In both the *cdc34-2* strain (Figure 6, Compare lanes 2 and 3) and *cdc4-1* strain (Figure 7, Compare lanes 2 and 4), ubiquitylated Gcn4 accumulated at a lower molecular weight than in congenic wild-type strains, indicative of a reduction in ubiquitylation. In agreement with a reduction of Gcn4 ubiquitylation, steady state Gcn4 levels were higher in *cdc4-1* and *cdc34-2* strains than in corresponding wild-type strains as demonstrated by western blotting of the input material. Interestingly, the amount of Gcn4 precipitated from the *cdc34-2* strain was much higher than from the *CDC34* strain, despite a decrease in high-molecular weight ubiquitin-Gcn4 conjugates (Figure 6, Lane 4). These experiments demonstrate that disruption of either the E2 enzyme Cdc34 or the F-box protein Cdc4 decreases—but does not block—Gcn4 ubiquitylation.

After confirming that Gcn4 ubiquitylation in *cdc34-2* and *cdc4-1* strains had reduced levels of ubiquitylation at 37°C, I asked whether Cdc34 and Cdc4 were required for transcription of the representative Gcn4 target gene *ARG1*. Work by Lipford *et al.* concludes that transcription of *ARG1* requires the ubiquitylation machinery (Lipford et al., 2005). However, these experiments were performed semi-quantitatively using reverse transcription coupled with ethidium bromide staining of PCR products. To quantitatively determine the effects on *ARG1* transcript levels, I performed reverse transcription coupled with quantitative PCR (RT-qPCR) to determine *ARG1* transcript levels following disruption of either Cdc34 (Figure 8A) or Cdc4 (Figure 8B). In both *CDC34* and *cdc34-2* strains at 30°C, *ARG1* transcript levels increased robustly in response to Gcn4 induction (SM) compared to uninduced controls (DMSO). At the non-permissive temperature 37°C, *ARG1* transcript levels in the *cdc34-2* strain were one-third that of transcript levels in the *CDC34* strain following Gcn4 induction (SM). In the case of *cdc4-1*, *ARG1* transcript levels were reduced by about one-third when compared to the *CDC4* strain at the non-permissive temperature 37°C. These data confirm that full response of *ARG1* transcript levels to Gcn4 induction requires functional Cdc34 and Cdc4. In addition, these results recapitulate the trend that

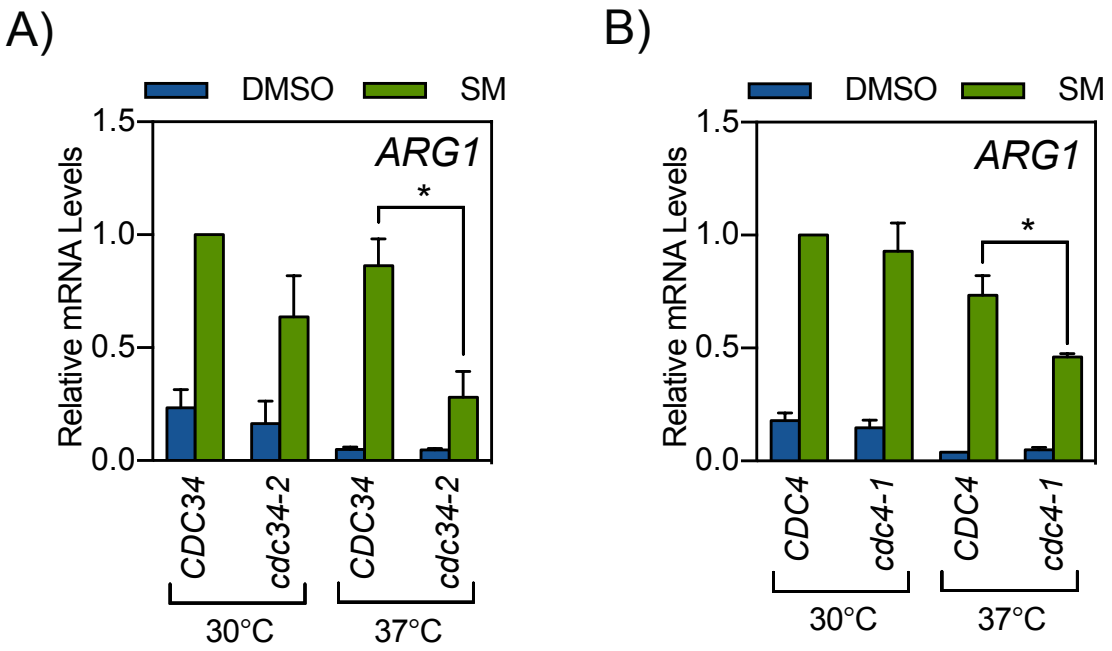

Figure 8. *ARG1* transcript levels decrease following disruption of Cdc34 and Cdc4. (A) *CDC34* (W303-1a) and *cdc34-2* (MT670) yeast were grown to log phase at 30°C in minimal media and then shifted to 37°C—or maintained at 30°C—for one hour as indicated. Strains were then treated with SM, or DMSO, for 1.5 hours, at which time RNA was collected and *ARG1* mRNA levels quantified by RT-qPCR. Relative mRNA levels for *ARG1* were normalized to the *CDC34* strain treated with SM at 30°C. n=3. (B) As in (A), except using *CDC4* (W303-1a) and *cdc4-1* (MT668) strains. n=3. Error bars represent SEM. (* significant at $p<0.05$)

ARG1 transcript levels are more sensitive to Cdc34 disruption than Cdc4 disruption, as was reported by Lipford *et al.* (Lipford et al., 2005).

Effects of Cdc34 nuclear exclusion on Gcn4 target gene transcript levels

To independently confirm the involvement of Cdc34 and Cdc4 in Gcn4 target gene transcription, I utilized the Anchor Away (AA) technique to conditionally deplete the nucleus of these proteins under the assumption that this would disrupt interaction with nuclear localized Gcn4 (Haruki et al., 2008). Briefly, the AA technique enables conditional export of a nuclear protein tagged with the FKBP-rapamycin binding (FRB) domain in a yeast strain containing the FKBP12-tagged ribosomal protein RPL13A (Figure 9A). Upon treatment with rapamycin (RAP), a tertiary complex forms between the FRB domain, rapamycin, and FKBP12. As RPL13A exits the nucleus for ribosomal assembly, the FRB-tagged target protein also exports due to this tertiary complex.

As growth in rich media requires nuclear Cdc34, Cdc4, and TBP, I performed spotting assays with AA strains targeting either Cdc34, Cdc4, TBP, or Gcn4 on media containing either DMSO or RAP (Figure 9B) to assay for a growth defect during RAP treatment (Blondel et al., 2000; Goebl et al., 1994). AA strains containing either Cdc34-FRB or TBP-FRB exhibited a growth defect as expected when either of these proteins are absent from the nucleus. However, an AA strain containing Cdc4-FRB did not exhibit a growth defect in the presence of RAP. Although genomic integration of the FRB-tagging cassette at the *CDC4* locus was verified by PCR, it remains to be determined as to whether the lack of a growth phenotype was due to Cdc4 nuclear localization being non-essential or a lack of expression of the FRB domain perhaps through an introduced mutation in the FRB coding sequence. As the AA *CDC4-FRB* strain did not exhibit the expected phenotype and nuclear exclusion was not validated, the AA *CDC4-FRB* strains was not used in my experiments.

Unsurprisingly, AA *GCN4-FRB* did not exhibit a growth defect during RAP treatment as *GCN4* is not required for growth in nutrient replete conditions. To determine the effects of RAP treatment in the AA *GCN4-FRB* strain, I performed a spotting assay with AA strains containing either Gcn4-FRB or TBP-FRB on plates containing SM to starve yeast of branched amino acids and create an

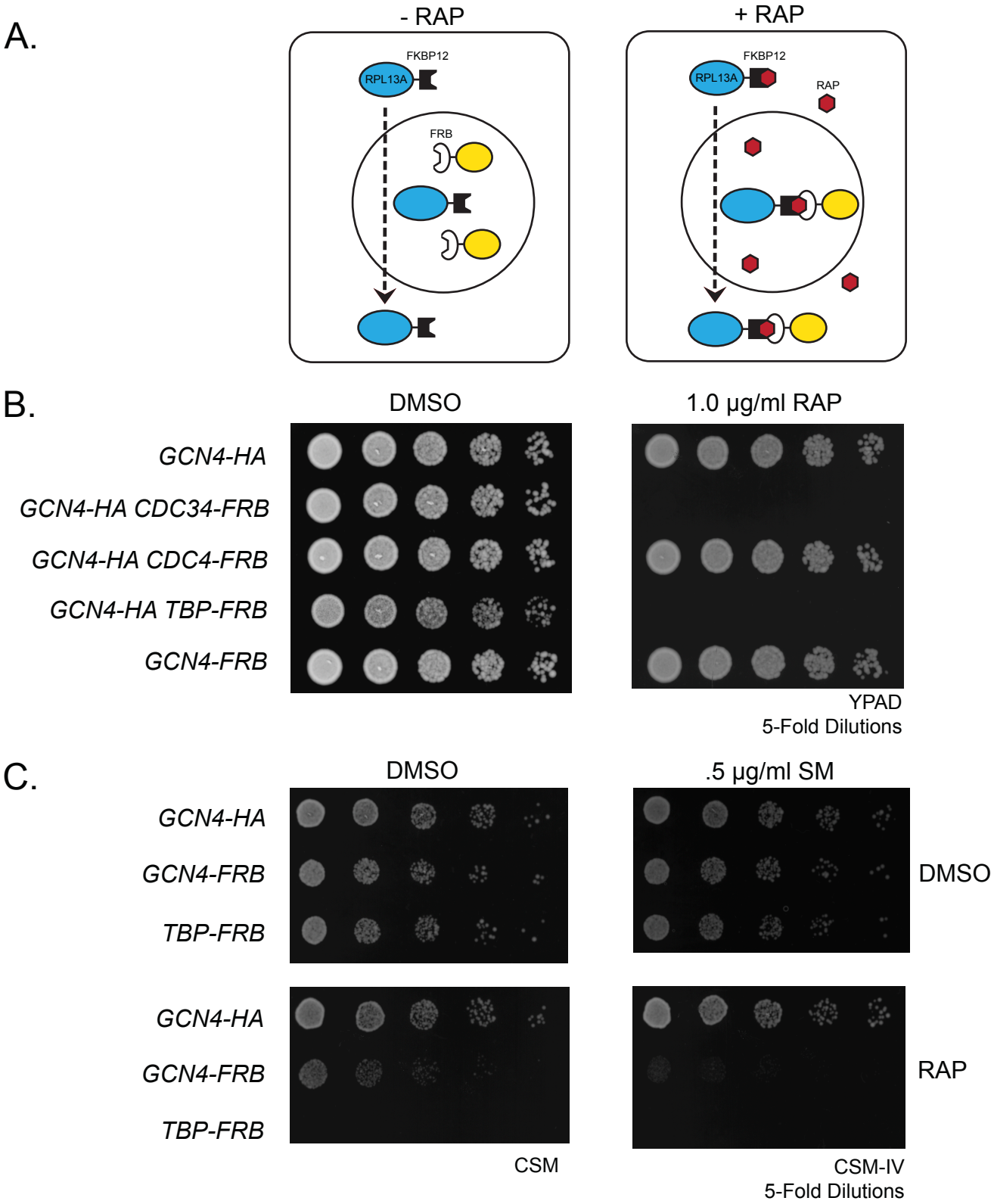

Figure 9. Nuclear exclusion of Cdc34, TBP, or Gcn4 confers a growth defect. (A) In the presence of rapamycin (+RAP), a tertiary complex forms containing the FRB domain fused to a target protein, rapamycin (RAP), and the FKBP12 domain fused to the ribosomal RPL13A protein. As the RPL13A protein exits the nucleus during ribosome assembly, so too does the target protein containing the FRB domain. (B) AA *GCN4-HA* (GHY139), AA *GCN4-HA CDC34-FRB* (GHY149), AA *CDC4-FRB* (GHY151), AA *GCN4-HA TBP-FRB* (GHY147), and AA *GCN4-FRB* (GHY145) yeast were spotting on YPAD agar plates containing either DMSO or 1.0 µg/mL rapamycin at 5-fold dilution per spot and grown at 30°C. (C) AA *GCN4-HA* (GHY139), AA *GCN4-FRB* (GHY145), and AA *TBP-FRB* (GHY147) yeast were spotted on CSM agar with DMSO and CSM-IV with 0.5 µg/mL SM in either the presence or absence of rapamycin (RAP) at 5-fold dilution per spot and grown at 30°C.

environment in which Gcn4 is required for growth (Zhang et al., 2008) (Figure 9C). In the presence of SM and RAP, the AA *GCN4-FRB* strain exhibited a growth defect. In sum, the growth defects observed for AA *CDC34-FRB* and AA *GCN4-FRB* strains during RAP treatment are commensurate with a phenotype expected during nuclear exclusion of either Cdc34 or Gcn4.

To determine the effects of Cdc34 nuclear exclusion on Gcn4 target gene transcript levels, I performed RT-qPCR to assay transcript levels of representative Gcn4 target genes in the AA *CDC34-FRB* strain (Figure 10A-D). In response to SM treatment, transcript levels of *ARG1* increased nearly fifty-fold whereas in the presence of RAP (SM, RAP), *ARG1* transcript levels increased to about half that achieved during SM treatment alone (SM). This decrease in *ARG1* transcript levels recapitulated the *ARG1* transcript levels observed during disruption of Cdc34 with the *cdc34-2* allele (Figure 8A). Additionally, *ARG1* transcript levels in the AA *GCN4-FRB* strain following RAP treatment were unresponsive to SM treatment (SM, RAP), validating the efficacy of RAP treatment in these experiments. I then expanded these RT-qPCR studies to determine the effects of targeting Cdc34 for nuclear exclusion on additional Gcn4 target genes: *ARG4* (Figure 10B), *CPA2* (Figure 10C), and *HIS4* (Figure 10D). Transcript levels of these three genes also decreased in response to SM and RAP treatment (SM, RAP) with *ARG4* transcript levels decreasing by about one-fourth and *CPA2* and *HIS4* transcript levels decreasing by about one-half of transcript levels compared to SM treatment alone (SM). These data support the notion that robust Gcn4 target gene transcription requires nuclear localized Cdc34 and Gcn4.

Effects of SCF subunit Skp1 disruption on ARG1 *transcript levels*

F-box proteins bind the SCF complex through contact with the Skp1 subunit (Figure 1B). Two temperature sensitive alleles, *skp1-11* (G160E and and R167K) and *skp1-12* (L8G), have been shown to disrupt interaction of F-box proteins with the SCF complex (Willems et al., 1996). The *skp1-11* allele preferentially disrupts activity of the SCF^{Cdc4} complex while the *skp1-12* allele preferentially disrupts activity of the SCF^{Grr1} complex (Patton et al., 1998). Therefore, I sought to determine whether Gcn4-mediated transcription was sensitive to Skp1 disruption using the *skp1-11* and *skp1-12* alleles. The strain containing the *skp1-11* allele exhibited no growth defect at 25°C or 30°C and growth arrest at 37°C (Figure 11). The strain containing the *skp1-12* allele

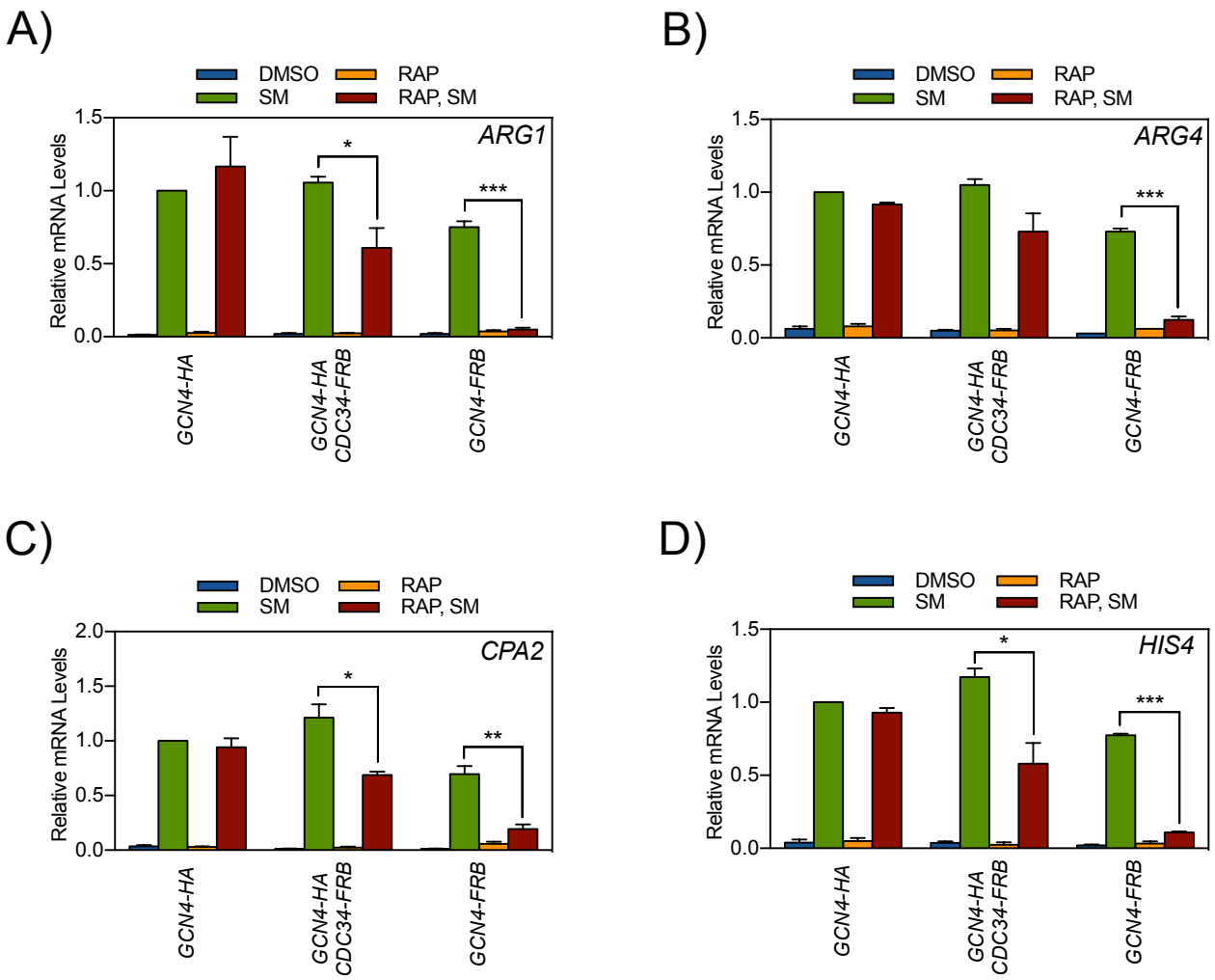

Figure 10. Gcn4 target gene transcript levels decrease in response to nuclear exclusion of Cdc34. Anchor Away strains expressing HA-tagged Gcn4 (GHY139), FKBP12-Rapamycin-binding domain (FRB)-tagged Cdc34 (GHY149) or FRB-tagged Gcn4 (GHY145), were grown to log phase in minimal media, treated with either DMSO or rapamycin for one hour, and then further treated with either DMSO or SM for 1.5 hours. RNA was collected, and *ARG1* (A), *ARG4* (B), *CPA2* (C), and *HIS4* (D) mRNA levels measured by RT-qPCR, as in A. Relative mRNA levels were normalized to the *GCN4-HA* strain treated with SM at 30°C. n=3. Error bars represent SEM. (* significant at $p<0.05$, ** significant at $p<0.01$, *** significant at $p<0.001$)

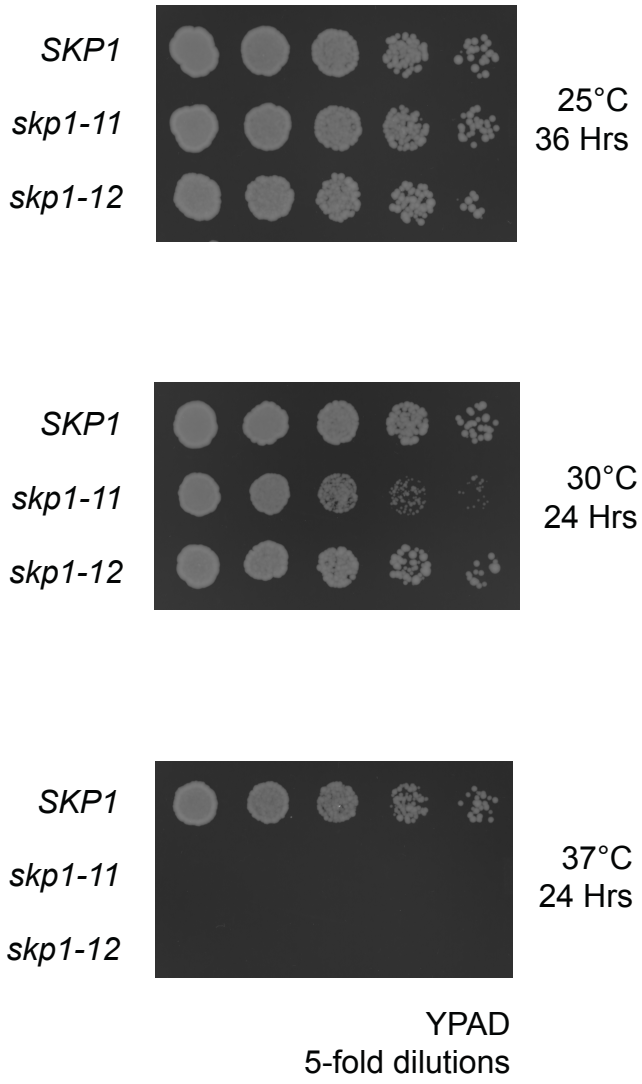

Figure 11. *skp1-11 and skp1-12* confer a growth defect at 37°C. *SKP1* (Y80), *skp1-11* (Y552), and *skp1-12* (Y554) yeast were spotted on YPAD agar plates at 5-fold dilution per spot and grown at the indicated temperatures for the indicated time before imaging.

exhibited no growth defect at 25°C, a small growth defect at 30°C, and growth arrest at 37°C (Figure 11). Using RT-qPCR, I determined that *ARG1* transcript levels following SM-treatment were reduced by about one-half in the *skp1-11* and *skp1-12* strains at the non-permissive temperature of 37°C when compared to the *SKP1* congenic strain (Figure 12). The Cdc4-specific allele *skp1-11* decreased *ARG1* transcripts to a statistically significant level while the *skp1-12* allele reproducibly reduced *ARG1* transcript levels, but not to a statistically significant level. These data provide further evidence that the SCF^{Cdc4} complex is required for Gcn4 target gene.

Effect of Cdc4 disruption on Gcn4 localization at chromatin

A central prediction based on the Spent/Stuck model is that the ubiquitylation machinery targeting Gcn4 is required for removal of Gcn4 from chromatin. Therefore, I hypothesized that disruption of the SCF^{Cdc4} complex would not disrupt Gcn4 localization on chromatin despite a reduction in target gene transcript levels. To test this notion, I utilized chromatin-immunoprecipitation (ChIP) to assay Gcn4 localization at the TATA-proximal Gcn4 UAS of *ARG1* in *CDC4* and *cdc4-1* strains induced for Gcn4 expression at the non-permissive temperature. I chose the *cdc4-1* allele to allow for greater specificity towards disrupting Gcn4 ubiquitylation as disruption of Cdc34 or Skp1 would also disrupt SCF complexes utilizing other F-box proteins. In the presence of the *cdc4-1* allele at the non-permissive temperature (37°C), Gcn4 levels at the UAS of *ARG1* was equivalent to levels detected in the congenic *CDC4* strain (Figure 13). These data support the Spent/Stuck model as Gcn4 remained bound to DNA during Cdc4 disruption despite a reduction in *ARG1* transcript levels.

Non-ubiquitylatable mutant of Gcn4

A caveat to studying Gcn4 ubiquitylation by disrupting the Cdc34 and Cdc4 is that disruption of the E2 and E3 will also affect other cellular processes involving these enzymes. Therefore, a decrease in transcript levels may be due to effects from disrupting these other processes instead of Gcn4 ubiquitylation. The best tool to study Gcn4 ubiquitylation while minimizing off-target effects is with a non-ubiquitylatable cis-mutant of Gcn4. To make this mutant, I generated K0-Gcn4 in which all 23 lysine residues of Gcn4 were mutated to arginine as ubiquitylation canonically targets lysine residues (Figure 2A). I verified that this mutant was not ubiquitylated

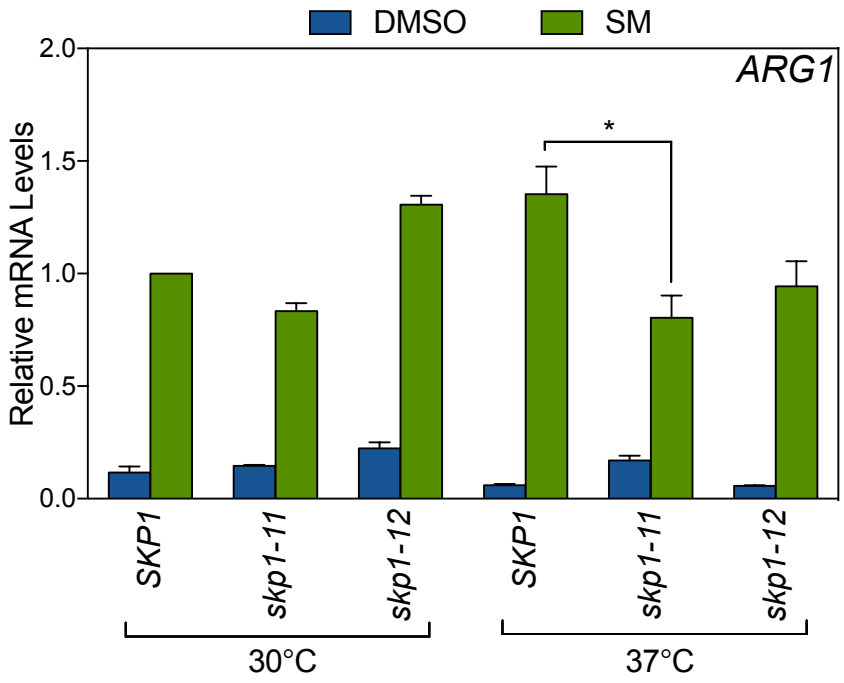

Figure 12. *ARG1* transcript levels decrease following disruption of Skp1. *SKP1* (Y80), *skp1-11* (Y552), and *skp1-12* (Y554) yeast were grown to log phase at 30°C in minimal media and then shifted to 37°C—or maintained at 30°C—for one hour as indicated. Strains were then treated with SM, or DMSO, for 1.5 hours, at which time RNA was collected and *ARG1* mRNA levels quantified by RT-qPCR. Relative mRNA levels for *ARG1* were normalized to the *SKP1* strain treated with SM at 30°C. n=3. Error bars represent SEM. (* significant at $p<0.05$)

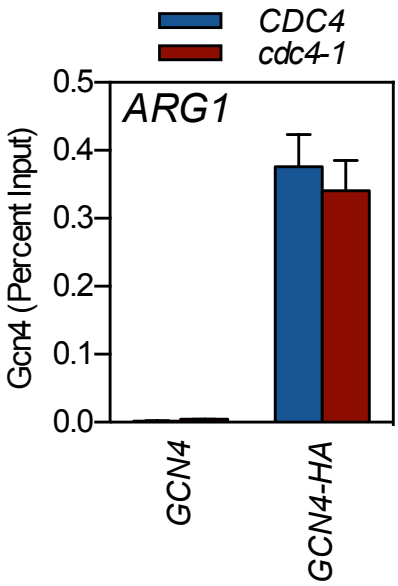

Figure 13. Levels of Gcn4 bound to the UAS of *ARG1* are unaffected following disruption of Cdc4. *CDC4 GCN4* (W303-1a), *CDC4 GCN4-HA* (GHY106), *cdc4-1 GCN4* (MT668), and *cdc4-1 GCN4-HA* (GHY107) strains were grown to log phase at 30°C in minimal media, shifted to the restrictive temperature of 37°C for one hour, and then induced with SM for an additional 1.5 hours. At this time, ChIP was performed with an antibody against the HA-epitope tag. Co-precipitating ARG1 promoter DNA was quantified by qPCR, expressed relative to the percentage of input DNA. n=3. Error bars represent SEM.

(Figure 14A) but found that K0-Gcn4 was detected at much lower levels at the UAS of *ARG1* compared to wild-type Gcn4 despite massive overexpression (Figure 14B). It is unknown whether the decrease in Gcn4 signal was due to a true decrease in Gcn4 levels at chromatin or whether mutation of the 23 lysine residues prevented efficient formaldehyde cross-linking during the ChIP protocol. Therefore, this mutant was not used in further RT-qPCR or ChIP experiments.

Discussion

If the Spent/Stuck model is correct, disruption of the ubiquitylation machinery targeting Gcn4 would result in a loss of target gene transcripts while levels of Gcn4 at target gene promoters would either increase or be unaffected. In this Chapter, I presented data in which representative Gcn4 target gene transcript levels decreased following disruption of Cdc34, Skp1, or Cdc4 using temperature sensitive alleles. I also demonstrated that targeting the Cdc34 enzyme using the anchor away technique resulted in decreased Gcn4 target gene transcript levels. Lastly, I showed that Gcn4 levels at *ARG1* were unaffected following Cdc4 disruption despite a decrease in *ARG1* transcript levels. In sum, these data are in agreement with the role of ubiquitylation proposed in the “Spent/Stuck” model.

Cdc34 or Cdc4 disruption on Gcn4 target gene transcript levels

Work from the Deshaies laboratory demonstrated that disruption of ubiquitylation via the *cdc34-2* and *cdc4-1* alleles resulted in a decrease in *ARG1* transcript levels when compared to a congenic wild-type control strain (Lipford et al., 2005). Their work also showed that *ARG1* transcript levels were lower in the *cdc34-2* strain than in the *cdc4-1* strain. Therefore, the work presented in this Chapter recapitulated the observations made by the Deshaies laboratory.

The observation that *ARG1* transcript levels were lower following disruption of Cdc34 than following disruption of Cdc4 is interesting. However, the difference between these two alleles in terms of their effect on *ARG1* transcript levels may be attributed to the efficiency in which the temperature sensitive alleles disrupt the proteins. In these experimental conditions, both Cdc34

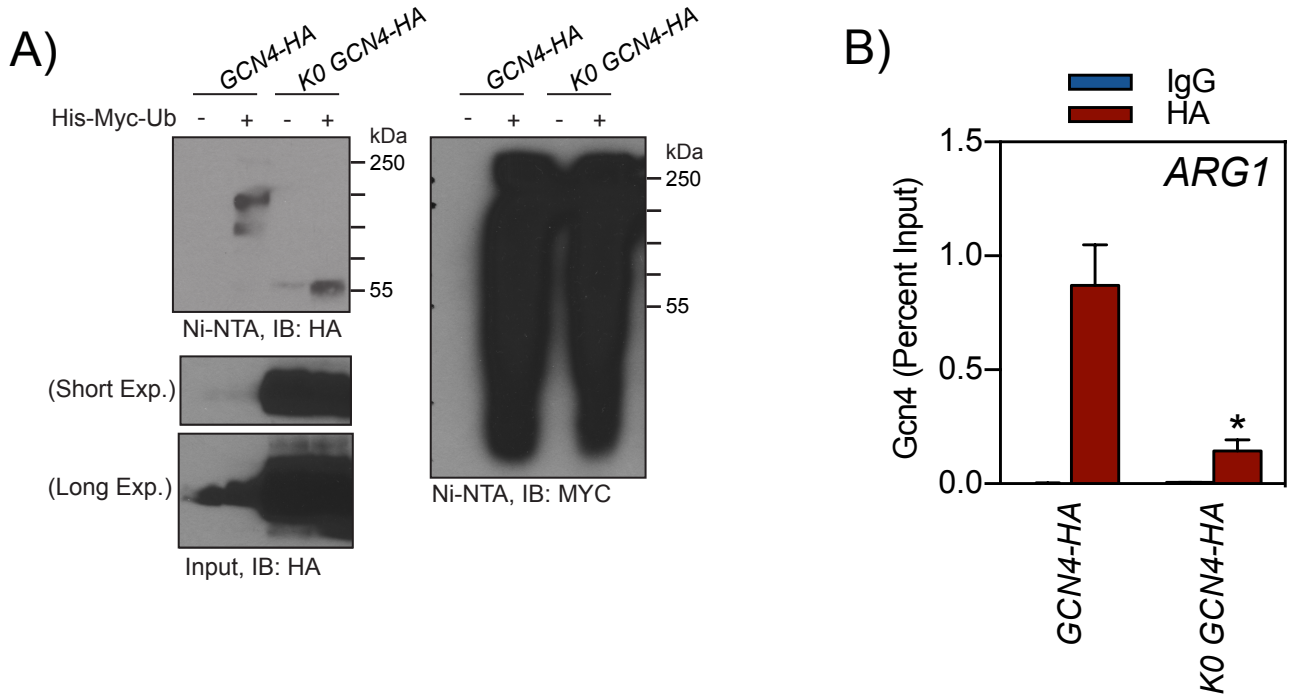

Figure 14. Lysine-free mutant K0 Gcn4 is detected at lower levels at the UAS of *ARG1* (A) *GCN4-HA* (GHY356) and *K0 GCN4-HA* (GHY052) yeast carrying either empty vector or a copper-inducible His-Myc-Ubiquitin expression plasmid (pUB221) were grown to log phase at 30°C in minimal media and treated with 0.5 mM $CuSO_4$ and 50 µM MG132 for one hour. Yeast were induced with 0.5 µg/ml SM for an additional 1.5 hours, at which time protein lysates were collected under denaturing conditions. Ubiquitin-conjugates were captured by nickel-resin (Ni-NTA) chromatography, resolved by SDS-PAGE, and probed for HA-tagged Gcn4 protein by western blotting. A sample of the input material to the nickel resin was also probed for HA-tagged Gcn4. IB, immunoblot. Ni-NTA pull-down material was also probed for total His-Myc-Ubiquitin. (B) *GCN4-HA* (GHY025) and *K0-GCN4-HA* (GHY052) yeast strains were grown to log phase at 30°C in minimal media and treated with either DMSO or MG132. After one hour, Gcn4 was induced with SM for 1.5 hours. At this time, ChIP was performed with either IgG or antibody against the HA epitope. Co-precipitating *ARG1* promoter DNA was quantified by qPCR, expressed relative to the percentage of input DNA. n=3. Error bars represent SEM. (* significant at $p<0.05$)

and Cdc4 retained some ubiquitylation activity as shown by the retention of ubiquitylated Gcn4 in both the *cdc34-2* and *cdc4-1* strains (Figures 6 and 7). An alternative explanation is that an SCF complex containing an F-box protein other than Cdc4, but still requiring Cdc34, may be required for transcription of *ARG1*. Therefore, the cdc34-2 allele would disrupt both SCF complexes. Supporting the role of an additional SCF complex for transcription is the data in which both the *skp1-11* and *skp1-12* alleles decreased *ARG1* transcript levels despite the specificity of the *skp1-11* allele towards SCF^{Cdc4} activity (Figure 12). Although not statistically significant, transcript levels in the *skp1-12* strain were consistently and reproducibly lower than in the congenic wild-type strain.

Effect of Cdc4 disruption on Gcn4 localization at chromatin

Following disruption of SCF^{Cdc4}, I did not observe changes in Gcn4 levels at the *ARG1* promoter. In the work reported by the Deshaies laboratory, Gcn4 detected on chromatin increased when compared to the congenic WT strain. However, the study from the Deshaies laboratory induced Gcn4 synthesis through leucine starvation while I utilized SM treatment. The difference between the observed results may be due to the strength of Gcn4 induction. Following SM treatment, Gcn4 binding sites may be saturated, thereby preventing an increase in signal.

The requirement for Gcn4 ubiquitylation to stimulate transcription is in agreement with what has been observed previously for other transcription factors such as Gal4, c-Myc, and LexA-VP16 (Kim et al., 2003; Muratani et al., 2005; Salghetti et al., 2001). How exactly a ubiquitin modification can be required for Gcn4 activity remains to be determined. The activation domains of many acidic transcriptional activators, including Gcn4, are inherently unstructured when unbound to binding partners (Brzovic et al., 2011). One hypothesis for the requirement of ubiquitin in stimulating transcription is that ubiquitin confers a structural conformation change or stabilization that facilitates interaction between a ubiquitylated activator and the transcriptional machinery. Future experiments to, at least in part, address this question could be ChIP experiments examining the recruitment of general transcription factors and coactivators following disruption of ubiquitylation. Alternatively, requisite ubiquitylation through Cdc34 and SCF^{Cdc4} may

target proteins other than Gcn4 such as histones, GTFs, or RNA polymerase II to facilitate transcription.

In this Chapter, I challenged central predictions based on the Spent/Stuck model of transcriptional activation through disruption of the E2 enzyme Cdc34 and the E3 enzyme SCF^{Cdc4} and determined the effects on transcript levels of Gcn4 target genes and Gcn4 levels on chromatin. In the next Chapter, I will further challenge the Spent/Stuck model by exploring the effects of proteasome inhibition.

CHAPTER IV

PROTEASOME-DEPENDENT TRANSCRIPTION OF GCN4 TARGET GENES

Introduction

The Spent/Stuck model proposes that ubiquitylation and proteolysis are required to clear promoters of bound, inactive, transcriptional activators in order to allow binding of active transcriptional activators for subsequent rounds of transcription. A central prediction based on this model is that ubiquitylation and proteolysis both function at the same step for transcription. Therefore, if the Spent/Stuck model is correct, proteasome inhibition would also result in a defect in target gene transcript levels while Gcn4 levels would be unaffected at promoters. In this Chapter, I present work probing the role of the proteasome in transcription of Gcn4 target genes.

The proteasome consists of two sub-complexes: the 19S regulatory particle and the 20S core. Hydrolysis of polypeptides occurs within the 20S core which contains three types of catalytic sites corresponding to three subunits: a tryptic site contained in the Pup1 subunit, a chymotryptic site contained in the Pre2 subunit, and a caspase-like site contained in the Pre3 subunit. Much emphasis has been placed on chymotryptic site inhibitors as this site is thought to account for the majority of protein degradation by the proteasome. Supporting the importance of the chymotryptic site for cellular processes, inhibition of the chymotryptic site in mammalian cells triggers cell cycle arrest and apoptosis (Richardson et al., 2006). In contrast, budding yeast continue through cell cycle progression despite inhibition of the chymotrypic site, presumably through compensation by the remaining two types of proteolytic sites (Fleming et al., 2002; Lee and Goldberg, 1998). Adding an additional layer of complexity to proteasome inhibition in budding yeast is the fact that chemical treatment often requires disruption of a drug-efflux pump such as Pdr5 to allow intracellular accumulation of chemical inhibitors (Liu et al., 2007).

To study the role of the proteasome in Gcn4 target gene transcription, I sought a method for comprehensive proteasome inhibition in order to minimize any potential effects from the

remaining catalytic sites. Previously in the Tansey laboratory, Collins *et al.* developed a method to comprehensively inhibit all three catalytic sites of the 20S proteasome in budding yeast through a combined chemical and genetic approach (Collins et al., 2010). In this method, the chymotryptic site is inhibited via the chemical inhibitor MG132 and the tryptic and caspase-like sites are inhibited through inactivating mutations in genes encoding the Pup1 (*pup1-T30A*) and Pre3 (*pre3-T20A*) subunits, respectively, expressed solely from plasmids. To allow for intracellular accumulation of MG132, this strain was *pdr5* null. Collins *et al.* demonstrated that complete 20S proteasome inhibition in the *pup1pre3pdr5* strain triggered an arrest in cell cycle progression and cell growth along with an increase in ubiquitin conjugates. However, our recent work revealed that the combination of the *pup1pre3* mutations and *pdr5* deletion triggered loss of mitochondrial DNA (mtDNA) through an unexplained mechanism, perhaps through accumulation of cellular toxins (Howard et al., 2012). If loss of mtDNA were due to irreparable DNA damage, this damage may also be present in genomic DNA, thereby altering genomic mechanisms and pathways. In contrast, we found that *pup1pre3* strains with genomically integrated *pup1-T30A* and *pre3-T20A* mutant alleles and retaining the *PDR5* gene did not lose mitochondrial DNA.

In this chapter, I present a modified version of the Collins *et al.* approach to comprehensively inhibit the proteasome while retaining the *PDR5* gene, thereby retaining mtDNA. I validated that this new method of proteasome inhibition triggered a growth arrest in liquid cultures. During proteasome inhibition, steady-state Gcn4 protein levels increased and accumulated in a polyubiquitylated state. I then determined that representative Gcn4 target gene transcript levels did not respond to SM treatment following proteasome inhibition and the loss of Gcn4 target gene transcripts correlated with a loss of Gcn4 localization at chromatin.

Results

Combined chemical-genetic proteasome inhibition in Saccharomyces cerevisiae

When combined with inactivating mutations in the *pup1* and *pre3* genes, deletion of the drug efflux gene *pdr5* resulted in loss of mitochondrial DNA (Collins et al., 2010; Howard et al., 2012). Therefore, I utilized the *pup1pre3PDR5* (Referred hereafter as *pup1pre3*) strain in my studies (Heinemeyer et al., 1997). To allow intracellular accumulation of MG132 in the presence of *PDR5*, I took advantage of the fact that MG132 sensitivity can be increased by treatment with 0.004% sodium dodecyl sulphate (SDS) and growth in media with L-proline as the sole nitrogen source (Liu et al., 2007). Cell cycle progression requires degradation of cyclins by the ubiquitin-proteasome system (Bloom and Cross, 2007). As a proxy for determining the efficacy of proteasome inhibition, I measured the optical density of liquid *PUP1PRE3* and *pup1pre3* budding yeast cultures grown in L-proline media containing 0.004% SDS and either DMSO or 50 μM MG132 (Figure 15). *PUP1PRE3* cultures seeded at an OD_{600} of 0.2 increased to an OD_{600} of about 4.5 after sixteen hours even in the presence of MG132. Liquid cultures of *pup1pre3* strains grew at a rate comparable to the *PUP1PRE3* strain, demonstrating that inhibition of the tryptic and caspase-like sites alone do not inhibit growth. However, the optical density of *pup1pre3* liquid cultures plateaued at an OD_{600} of around 1.2 beginning at ten hours compared to an OD_{600} of about 2.0 for *pup1pre3* cultures treated with DMSO. These data suggest that the modified approach of complete proteasome inhibition in the presence of *PDR5* is a viable method for proteasome inhibition that can used in this study.

Effects of proteasome inhibition on Gcn4 target gene transcript levels

To interrogate the role of the proteasome for transcription of Gcn4 target genes, I asked whether the increase in Gcn4 target gene transcripts following SM treatment required proteasome function. Based on the Spent/Stuck model, I hypothesized that proteasome inhibition would disrupt responsiveness to SM treatment. To do this, I treated *pup1pre3* strains with SM in the absence (SM) or presence (SM, MG132) of proteasome inhibition and determined steady-state transcript levels of the representative Gcn4 target genes *ARG1* (Figure 16A), *ARG4* (Figure 16B), *CPA2* (Figure 16C), and *HIS4* (Figure 16D) by RT-qPCR. In the case of all four genes, transcript

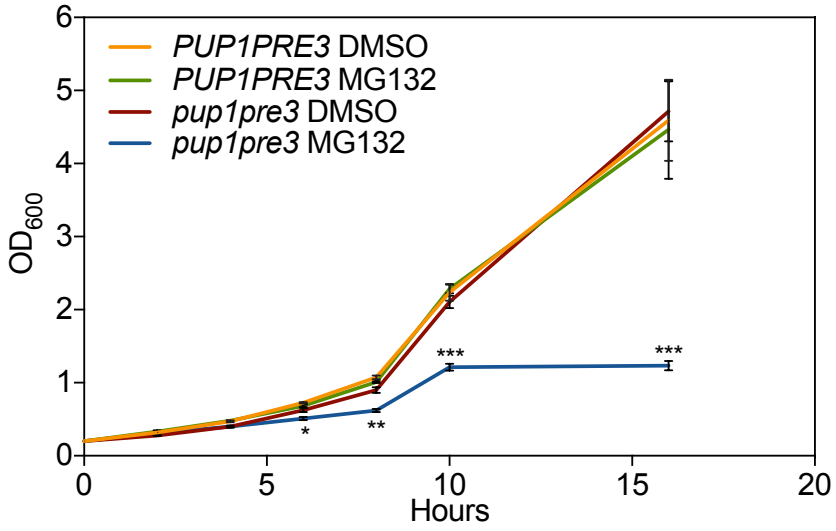

Figure 15. Combined chemical and genetic inhibition, but not chemical inhibition, of the proteasome confers growth arrest of liquid yeast cultures. *PUP1PRE3* (WCG4a) and *pup1pre3* (YUS5) were grown in complete synthetic medium (CSM) containing 0.1% proline, SDS added to 0.004%, and treated with either DMSO or 50 μM MG132. Growth at 30°C was measured as an increase in the absorbance (A600 nm) of the culture. n=3. Error bars represent SEM. (* significant at $p<0.05$, ** significant at $p<0.01$, *** significant at $p<0.001$)

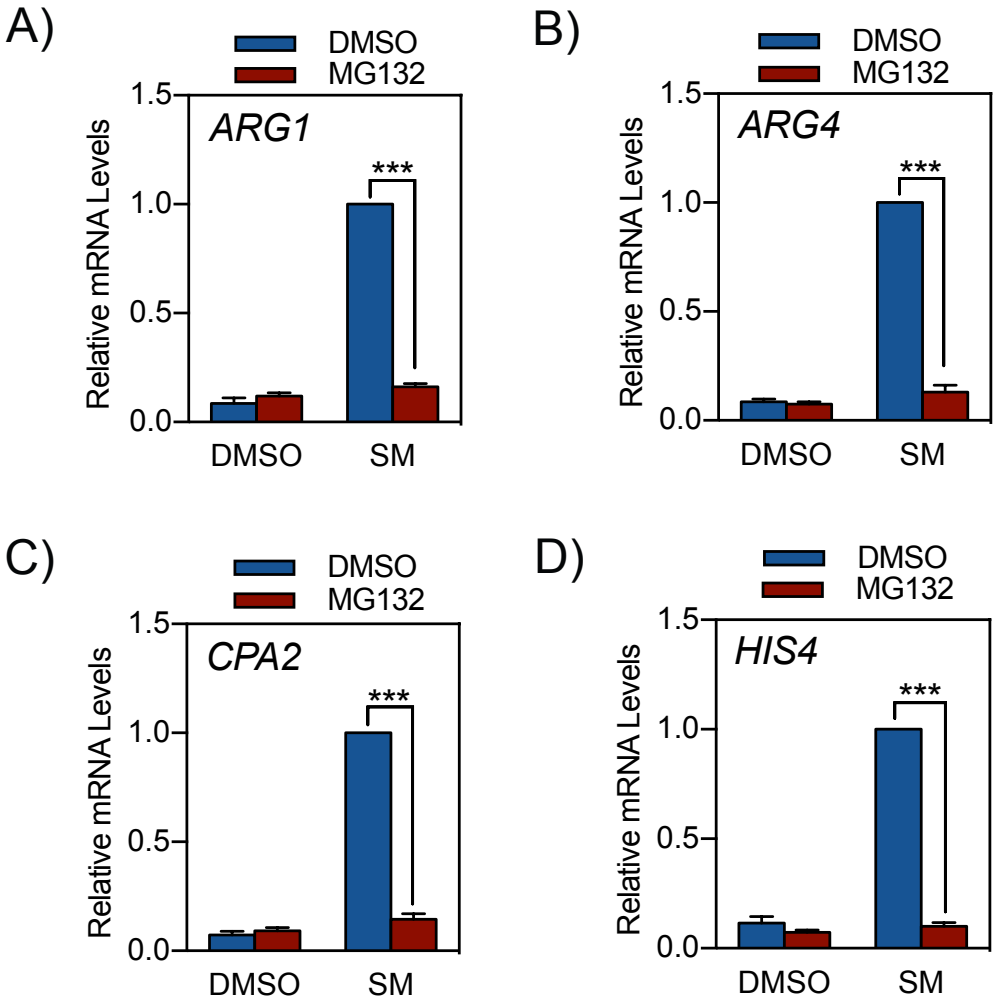

Figure 16. Gcn4 target gene transcript levels do not respond to SM treatment following proteasome inhibition. Yeast bearing the *pup1–T30A pre3–T20A* mutations (GHY010) were grown to log phase in minimal media and treated with either DMSO or MG132 for one hour. Strains were then treated with SM, or DMSO, for 1.5 hours, at which time RNA was collected and *ARG1* (A), *ARG4* (B), *CPA2* (C) and *HIS4* (D) mRNA levels quantified by RT-qPCR. Relative mRNA levels were then normalized to the SM-induced, DMSO-treated, sample for each gene. n=4. Error bars represent SEM. (*** significant at p<0.001)

levels increased by over ten-fold following SM treatment when compared to uninduced DMSO controls. However, the responsiveness of transcript levels to SM-treatment was lost during proteasome inhibition as transcript levels in SM, MG132-treated cultures were comparable to their corresponding uninduced controls. These data reveal that proteasome function is required for an increase in Gcn4 target gene transcript levels following SM treatment.

Effects of proteasome inhibition on Gcn4 protein levels

Amino acid starvation triggers transcription of Gcn4 target genes by stimulating an increase in Gcn4 synthesis (Hinnebusch, 1984). An alternative hypothesis for the loss Gcn4 target gene transcripts following proteasome inhibition is that proteasome inhibition may disrupt Gcn4 protein synthesis. To determine steady-state cellular Gcn4 protein levels following SM treatment and proteasome inhibition, I extracted protein from yeast cultures treated in the various experimental conditions and performed western blot analysis against HA-tagged Gcn4 (Gcn4-HA) (Figure 17). In response to SM-treatment, steady-state levels of both unmodified and modified Gcn4-HA increased when compared to that in the uninduced control (DMSO). These data demonstrate that Gcn4 remains present in the cell following proteasome inhibition, thereby arguing against a loss of Gcn4 protein as a reason for the decrease in target gene transcripts.

Effects of proteasome inhibition on Gcn4-ubiquitin conjugates

Following proteasome inhibition, Gcn4 accumulated in a high molecular weight form, indicative of a post-translationally modified protein. As mentioned, Gcn4 is a highly unstable protein targeted for degradation by ubiquitylation. Additionally, Gcn4 can be SUMOylated at chromatin through a process that stimulates its degradation (Rosonina et al., 2012). Therefore, I hypothesized that the highly modified forms of Gcn4 were, at least in part, ubiquitylated species of Gcn4 that most likely accumulated due to the proteasome's inability to degrade ubiquitylated Gcn4. To test this hypothesis, I isolated protein under denaturing conditions from yeast strains expressing His-Myc-tagged ubiquitin and precipitated ubiquitylated proteins through nickel-affinity chromatography (Figure 18). I then performed western blot analysis against Gcn4-HA to determine levels of ubiquitylated Gcn4. I found that Gcn4 was polyubiquitylated in strains following proteasome

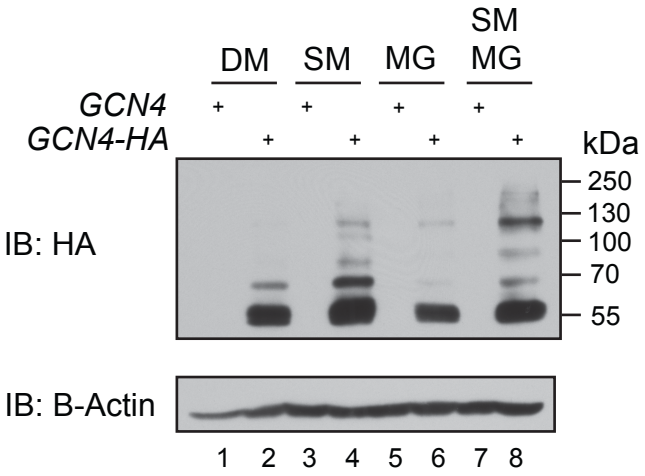

Figure 17. Yeast retain Gcn4 protein following proteasome inhibition. Yeast expressing either native Gcn4 (GHY010) or HA-tagged Gcn4 (GHY025) were grown to log phase in minimal media and treated with either DMSO or MG132 (MG) for one hour. Strains were then treated with SM, or DMSO (DM), for 1.5 hours, at which time protein was extracted, resolved by SDS-PAGE, and subject to western blotting with antibodies against the HA-epitope or β-actin.

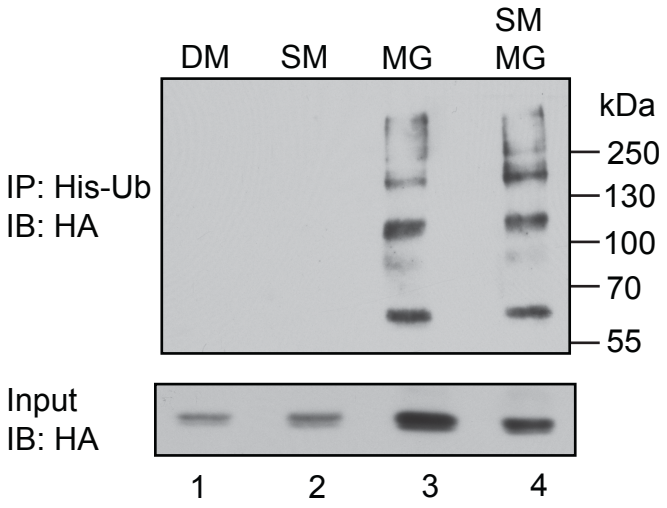

Figure 18. Ub-Gcn4 conjugates accumulate following proteasome inhibition. *GCN4-HA* (GHY356) yeast carrying a copper-inducible His-Ub expression plasmid (pUB221) were grown to log phase in minimal media and treated with CuSO4 and either DMSO (DM) or MG132 (MG) for one hour. Yeast were induced with SM, or DMSO, for an additional 1.5 hours, at which time protein lysates were collected under denaturing conditions. Ubiquitin-conjugates were captured by nickel-resin (Ni-NTA) chromatography, resolved by SDS-PAGE, and probed for HA-tagged Gcn4 protein by western blotting. A sample of the input material to the nickel resin was also probed for HA-tagged Gcn4. IB, immunoblot.

inhibition suggesting that the highly modified forms of Gcn4 were, at least in part, ubiquitylated species.

Effect of Cdk-dependent phosphorylation on proteasome-dependent Gcn4 target gene transcripts

Srb10 and Pho85 phosphorylate Gcn4 which stimulates Gcn4 ubiquitylation and degradation. Lipford *et. al* reported that blocking phosphorylation by these kinases through mutation of five consensus Cdk target residues of Gcn4 (3T2S-Gcn4) bypasses the requirement for the proteasome for Gcn4 target gene transcription (Figure 2A). In light of this work, I hypothesized that phosphorylation may function as an inactivating mark that locks Gcn4 into a state requiring proteasome function. To test this concept, I assayed representative Gcn4 target gene transcript levels in *3T2S-GCN4* strains to determine whether blocking Cdk-dependent phosphorylation conferred resistance to proteasome inhibition for target gene transcript levels. Following SM treatment, *ARG1* transcript levels in *3T2S-GCN4* strains were nearly three-fold higher than levels found in *GCN4* strains. However, following SM treatment and proteasome inhibition (SM,MG132), *ARG1* transcript levels were only one-fourth that found following SM treatment alone (SM) (Figure 19A). Additionally, sensitivity to proteasome inhibition was observed for transcript levels of the Gcn4 target genes *ARG4* (Figure 19B), *CPA2* (Figure 19C), and *HIS4* (Figure 19D). Therefore, *ARG1* transcript levels appear to be sensitive to proteasome inhibition in the presence of 3T2S-Gcn4. In the context of the Spent/Stuck model, phosphorylation by Srb10 or Pho85 can not “lock” Gcn4 into a state that requires proteasome function.

My data demonstrating that Gcn4 target gene transcript levels were sensitive to proteasome inhibition in the *3T2S-GCN4* strain is in direct contrast to work published by Lipford et. al. In order to account for these contrasting results, I sought to determine whether 3T2S-Gcn4 in my strains behaved similarly to that in strains previously published. Lipford *et al*. published that the mutations in 3T2S-Gcn4 decreased Gcn4 ubiquitylation. To determine the ability of 3T2S-Gcn4 to bypass ubiquitylation in my strain, I performed nickel affinity chromatography of protein isolated from strains expressing either WT Gcn4 or 3T2S-Gcn4, and His-Myc-Ub and performed western blot analysis targeting Gcn4 (Figure 20). As expected, I found that 3T2S-Gcn4 had decreased levels of polyubiquitin modifications. However, 3T2S-Gcn4 retained a mono-ubiquitylated form

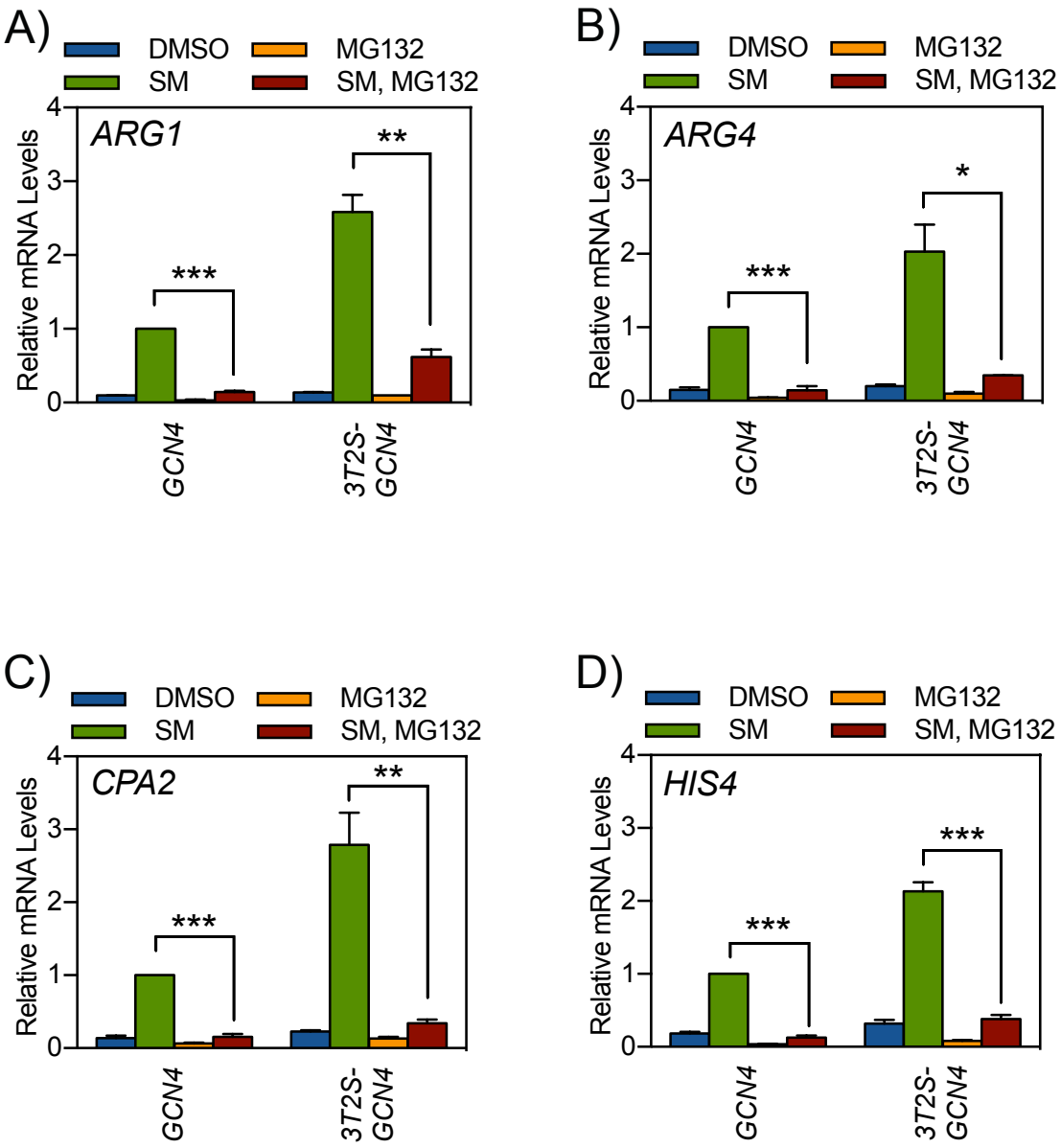

Figure 19. Gcn4 target gene transcript levels decrease following proteasome inhibition in yeast containing phospho-site mutant *3T2S-GCN4.* *GCN4* (GHY010) and *3T2S-GCN4* (GHY014) strains were grown to log phase at 30°C in minimal media and treated with either DMSO or MG132. After one hour, strains were treated with either DMSO or SM for 1.5 hours, RNA harvested, and processed as described to measure mRNA levels from the *ARG1* (A), *ARG4* (B), *CPA2* (C), and *HIS4* (D) loci. n=3. Error bars represent SEM. (* significant at p<0.05, ** significant at p<0.01, *** significant at p<0.001)

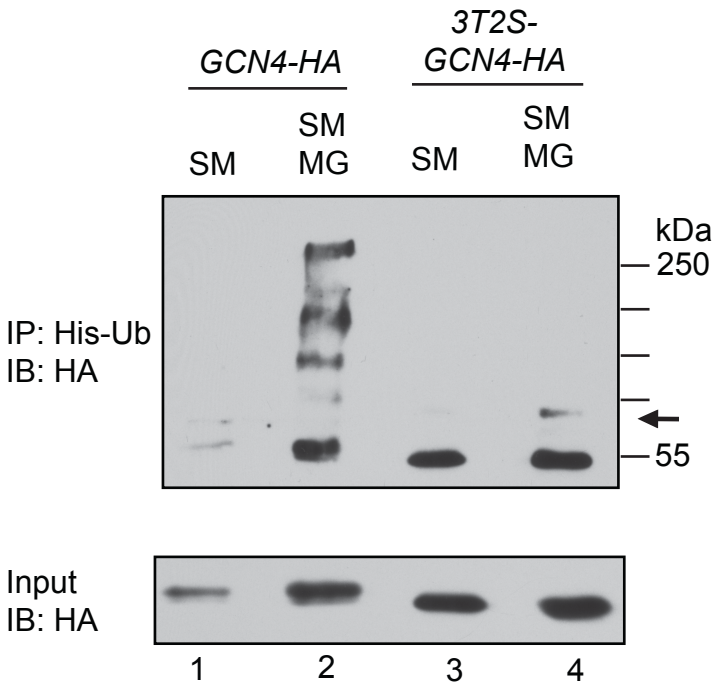

Figure 20. Phospho-site mutant 3T2S-Gcn4 is mono-ubiquitylated following proteasome inhibition. *pup1–T30A pre3–T20A GCN4-HA* (GHY356) and *pup1–T30A pre3–T20A 3T2S-GCN4-HA* (GHY360) yeast carrying a copper-inducible His-Myc-Ubiquitin expression plasmid (pUB221) were grown to log phase at 30°C in minimal media and treated with 0.5 mM $CuSO_4$ and either DMSO or 50 μM MG132 for one hour. Yeast were induced with 0.5 μg/ml SM, or a DMSO control, for an additional 1.5 hours, at which time protein lysates were collected under denaturing conditions. Ubiquitin-conjugates were captured by nickel-resin (Ni-NTA) chromatography, resolved by SDS-PAGE, and probed for HA-tagged Gcn4 protein by western blotting. A sample of the input material to the nickel resin was also probed for HA-tagged Gcn4. IB, immunoblot. A single Ub-conjugate of Gcn4 (arrow) persists in the 3T2S Gcn4 mutant.

during proteasome inhibition, suggesting that—contrary to the previous report—mutation of these five residues reduces, but does not eliminate, ubiquitylation under my experimental conditions.

Effects of proteasome inhibition on Gcn4 levels at the UAS of Gcn4 target genes

The function of the proteasome in the Spent/Stuck model is to degrade inactive, promoter-bound Gcn4 and allow for fresh activator binding. Therefore, I hypothesized that Gcn4 would remain bound to promoters during proteasome inhibition, similarly to what I observed for Cdc4 disruption (Figure 13) and to what has been previously shown by the Deshaies laboratory (Lipford et al., 2005). To challenge this hypothesis, I performed chromatin immunoprecipitation (ChIP) to measure Gcn4 levels at the *ARG1* promoter following SM induction and proteasome inhibition (Figure 21A). Surprisingly, I found that Gcn4 localization at the Gcn4 binding site of *ARG1* was decreased by about ten-fold following proteasome inhibition (SM, MG132) when compared to induction alone (SM), suggesting that proteasome function is required for detection of Gcn4 on chromatin. Additionally, signal for the TATA binding protein (TBP) decreased about five-fold following proteasome inhibition as determined by ChIP of TBP (Figure 21B).

In light of the loss of Gcn4 signal following proteasome inhibition, I wanted to determine whether the loss of Gcn4 signal was unique to the *ARG1* locus or a broad phenomenon for Gcn4 target genes. I performed ChIP to determine Gcn4 levels following proteasome inhibition at ten additional genes with mapped Gcn4 binding sites: *ARG4*, *ARG5*, *ARO4*, *CPA2*, *HIS4*, *HIS7*, *LEU3*, *LYS1*, *SNZ1*, and *THR4* (Figure 21A). Gcn4 levels detected at each gene decreased following proteasome inhibition (SM, MG132) when compared to induction alone (SM). These data reveal that the loss of Gcn4 at promoters following proteasome inhibition was not unique to *ARG1* but occurred at a wide-array of Gcn4 target genes. These data also suggest that, although both Cdc4 and the proteasome are required for a full response in *ARG1* transcript levels to SM-treatment, these UPS components function at different steps for transcription of Gcn4 target genes.

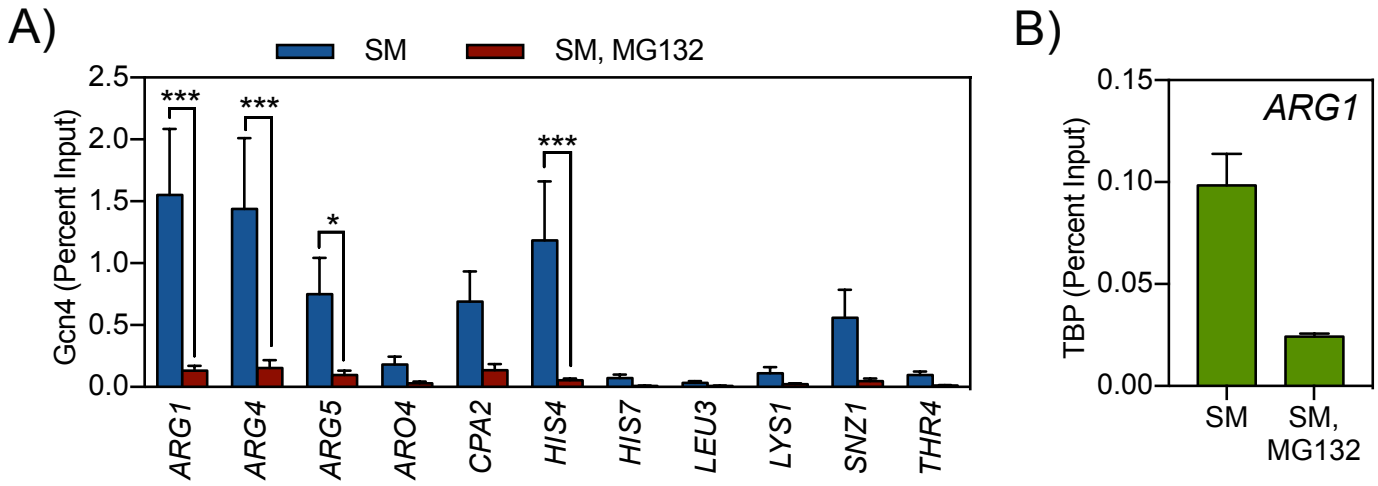

Figure 21. Gcn4 levels at the UAS of representative Gcn4 target genes decrease following proteasome inhibition. (A) *GCN4-HA* (GHY025) yeast were grown to log phase at 30°C in minimal media, treated with either DMSO or MG132 for one hour, and induced with SM for 1.5 hours. ChIP was performed using antibodies against the HA-epitope tag. Co-precipitating DNAs from the anti-HA ChIP were quantified by qPCR using primer pairs that amplify Gcn4 binding sites in the indicated genes. n=3. (B) Same as in (A) except using antibodies againt TBP and primers that amplify the *ARG1* TATA box. n=3. Error bars represent SEM. (* significant at $p<0.05$, ** significant at $p<0.01$, *** significant at $p<0.001$)

Effects of Gcn4 epitope-tagging on chromatin localization following proteasome inhibition

The loss of Gcn4 at *ARG1* was surprising considering that previous work by Lipford *et. al* demonstrated an increase in Gcn4 on chromatin following proteasome inhibition via MG132 treatment (Lipford et al., 2005). In an attempt to reconcile my data with this previously published work, I first asked whether I could reproduce the observation made by Lipford *et. al* using both their yeast strain (RJD) and method of Gcn4 induction. In their work, Gcn4 was induced through growth in leucine drop-out media. Using RT-qPCR, I confirmed that *ARG1* transcript levels in RJD strains grown in leucine drop-out media decreased following proteasome inhibition (MG132) (Figure 22A). Also in agreement the Lipford *et al*. study, Gcn4 signal at the *ARG1* promoter was unaffected following proteasome inhibition despite a corresponding decrease in *ARG1* transcript levels (Figure 22B).

I next asked whether the retention of Gcn4 on chromatin in the RJD strain following proteasome inhibition was due to the method of induction. I performed ChIP in the RJD strain induced with SM treatment in order to determine whether these conditions recapitulated results seen using leucine starvation. In agreement with the results obtained following leucine starvation, Gcn4 protein levels following proteasome inhibition detected at the *ARG1* promoter were unaffected (Figure 23). These data suggest that the difference in results between my study and the Lipford *et al*. study is not due to the method of Gcn4 induction.

Last, I sought to determine whether the epitope tag may account for these differences. In my studies, I utilized a 3xHA tag while Lipford *et al.* utilized a 9xMyc tag. To determine whether the epitope tag may influence the detection of Gcn4 on chromatin by ChIP following proteasome inhibition, I tagged Gcn4 in the *pup1pre3* strain with the 9xMyc epitope tag. I then performed a ChIP experiment with this *pup1pre3 GCN4-9xMyc* strain as I did previously with the *pup1pre3 GCN4-3xHA* strain. In contrast to the loss of Gcn4-3xHA signal at the *ARG1* promoter following proteasome inhibition, Gcn4-9xMyc signal remained unchanged following proteasome inhibition (Figure 24). These data suggest that the addition of the 9x-Myc epitope to Gcn4 influences the ability to detect Gcn4 during complete proteasome inhibition.

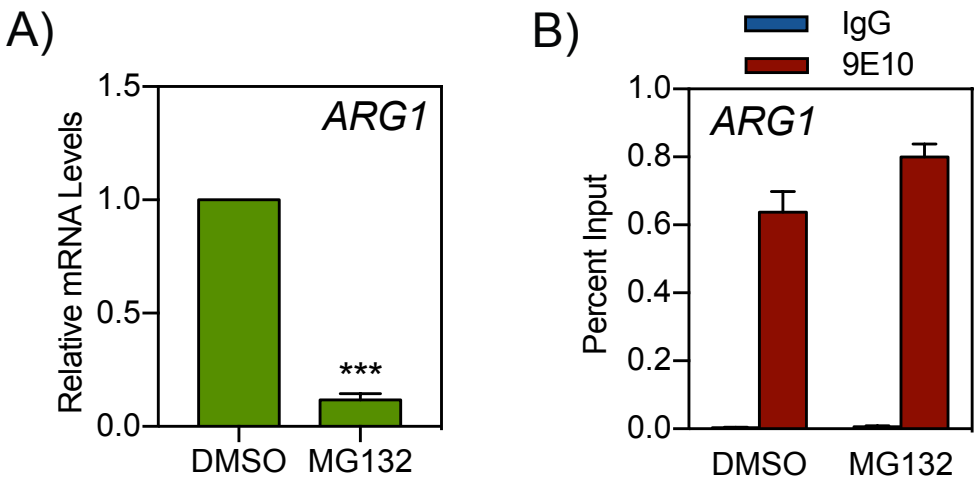

Figure 22. Gcn4-9xMyc levels at the UAS of *ARG1* are unaffected in the *Lipford et al.* strain following leucine starvation and proteasome inhibition. (A) *GCN4-MYC* (RJD3037) yeast were grown to log phase at 30°C in minimal media and treated with either DMSO or MG132. After one hour, strains were shifted to leucine drop-out media for 30 minutes, RNA harvested, and processed as described to measure mRNA levels from the *ARG1* locus. n=3. (B) *GCN4-MYC* yeast treated as in (A) and ChIP was performed using the 9E10 antibody against the Myc-epitope tag. Co-precipitating *ARG1* promoter DNA was quantified by qPCR. n=3. Error bars represent SEM. (*** significant at $p<0.001$)

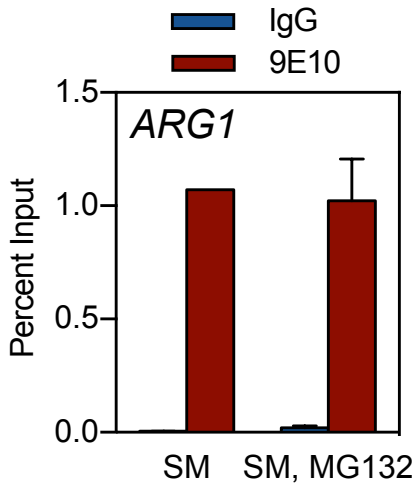

Figure 23. Gcn4-9xMyc levels at the UAS of *ARG1* are unaffected in the Lipford *et. al* strain following SM treament and proteasome inhibition. *GCN4-MYC* (RJD3037) yeast were grown to log phase at 30°C in minimal media and treated with either DMSO or MG132. After one hour, strains were induced with SM for 1.5 hours and ChIP was performed using the 9E10 antibody against the Myc-epitope tag. Co-precipitating *ARG1* promoter DNA was quantified by qPCR. n=3. Error bars represent SEM.

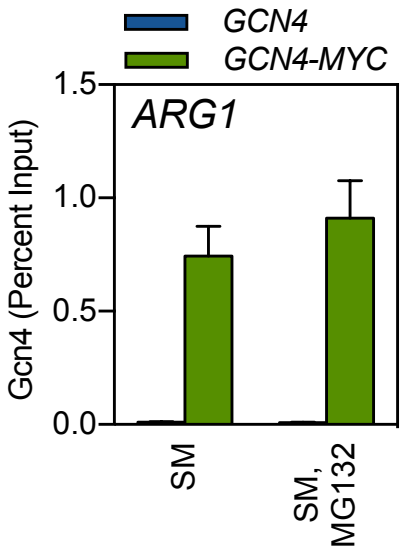

Figure 24. Gcn4-9xMyc levels at the UAS of *ARG1* are unaffected in strains generated in this study following proteasome inhibition and SM treatment. *GCN4-MYC* (GHY021) yeast were grown to log phase at 30°C in minimal media and treated with either DMSO or MG132. After one hour, strains were induced with SM for 1.5 hours and ChIP was performed using the 9E10 antibody against the Myc-epitope tag. Co-precipitating *ARG1* promoter DNA was quantified by qPCR. n=3. Error bars represent SEM.

The observation that Gcn4-HA detected at chromatin decreased following proteasome inhibition while Gcn4-Myc remained unchanged brought up the question of what happens to native, endogenous Gcn4 levels at promoters following proteasome inhibition. In order to determine the effect of proteasome inhibition on native Gcn4, I performed ChIP in strains containing untagged Gcn4 using an anti-Gcn4 polyclonal antibody. In agreement with the loss of Gcn4-HA signal at the *ARG1* promoter following SM treatment and proteasome inhibition (SM, MG132), native Gcn4 levels decreased to levels found in the uninduced control (DMSO) (Figure 25). These results reveal that levels of native, untagged Gcn4 decrease at promoters in response to proteasome inhibition.

Discussion

I began this chapter by presenting a modified approach to combined chemical-genetic proteasome inhibition in order to more tightly inhibit the proteasome in my studies. I found that transcript levels of representative Gcn4 target genes decreased following proteasome inhibition despite Gcn4 remaining present in the cell. Contrary to previous work from others, I demonstrated that Gcn4 target gene transcript levels decreased in response to proteasome inhibition in a strain containing the phospho-site mutant 3T2S-Gcn4. Lastly, I showed that Gcn4 levels detected at promoters of target genes decreased following proteasome inhibition. The decrease in Gcn4 signal following proteasome inhibition was seen for both native Gcn4 and 3xHA-tagged Gcn4, but not 9x-Myc-tagged Gcn4, suggesting that tagging Gcn4 with the 9x-Myc epitope tag alters either the ability to detect Gcn4 or the behavior of Gcn4 following proteasome inhibition.

Combined chemical-genetic proteasome inhibition in Saccharomyces cerevisiae

Neither chemical inhibition of the proteolytic chymotryptic site via MG132 treatment nor genetic inhibition of the caspase and caspase-like sites through inactivating point-mutations were sufficient to arrest growth in liquid budding yeast cultures. The demonstration that growth arrest occurred only during combined chemical-genetic proteasome inhibition supports the idea of a compensatory mechanism by remaining proteolytic sites during partial proteasome inhibition in

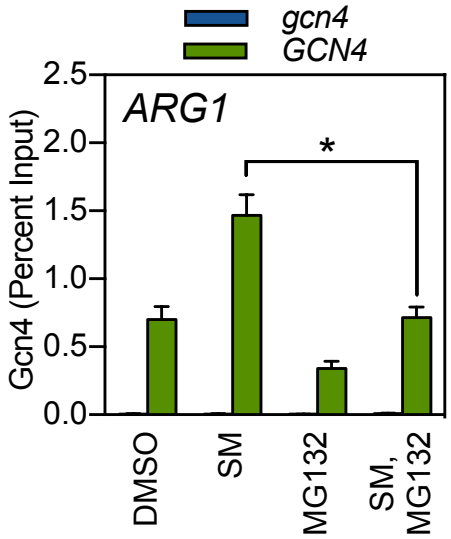

Figure 25. Native Gcn4 levels decrease at the UAS of *ARG1* following SM treatment and proteasome inhibition. *gcn4* (GHY004) and *GCN4* (GHY010) yeast strains were grown to log phase at 30°C in minimal media and treated with either DMSO or MG132. After one hour, Gcn4 was induced with SM for 1.5 hours. At this time, ChIP was performed with a polyclonal antibody against Gcn4. Co-precipitating *ARG1* promoter DNA was quantified by qPCR, expressed relative to the percentage of input DNA. n=3. Error bars represent SEM. (* significant at $p<0.05$)

yeast. This new approach for proteasome inhibition provides a useful tool that minimizes confounding experimental results through remaining proteolytic activity. Additionally, this new method allows for future studies of the role of the proteasome in Gal4-mediated transcriptional activation as the previous method of chemical-genetic proteasome inhibition utilized a *gal-* strain while this strain responds to galactose treatment (Collins et al., 2010).

Effects of proteasome inhibition on Gcn4 target gene transcript levels

Previous work demonstrated that chemical inhibition of the proteasome through MG132 treatment resulted in a decrease in *CPA2* and *HIS4* transcript levels and Gcn4 LacZ reporter gene transcript levels (Lipford et al., 2005). This same study also showed that disruption of the proteasome with a strain containing both the temperature sensitive *pre1-1* and *pre4-1* alleles had decreased *HIS4* transcript levels. My data demonstrating the loss of *ARG1*, *ARG4*, *CPA2*, and *HIS4* transcript levels following combined chemical-genetic proteasome inhibition are in agreement with these previous experiments. These results are also in agreement with the prediction of the Spent/Stuck model in which proteasome inhibition blocks transcription due to accumulation of inactive Gcn4. However, these experiments do not exclude the possibility that proteasome inhibition may block transcription through an indirect mechanism as combined chemical-genetic proteasome inhibition would disrupt a plethora of cellular processes that require proteolysis including cell cycle progression.

Effects of Cdk-dependent phosphorylation on proteasome-dependent Gcn4 target gene transcript levels

The decrease in Gcn4 target gene transcript levels in the *3T2S-GCN4* strain following proteasome inhibition does not agree with previous work by Lipford *et al*. One factor that may account for this difference is that Lipford *et al*. measured transcript levels through a qualitative approach in which PCR products were imaged by ethidium bromide staining. This is opposed to my studies in which I quantitatively determined transcript levels with RT-qPCR. The ability to accurately distinguish changes in transcript levels by imaging ethidium bromide stained amplicons requires demonstration that amplicons were isolated from PCR reactions during exponential amplification. If not, amplicon intensity does not correlate with input template.

However, this control was not included. Interestingly, I observed a two-fold increase in *HIS4* transcript levels in the presence of 3T2S-Gcn4 compared to WT Gcn4. However, Lipford *et al.* did not observe this difference between *GCN4* and *3T2S-GCN4* strains as *HIS4* transcript levels were comparable.

Another factor that may account for the difference between this study and that by Lipford *et al*. is that 3T2S-Gcn4 may behave differently in the two different strains, perhaps due to the type of epitope tag attached to 3T2S-Gcn4 or the stringency of proteasome inhibition. Using the combined chemical and genetic approach for proteasome inhibition, I observed a mono-ubiquitylated specie of 3T2S-Gcn4 whereas Lipford *et al.* used MG132 treatment alone and did not see this form of Gcn4. Other studies examining the role of phosphorylation in Gcn4 turnover may not have observed mono-ubiquitylated 3T2S-Gcn4 as the phospho-mutant was analyzed through alteration in half-life and not through ubiquitylation assays examining ubiquitin-Gcn4 conjugates (Chi et al., 2001). Since mono-ubiquitylation is insufficient to stimulate degradation by the proteasome, mono-ubiquitylation could have occurred while still stabilizing Gcn4 proteins.

3T2S-Gcn4 mono-ubiquitylation is very interesting considering that mono-ubiquitylation can regulate activity of other transcription factors (van der Horst et al., 2006; Wu et al., 2007). Whether the same mono-ubiquitylation event targeting 3T2S-Gcn4 targets wild-type Gcn4 remains to be determined. Increased cellular levels of 3T2S-Gcn4 may force interaction between 3T2S-Gcn4 and an E3 enzyme that it would otherwise not come in contact with. It also remains to be determined which E2 and E3 enzyme mediates this modification. The SCF^{Cdc4} E3 enzyme requires phosphorylation of the degron to stimulate interaction due to necessary electrostatic interactions between phosphates and the WD40 domain of Cdc4 (Orlicky et al., 2003). If the 3T2S-Gcn4 mutant is truly non-phosphorylatable, I would predict a different E3 enzyme. Alternatively, 3T2S-Gcn4 could still be phosphorylated but not at a Cdk consensus target residue. Mapping the location of this mono-ubiquitylation site through either lysine-mutational analysis or mass-spectrometry could allow for the generation of a combined 3T2S-Gcn4/non-ubiquitylated mutant to determine the significance of 3T2S-Gcn4 mono-ubiquitylation.

Effects of proteasome inhibition on Gcn4 levels at the UAS of Gcn4 target genes

The decrease in Gcn4 levels at chromatin following proteasome inhibition was surprising considering previous work showed an increase in Gcn4 localization at the *HIS4* promoter during MG132 treatment (Lipford et al., 2005). The difference between these two studies can be accounted for by my data demonstrating that the addition of a 9xMyc epitope to Gcn4 alters the ChIP signal following proteasome inhibition when compared to ChIP of either native Gcn4 or 3xHA epitope-tagged Gcn4. As epitope-tagging of Gcn4 was performed at the C-terminus adjacent to the DNA binding domain of Gcn4 and the 9xMyc epitope is much larger than the 3xHA epitope, the 9xMyc epitope may help stabilize DNA binding following proteasome inhibition or disrupt protein-protein interactions that may be required for loss of Gcn4 from chromatin.

The fact that the level of untagged Gcn4 signal decreased following proteasome inhibition suggests that the level of endogenous, native Gcn4 decreases at chromatin. ChIP experiments against native Gcn4 utilized a polyclonal Gcn4 antibody. Therefore, Gcn4 can be recognized at multiple epitopes during the ChIP procedure, reducing the likelihood that a decrease in signal is due to epitope masking. Although both Gcn4-3xHA and Gcn4 levels detected on chromatin were reduced following proteasome inhibition, the fold reduction was much greater in the Gcn4-3xHA ChIP. This may be due to higher sensitivity in detecting Gcn4-HA with the anti-HA antibody compared to the Gcn4 polyclonal antibody.

A central prediction of the Spent/Stuck model is that proteasome inhibition blocks the removal of Gcn4 from chromatin during transcription. Therefore, I hypothesized that proteasome inhibition would either have no effect on, or increase, Gcn4 levels at promoters. However, detected Gcn4 levels actually decreased following proteasome inhibition. These data do not support the Spent/Stuck model in its current form and instead support the proteasome functioning at a different requisite step for transcription. In combination with my data from Chapter 3 demonstrating that Gcn4 remains at chromatin during Cdc4 disruption, the loss of Gcn4 chromatin localization following proteasome inhibition suggests that Cdc4 and the proteasome act at different steps for Gcn4 target gene transcription. These results lead me to shift my focus to determining how proteasome inhibition may trigger a loss of Gcn4 signal at promoters.

CHAPTER V

PROTEASOME-DEPENDENT LOCALIZATION OF GCN4 ON CHROMATIN

Introduction

The surprising loss of Gcn4 signal at promoters in response to proteasome inhibition invalidates the Spent/Stuck model in its present form. In order to determine how proteasome inhibition triggers a loss of Gcn4 signal at promoters, I examined three potential mechanisms in which the proteasome may function. First I examined whether proteasome inhibition may block import of Gcn4 from the cytoplasm into the nucleus. Next, I examined whether proteasome inhibition alters the nucleosome arrangement in promoters in such a way as to block Gcn4 recognition sequences. Last, I examined whether proteasome inhibition prevents Gcn4 binding by alterations in the arginine repression (ArgR) complex.

In this Chapter, I demonstrate that Gcn4 localized to the nucleus irrespective of proteasome inhibition and that Gcn4 binding sites at *ARG1* and *HIS4* appear vacant of nucleosomes, thus accessible by Gcn4, following proteasome inhibition. I also present data demonstrating that the arginine repression complex is not responsible for the loss of target gene transcript levels following proteasome inhibition.

Results

Nuclear localization of Gcn4 during complete proteasome inhibition

A simple explanation as to why Gcn4 is not detected at chromatin following proteasome inhibition is that proteasome inhibition prevents Gcn4 from entering the nucleus. To assay whether proteasome inhibition excludes Gcn4 from the nucleus, I visualized sub-cellular localization of GFP-tagged Gcn4 (Gcn4-GFP) by fluorescent microscopy. To demarcate the nucleus, I also

visualized histone H2B tagged with mCherry (Htb2-mCherry). By determining the colocalization of these two proteins, I could deduce whether Gcn4 was nuclear localized.

Following SM treatment, the majority of yeast cells contained discreet regions of Gcn4-GFP localization (Figure 26A). Although the intensity of these distinct regions varied from cell to cell, the majority of cells did contain a region of peak signal. These discrete regions colocalized with Htb2-mCherry (Figure 26B-C), suggesting that Gcn4-GFP colocalizes with chromatin, thus the nucleus, during SM treatment. Following SM treatment and proteasome inhibition (SM, MG132), Gcn4-GFP again localized in discrete regions within the cell which colocalized with Htb2-mCherry. In sum, these data support the notion Gcn4-GFP localizes within the nucleus despite proteasome inhibition. Therefore, proteasome inhibition does not inhibit chromatin binding of Gcn4, and therefore transcription of target genes, through nuclear exclusion.

Effect of proteasome inhibition on nucleosome arrangement at the ARG1 and HIS4 promoters

In the case of *HIS4*, binding of Gcn4 to chromatin at recognition sequences requires chromatin opening at the promoter through a Rap1 or Abf1-mediated process to make Gcn4 binding sites accessible and allow for transcription (Devlin et al., 1991; Yarragudi et al., 2004; Yu and Morse, 1999). Therefore, I asked whether the presence and/or locations of nucleosomes within Gcn4 target gene promoters changed following proteasome inhibition. To determine nucleosome positions at a resolution higher than by ChIP, I performed a nucleosome mapping assay. Here, chromatin is treated with micrococcal nuclease to digest DNA that is unprotected by nucleosome occupancy. By coupling this strategy with tiling qPCR along the *ARG1* and *HIS4* loci, I was able to infer nucleosome locations through peaks in qPCR signal due to protection from nuclease digestion (Figure 27).

During basal transcription of *ARG1* in uninduced conditions (DMSO), a distinct site of nuclease-protection occurred at the *ARG1* TATA box (Figure 27A) which was adjacent to, but not covering, the two Gcn4 binding sites. In the *ARG1* ORF, nuclease protection occurred in distinct, orderly peaks, suggesting the presence of evenly distributed, well-ordered nucleosomes. Following SM treatment (SM), the TATA box-localized region of nuclease protection decreased in intensity and

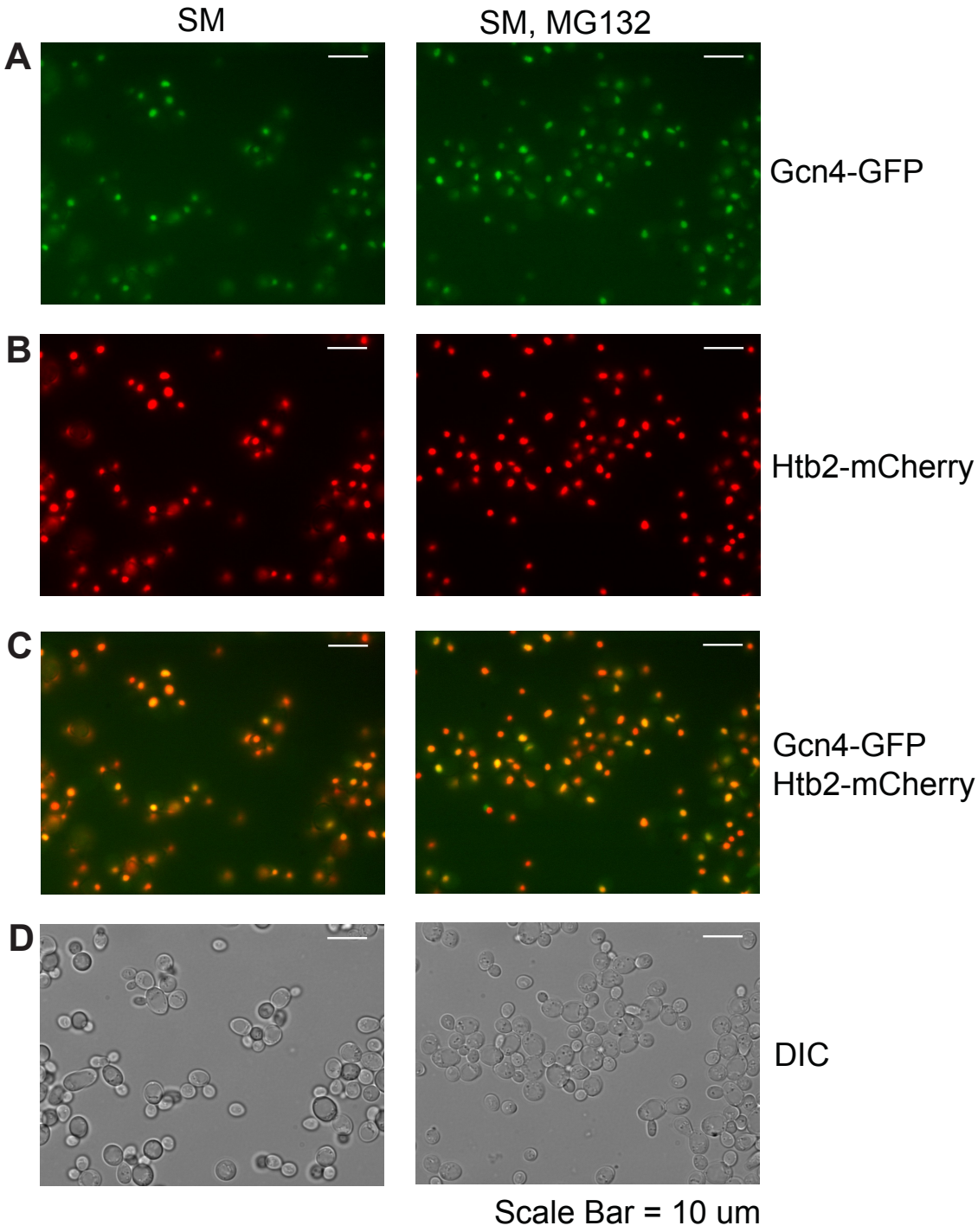

Figure 26. Gcn4 remains localized in the nucleus following proteasome inhibition. *GCN4-GFP HTB2-mCherry* (GHY339) yeast were grown to log phase at 30°C in minimal media, treated with either DMSO or MG132 for one hour, and induced with SM for 1.5 hours. Samples were imaged using either fluorescent microscopy for Gcn4-GFP (A), Htb2-mCherry (B), or differential interference contrast microscopy (D). Scale bars represent 5 μm.

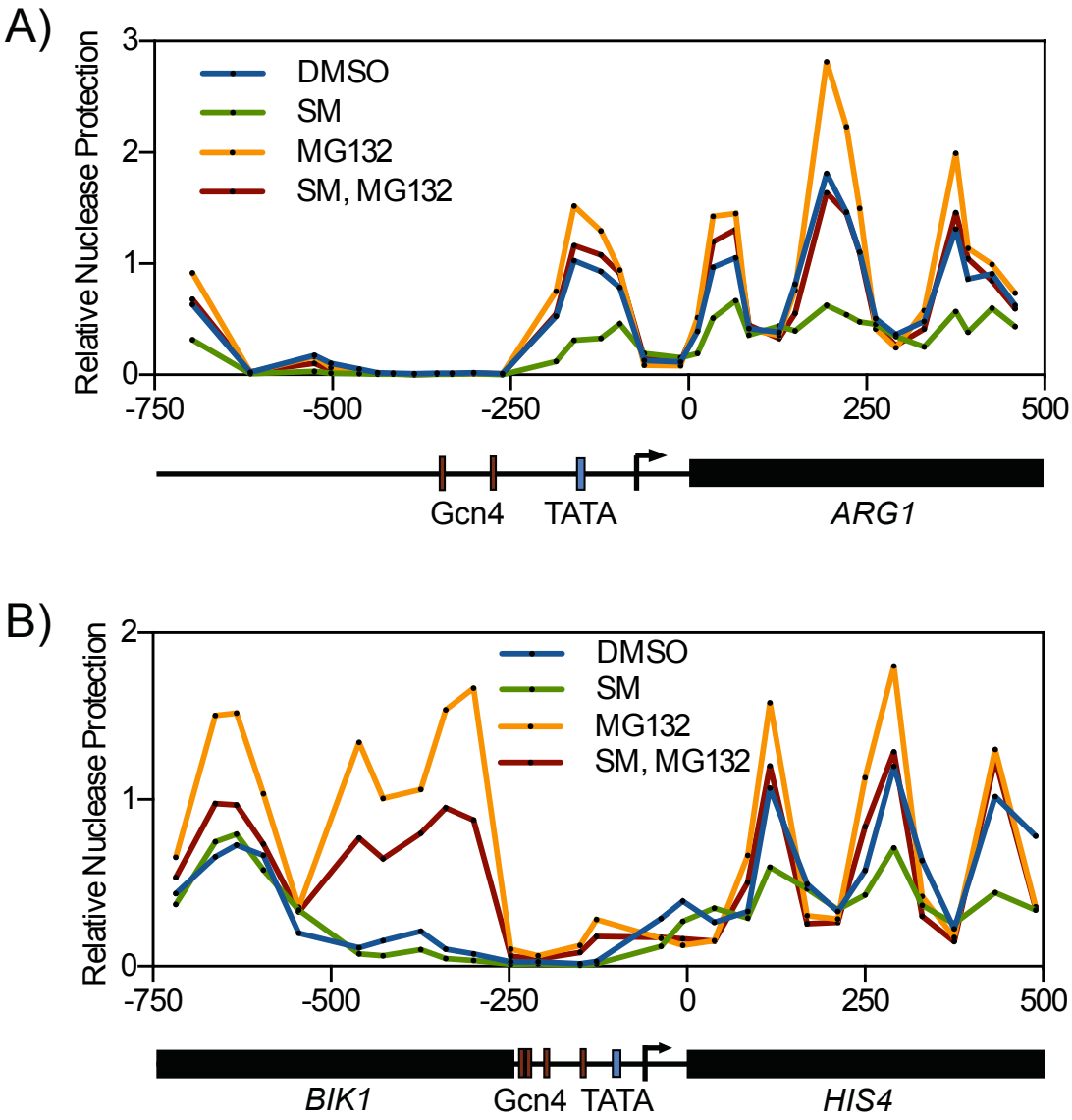

Figure 27. *ARG1* and *HIS4* promoters are depleted of nucleosomes irrespective of proteasome inhibition. (A) *GCN4* yeast (GHY010) were grown to log phase at 30°C in minimal media, treated with DMSO or MG132, induced with SM or a DMSO control for an additional 1.5 hours, and nucleosome occupancy mapped by MNase digestion, coupled with tiled primer sets spanning *ARG1*. qPCR data were normalized to the signal from a *GAL1-10* promoter-localized nucleosome. Data points represent an average of two independent experiments. (B) As in (A), except monitoring nucleosome positioning surrounding the *HIS4* locus. Data points represent an average of two independent experiments.

broadened, but did not cover Gcn4 binding sites. Within the *ARG1* ORF following SM treatment (SM), peaks of nuclease protection were low in intensity and very disordered compared to that in the uninduced samples (DMSO). Following proteasome inhibition and irrespective of SM treatment (MG132 and SM, MG132), nuclease protection in both the *ARG1* promoter and ORF increased but only at sites previously observed for nuclease protection in the uninduced samples (DMSO). Most importantly, Gcn4 binding sites in the *ARG1* promoter remained sensitive to nuclease treatment following proteasome inhibition (MG132 and SM, MG132). The retention of nuclease sensitivity at Gcn4 binding sites following proteasome inhibition was also observed at the *HIS4* gene (Figure 27B). Nuclease protection was undetermined at the *HIS4* TATA box due to the inability to design unique qPCR primers for this AT-rich region. In sum, these data suggest that Gcn4 binding sites at both *ARG1* and *HIS4* contain little, if any, nucleosomes following proteasome inhibition. Interestingly, nucleosome density at the *HIS4*-adjacent gene *BIK1,* which is not regulated by Gcn4*,* is increased in response to MG132, demonstrating that proteasome function is involved in mediating some aspect of nucleosome dynamics that is yet to be described.

Effects of the ArgR complex on proteasome-dependent Gcn4 target gene transcript levels

To date, no global inhibitor of Gcn4 has been described that prevents transcription of all Gcn4 target genes. However, a subset of Gcn4 target genes encoding enzymes involved in arginine anabolism and catabolism are regulated by the arginine repression (ArgR) complex which consists of four subunits: Arg80, Arg81, Arg82, and Mcm1 (Messenguy and Dubois, 2003). In the presence of arginine, a complex consisting of these four subunits forms and binds Arginine Control (ARC) elements in promoters of genes regulated by this complex. To determine whether proteasome inhibition prevents transcription of *ARG* genes through the accumulation or activation of the ArgR transcriptional inhibitor complex, I used RT-qPCR to determine transcript levels of the ArgR regulated gene *ARG1* (Figure 28A) and of the ArgR unregulated gene *HIS4* (Figure 28B) in strains with (*ARG80*) or without (*arg80*) ArgR function.

Even in the absence of SM induction (DMSO), *ARG1* transcript levels in the *arg80* strain were nearly ten-fold higher than *ARG1* transcript levels in the *ARG80* strain (Figure 28A). During SM

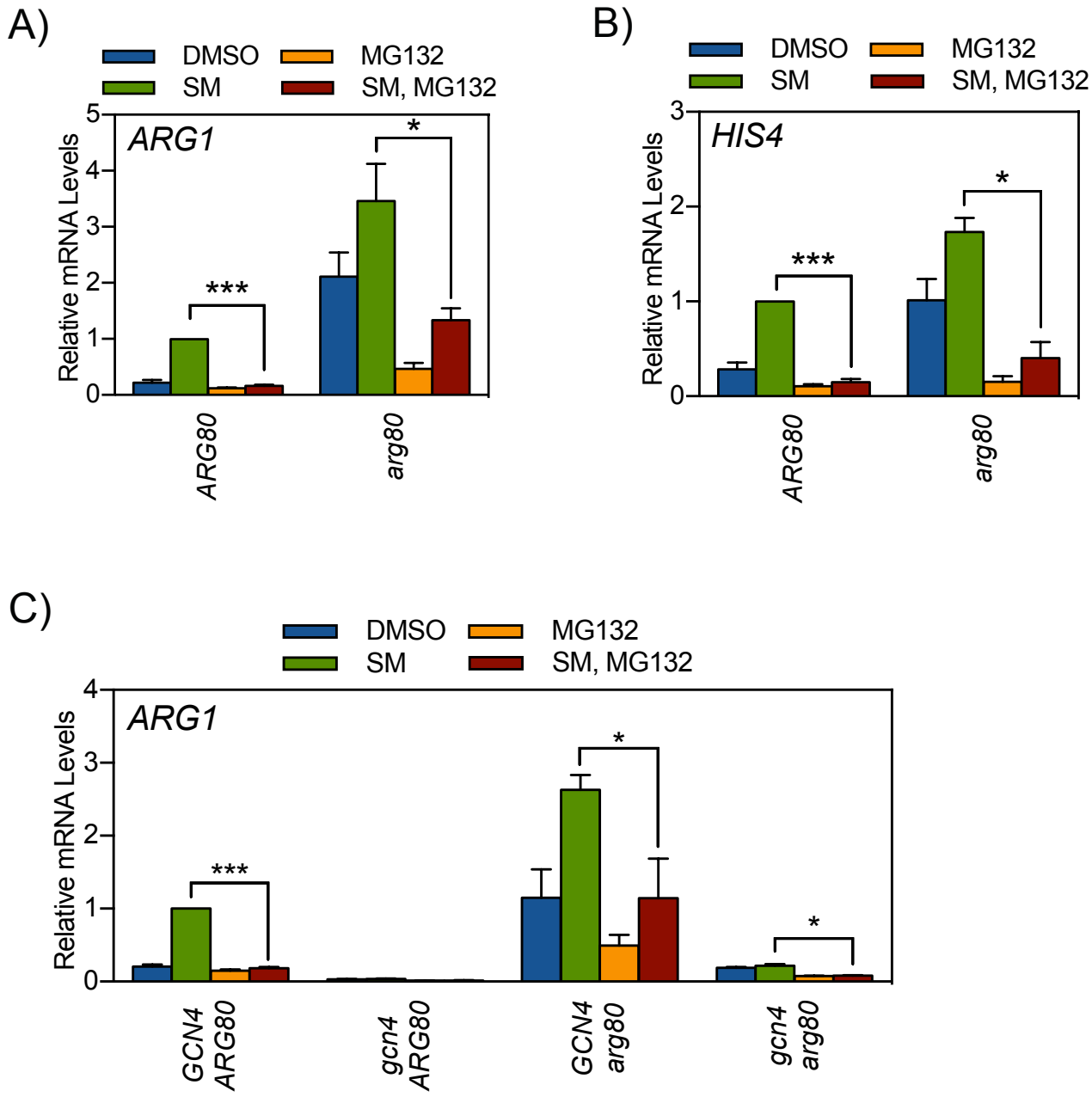

Figure 28. Decrease in Gcn4 target gene transcript levels following proteasome inhibition is not due to the ArgR complex. *ARG80* (GHY010) and *arg80* (GHY081) strains were grown to log phase in minimal media and treated with either DMSO or MG132. After one hour, strains were treated with DMSO or SM for 1.5 hours, RNA harvested, and *ARG1* (A) and *HIS4* (B) mRNA levels quantified by RT-qPCR. Each qPCR reaction was normalized to the SM-treated *ARG80* sample. n=3. (C) Same as in (A) except using *GCN4 ARG80* (GHY010), *gcn4 ARG80* (GHY004), *GCN4 arg80* (GHY081), and *gcn4 arg80* (GHY079) strains. n=4. Error bars represent SEM. (* significant at $p<0.05$, *** significant at $p<0.001$)

treatment (SM), *ARG1* transcript levels in *arg80* strains were over three times that of *ARG1* transcript levels detected in *ARG80* strains. However, following SM treatment and proteasome inhibition (SM, MG132), *ARG1* transcript levels in *arg80* strain decreased to below that of *ARG1* transcript levels in the uninduced cultures (DMSO), demonstrating that the loss of *ARG1* transcript levels following proteasome inhibition does not occur as a result of the ArgR complex. The remaining *ARG1* transcript levels following proteasome inhibition (SM, MG132) were dependent on Gcn4 as *ARG1* transcript levels following SM treatment and proteasome inhibition (SM, MG132) in the *GCN4 arg80* strain were less than that in the *gcn4 arg80* strain (Figure 28C). Interestingly, *HIS4* transcript levels in uninduced *arg80* strains (DMSO) were increased compared to *ARG80* strains, although to a lesser degree than that seen for *ARG1* transcript levels (Figure 28B). The increase in *HIS4* transcript levels occurred despite *HIS4* not containing a characterized ArgR recognition sequence in the *HIS4* promoter. These results demonstrate that the loss of target gene transcript levels following proteasome inhibition does not occur through a mechanism requiring the ArgR complex.

Discussion

In this Chapter, I report that Gcn4 was localized within the nucleus despite inhibition of the proteasome. I also found that the Gcn4 binding sites in the promoter regions of *ARG1* and *HIS4* remained nucleosome-free following proteasome inhibition, suggesting that nucleosomes do not physically block Gcn4 binding following proteasome inhibition. I also determined that the loss of *ARG1* transcript levels following proteasome inhibition did not occur through the ArgR complex.

Nuclear localization of Gcn4 following proteasome inhibition

Regulated nuclear localization in response to stimuli has been studied for multiple transcription factors including Msn2, Gln3, and Mig1 (Beck and Hall, 1999; De Vit et al., 1997). Additionally, nuclear localization of some transcription factors can be regulated through ubiquitylation. In the case of p53, mono-ubiquitylation of p53 stimulates export from the nucleus, while poly-ubiquitylation of p53 stimulates degradation (Li et al., 2003). In contrast, Gcn4 activity is regulated

at the point of protein synthesis and remains localized in the nucleus even during growth in uninduced conditions.

The notion that Gcn4 is constitutively imported into the nucleus does not eliminate the possibility that proteasome inhibition may perturb the cell in such a way as to inhibit normal function of the nuclear import machinery. Arguing against this point is the observation that Gcn4-GFP colocalized with Htb2-mCherry irrespective of proteasome inhibition, suggesting that Gcn4 remains predominantly localized within the nucleus despite proteasome disruption. This suggests that the loss of Gcn4 from chromatin is not a result of nuclear exclusion of Gcn4.

Effects of proteasome inhibition on nucleosome arrangement at the ARG1 and HIS4 promoters

Genome-wide yeast studies have shown that nucleosome occupancy at regulatory regions inversely correlates with transcription of the genes these regions regulate (Lee et al., 2004; Lee et al., 2007). Interestingly, a distinct peak in nuclease protection, indicative of nucleosome occupancy, was present at the *ARG1* TATA box. The level of nuclease protection at the TATA box in the various Gcn4 induction and proteasome inhibition conditions (Figure 27) correlated with corresponding levels of *ARG1* transcripts (Figure 16A). This in agreement with previous studies that observed a decrease in the TATA localized nucleosome at *ARG1* when transcription was induced (Crisucci and Arndt, 2012; Govind et al., 2010). Therefore, the TATA-localized nucleosome at *ARG1* may act as a mechanism of regulation as this nucleosome would need displaced for TBP to bind the TATA box and facilitate transcription.

During transcription of *ARG1* and *HIS4* (SM), the ORF-localized nucleosomes were irregularly spaced as demonstrated by the lack of distinct, prominent peaks as shown in uninduced cultures (DMSO) in the nucleosome protection assay. This nucleosome organization is in agreement with work from the Arndt group which observed similar patterns during SM treatment (Crisucci and Arndt, 2012). This irregular pattern is indicative of nucleosome displacement by transcriptional machinery passing along the gene to produce the RNA strand (Adams and Workman, 1993; Teves et al., 2014; Workman, 2006). In support of this idea, nuclease protection in the ORF inversely correlated with *ARG1* and *HIS4* transcript levels. Despite the effects of proteasome

inhibition on nucleosomes at the TATA box and ORF, Gcn4 binding sequences at both *ARG1* and *HIS4* remained sensitive to nuclease digestion. These data do not support a mechanism in which proteasome inhibition triggers a loss of Gcn4 from recognition sequences due to nucleosomes covering Gcn4 recognition sequences in the promoter.

Effects of the ArgR complex on proteasome-dependent Gcn4 target gene transcript levels

The ArgR complex assembles at ARC elements in the *ARG1* promoter in the presence of arginine to inhibit transcription of many arginine synthesis genes including *ARG1*. Congruent with the repressive function of the ArgR complex, the *arg80* strain contained higher levels of *ARG1* transcripts than the *ARG80* strain even in the absence of SM treatment (Figure 28A and C). Following proteasome inhibition, *ARG1* transcripts decreased to levels below that observed in intreated cultures. Therefore, reduction of transcript levels following proteasome inhibition does not occur through an ArgR dependent process. Interestingly, *HIS4* transcript levels in the *arg80* strain were higher than in the *ARG80* strain, despite *HIS4* not being directly regulated by the ArgR complex (Figure 28B). However, the difference in transcript levels between *ARG80* and *arg80* strains was greater for *ARG1* transcripts than for *HIS4* transcripts, suggesting that the effects on *HIS4* transcript levels may be an indirect consequence of ArgR disruption. One potential explanation is that disruption of the ArgR complex may affect Gcn4 synthesis or degradation, thereby causing an increase in Gcn4 protein levels and a global increase in target gene transcript levels. Further experiments will be required to determine the effect of ArgR complex disruption on Gcn4 protein levels.

In this Chapter, I examined changes extrinsic to Gcn4 following proteasome inhibition that may account for the decrease in Gcn4 levels following proteasome inhibition. In the next Chapter, I focus on whether proteasome inhibition triggers a loss of Gcn4 from chromatin through a mechanism intrinsic to Gcn4. Based on my work in Chapter 4, I know that Gcn4 is highly ubiquitylated following proteasome inhibition (Figure 18). This led me to study a potential mechanism in which Gcn4 ubiquitylation could trigger this loss.

CHAPTER VI

ROLE OF CDC48 IN PROTEASOME-DEPENDENT GCN4 LOCALIZATION AT PROMOTERS

Introduction

In the previous Chapter, I present evidence that the decrease in both the levels of Gcn4 target gene transcripts and levels of Gcn4 detected on chromatin were not due to alterations in Gcn4 nuclear localization, nucleosome arrangement in promoter regions of target genes, or perturbation on the ArgR complex. Therefore, I next focused on whether proteasome inhibition may alter Gcn4 in such a way as to affect its ability to associate with DNA. Gcn4 is a highly unstable protein accumulates in a polyubiquitylated form following proteasome inhibition (Figure 18). Lysine residues occur throughout Gcn4, within the DNA binding domain. Therefore, ubiquitylation may sterically inhibit recognition of DNA. Ubiquitylation of some proteins has been reported to inhibit chromatin interaction by stimulating interaction with the Cdc48 complex, a homo-hexameric complex that extracts ubiquitylated proteins from chromatin. A few of these examples include the RNA polymerase II subunit Rbp1 following UV irradiation (Verma et al., 2011), the transcriptional repressor alpha-2 (Wilcox and Laney, 2009), and the transcriptional activator LexA-VP16 when fused to a non-cleavable mutant of ubiquitin (Ndoja et al., 2014). Therefore, I hypothesized that the decrease in Gcn4 signal at chromatin following proteasome inhibition may be due to recognition of ubiquitylated Gcn4 by the Cdc48 complex which stimulates stripping of Gcn4 from DNA.

In this chapter, I report that the *cdc48-3* allele rescued Gcn4 binding to chromatin along with target gene transcript levels following proteasome inhibition. I also report that Cdc48 and Gcn4 interact with one another, and the loss of target gene transcript levels following proteasome inhibition did not occur though a single, non-essential Cdc48 adapter protein. I also demonstrate that the effects of Cdc48 disruption on Gcn4-mediated transcription is in contrast to the effects of Cdc48 disruption on Gal4-mediated transcription, suggesting that Cdc48 does not function at a single step common to both transcriptional activators.

Effects of the Cdc48 complex on proteasome-dependent Gcn4 levels at the UAS of Gcn4 target genes

Considering that the Cdc48 complex can remove ubiquitylated proteins from chromatin and that Gcn4 accumulates in a polyubiquitylated state following proteasome inhibition, I hypothesized that Cdc48 could recognize ubiquitylated Gcn4 following proteasome inhibition and prevent association with chromatin. To test this hypothesis, I disrupted Cdc48 in a strain containing the *cdc48-3* allele and performed ChIP in order to determine whether disruption of Cdc48 rescued Gcn4 binding at the UAS of Gcn4 target genes following proteasome inhibition (Sato and Hampton, 2006). As I observed previously (Figure 21), Gcn4 levels detected at the *ARG1* (Figure 29A), *ARG4* (Figure 29B), *CPA2* (Figure 29C), and *HIS4* (Figure 29D) promoters following SM treatment and proteasome inhibition (SM, MG132) decreased by about half in the *CDC48* strain compared to levels found in SM-treated cultures without proteasome inhibition (SM). However, Gcn4 signals at all four representative Gcn4 target genes were unaffected by proteasome inhibition in the *cdc48-3* strain which supports the hypothesis that the loss of Gcn4 signal at promoters following proteasome inhibition occurs through a Cdc48-dependent mechanism.

Effects of the Cdc48 complex on proteasome-dependent Gcn4 target gene transcript levels

I next asked whether the *cdc48-3* allele also rescued transcript levels of Gcn4 target genes following proteasome inhibition. Using RT-qPCR, I determined transcript levels of the representative Gcn4 target genes *ARG1* (Figure 30A), *ARG4* (Figure 30B), *CPA2* (Figure 30C), and *HIS4* (Figure 30D) in *CDC48* and *cdc48-3* strains following SM treatment and proteasome inhibition. In the case of the *CDC48* strain, transcript levels of the representative target genes increased in response to SM treatment (SM) while this response was reduced following proteasome inhibition (SM, MG132). Irrespective of SM treatment, transcript levels of all four representative target genes in the *cdc48-3* strain were two- to three-fold higher than that found in induced *CDC48* cultures (SM), depending on the target gene. Most importantly, transcript levels of the representative target genes remained at this high level following proteasome inhibition (SM,

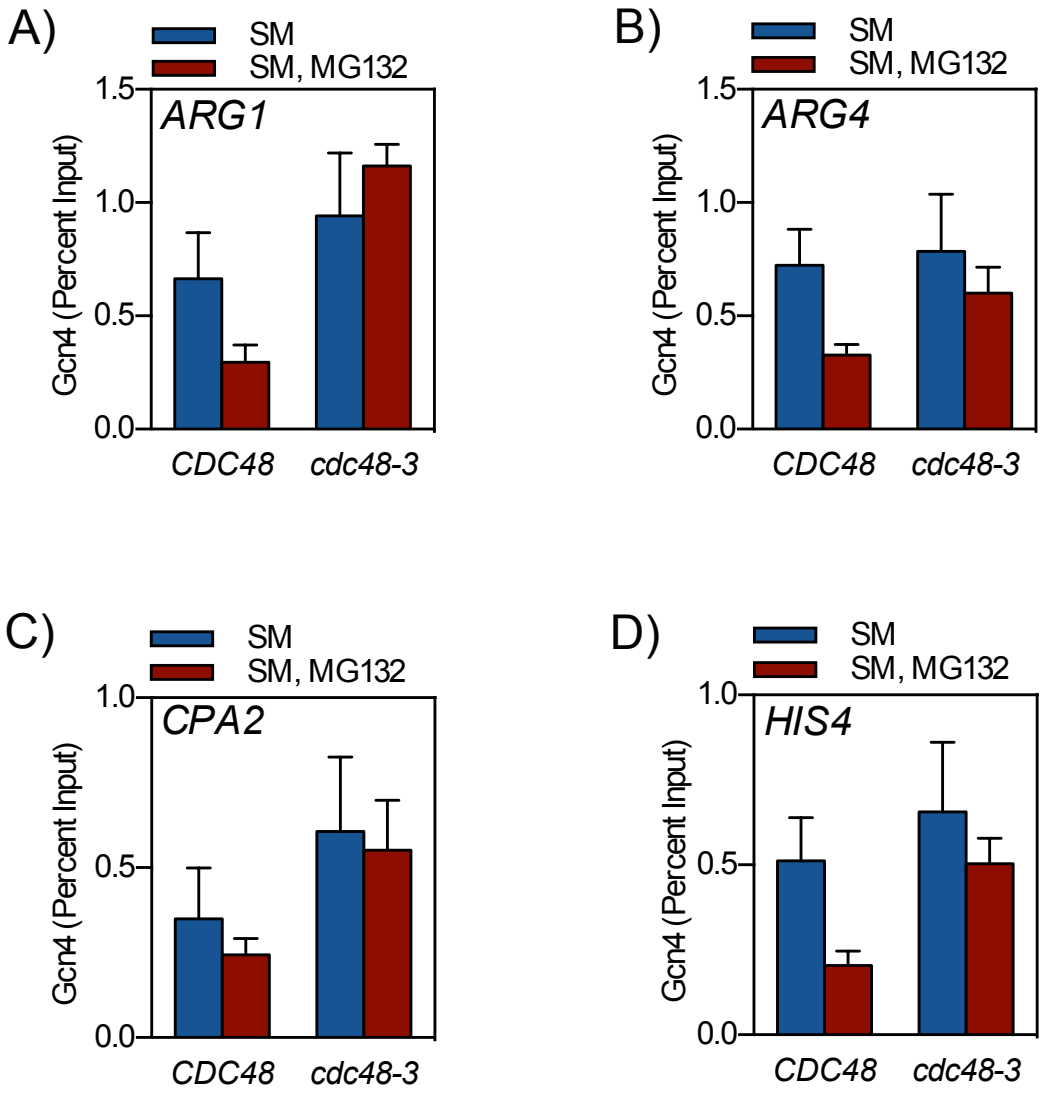

Figure 29. Disruption of the Cdc48 complex confers resistance to proteasome inhibition for levels of Gcn4 binding at the UAS of representative Gcn4 target genes. *CDC48 GCN4-HA* (GHY116) and *cdc48-3 GCN4-HA* (GHY118) strains were grown to log phase at 30°C in minimal media, treated with either DMSO or MG132 for one hour, and induced with SM for 1.5 hours. ChIP was then performed using antibodies against the HA-epitope tag. Co-precipitating *ARG1* (A), *ARG4* (B), *CPA2* (C), or *HIS4* (D) promoter DNAs were quantified by qPCR, expressed relative to the percentage of input DNA. n=3. Error bars represent SEM.

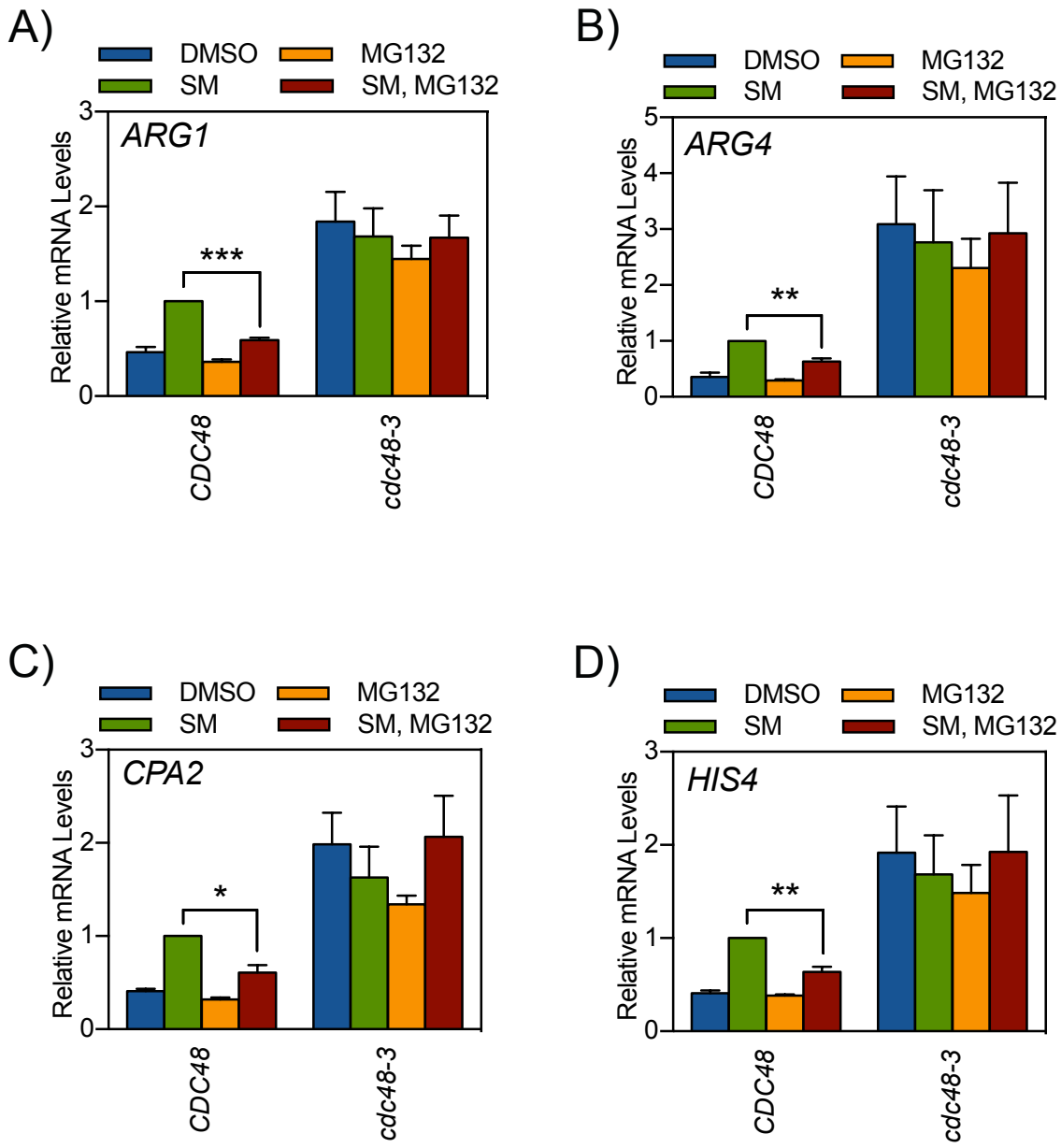

Figure 30. Disruption of the Cdc48 complex confers resistance to proteasome inhibition for Gcn4 target gene transcript levels. *CDC48* (RHY2455) and *cdc48-3* (RHY2457) strains were grown to log phase at 30°C in minimal media and treated with either DMSO or MG132. After one hour, strains were treated with either DMSO or SM for 1.5 hours, RNA harvested, and processed as described to measure mRNA levels from the *ARG1* (A), *ARG4* (B), *CPA2* (C), and *HIS4* (D) loci. n=4. Error bars represent SEM. (* significant at p<0.05, ** significant at p<0.01, *** significant at p<0.001)

MG132). This result suggests that rescuing promoter binding of Gcn4 through the *cdc48-3* allele is sufficient to rescue transcript levels of the target genes following proteasome inhibition. This also suggests that proteasome function is not required for transcription when the Cdc48 complex is disrupted.

The Cdc48 complex plays a role in maintaining genomic integrity by functioning in DNA replication and DNA damage repair (Franz et al., 2016). To rule out the possibility that proteasome resistance in the *cdc48-3* strain was due to an unknown, unlinked mutation, I mutated the *cdc48-3* allele to wild-type *CDC48* and determined whether this restored sensitivity of *ARG1* transcript levels to proteasome inhibition (Figure 31). As observed previously, *ARG1* transcript levels in the *CDC48* strain decreased following proteasome inhibition (SM, MG132) while *ARG1* transcript levels in the *cdc48-3* strain were unchanged (SM, MG132) when compared to their corresponding SM-treated cultures (SM). In the *cdc48-3::CDC48* strain, *ARG1* transcript levels were higher than in the *CDC48* strain even in uninduced conditions (DMSO), suggesting the *cdc48-3* strain may contain secondary mutations that increase *ARG1* transcript levels. However, *ARG1* transcript levels decreased following induction and proteasome inhibition (SM, MG132) compared to SM treatment alone (SM), demonstrating that the *cdc48-3* allele is required for resistance of *ARG1* transcript levels following proteasome inhibition.

Gcn4 interaction with Cdc48

If Cdc48 acts on the Gcn4 protein, Cdc48 should physically associate with Gcn4. To determine whether Cdc48 associates with Gcn4, I immunoprecipitated Gcn4 from protein extracts obtained during SM treatment and proteasome inhibition and probed for co-immunoprecipitation of Cdc48 by western blotting (Figure 32). Supporting the notion that Cdc48 associates with Gcn4, Cdc48 co-immunoprecipitated with Gcn4 at a level above background binding to an untagged-Gcn4 negative control (Compare lanes 1 and 3). I also determined that Cdc48 did not robustly co-immunoprecipitate with the non-ubiquitylated lysine-free K0-Gcn4 mutant generated in Chapter 3 (Compare lanes 3 and 5) which agrees with the concept that ubiquitylation is required for recognition by the Cdc48 complex.

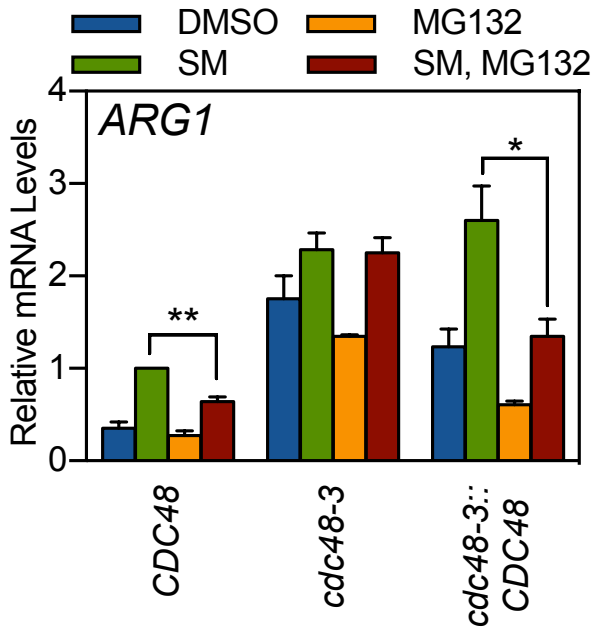

Figure 31. Resistance of *ARG1* transcript levels to proteasome inhibition in the *cdc48-3* strain is not due to secondary mutations. *CDC48* (RHY2455), *cdc48-3* (RHY2457) and *cdc48-3::CDC48* (GHY279) strains were grown to log phase at 30°C in minimal media and treated with either DMSO or MG132. After one hour, strains were treated with either DMSO or SM for 1.5 hours, RNA harvested, and processed as described to measure mRNA levels from the *ARG1* loci. n=4. Error bars represent SEM. (* significant at $p<0.05$, ** significant at $p<0.01$)

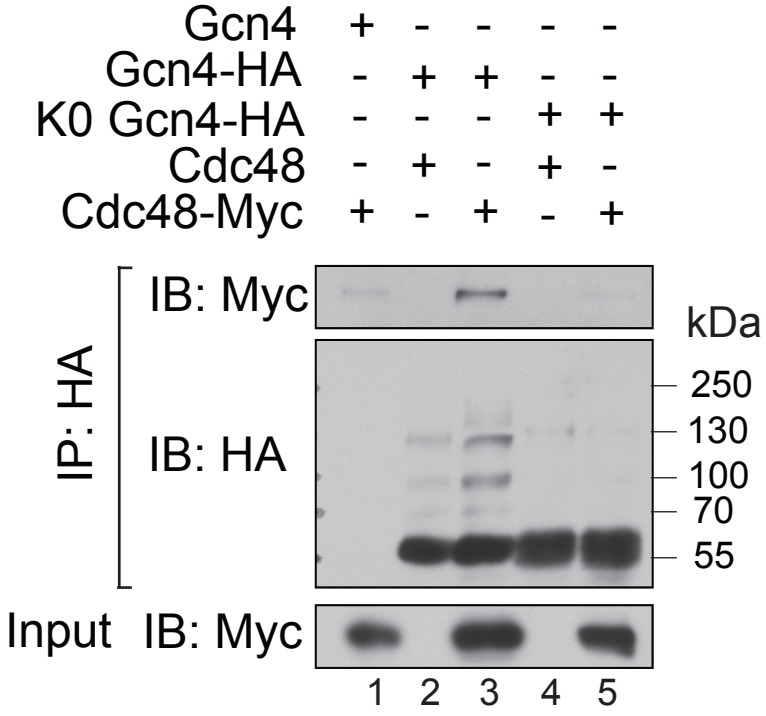

Figure 32. Gcn4 associates with Cdc48. *GCN4 CDC48-MYC* (GHY285), *GCN4-HA CDC48* (GHY025), *GCN4-HA CDC48-MYC* (GHY287), *K0-GCN4-HA CDC48* (GHY124), and *K0-GCN4-HA CDC48-MYC* (GHY293) yeast were grown to log phase at 30°C in minimal media and treated with MG132. After one hour, Gcn4 was induced with SM for 1.5 hours. Protein lysates were collected, Gcn4-HA immunoprecipitated (IP) via an anti-HA antibody, and IPs probed with antibodies against the Myc- (Cdc48) and HA- (Gcn4) epitope tags. A sample of the input material to the IP was also probed for Myc-tagged Cdc48.

Effect of Cdc48 cofactors on Gcn4 target gene transcript levels

Cdc48 recognizes ubiquitylated substrates through multiple cofactors, some of which are nonessential in budding yeast (*UBX1-7*). To determine whether a single, nonessential cofactor could be mapped as that which recognizes Gcn4, I assayed *ARG1* transcript levels in single *ubx* deletion strains under the assumption that deletion of the Gcn4-targeting cofactor would phenocopy of *ARG1* transcript levels in the *cdc48-3* strain following proteasome inhibition. However, *ARG1* transcript levels in each of the seven *ubx* deletion strains decreased to levels of that found in the *UBX* strain following proteasome inhibition (Figure 33). Therefore, a single, nonessential Ubx cofactor does not appear to function in relieving the sensitivity of *ARG1* transcript levels to proteasome inhibition. These data do not exclude the possibility that action by Cdc48 may involve one or both of the essential Cdc48 cofactors Ufd1 or Npl4, or that Cdc48 may utilize multiple, redundant Ubx proteins.

Effects of Cdc48 disruption on GAL10 transcript levels

The effects of the *cdc48-3* allele on Gcn4 target gene transcript levels is in contrast to what we have reported for the effects of *cdc48-3* on the Gal4 target gene *GAL10* (Bonizec et al., 2014). In the *GAL10* study, Cdc48 was disrupted with the *cdc48-3* allele at 37°C as opposed to 30°C. To determine whether the difference in temperatures accounted for the opposite effect on *GAL10* transcript levels, I utilized RT-qPCR to determine *GAL10* transcript levels in response to treatment with galactose (GAL) in the *cdc48-3* strain at both 30°C and 37°C. *GAL10* transcript levels were decreased in the *cdc48-3* strain at both 30°C and 37°C when compared to levels in the congenic *CDC48* strain (Figure 34). These data verify that the *cdc48-3* strain used in these two different studies behave similarly and that the opposite effect of *cdc48-3* on Gcn4 target genes and *GAL10* is not due to the temperature at which the strain is grown.

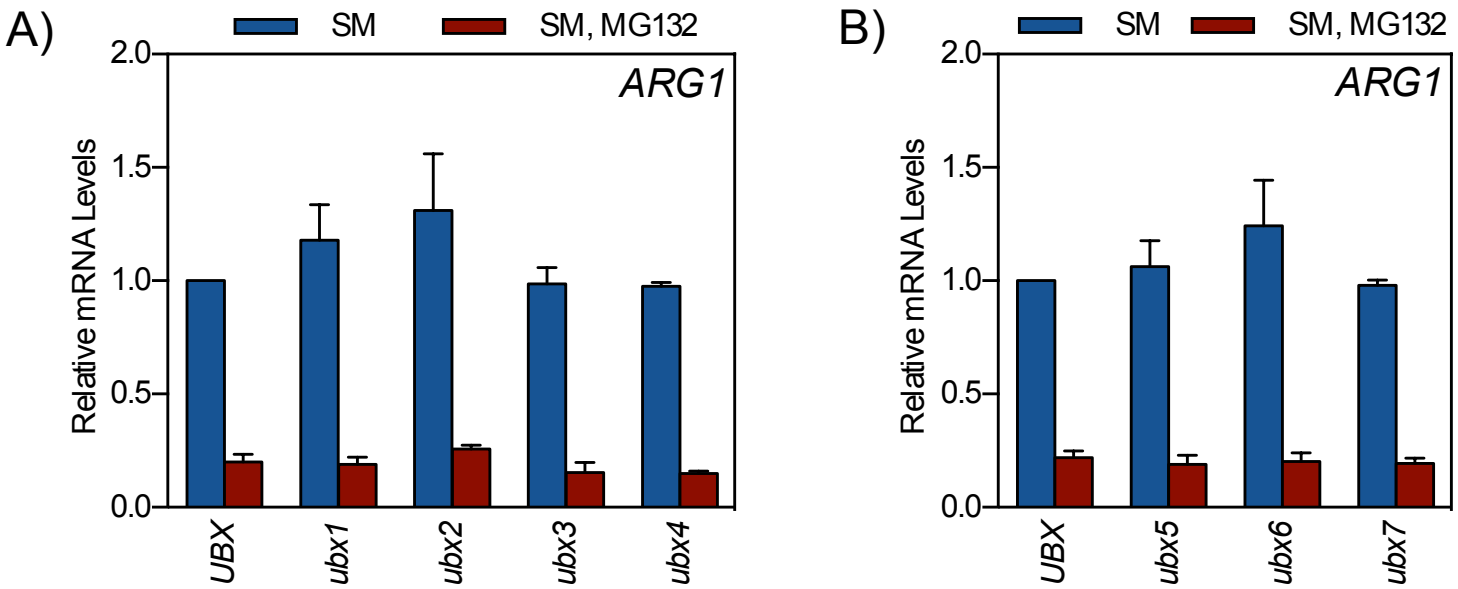

Figure 33. Deletion of a single Ubx adapter protein does not confer resistance of proteasome inhibition for *ARG1* transcript levels. (A) *UBX* (GHY010), *ubx1* (GHY161), *ubx2* (GHY189), *ubx3* (GHY165), and *ubx4* (GHY185) strains were grown to log phase at 30°C in minimal media and treated with either DMSO or MG132. After one hour, strains were treated with SM for 1.5 hours, RNA harvested, and processed as described to measure mRNA levels from the *ARG1* loci. n=3. (B) Same as in (A), except with *UBX* (GHY010), *ubx5* (GHY168), *ubx6* (GHY170), and *ubx7* (GHY171) strains. Error bars represent SEM.

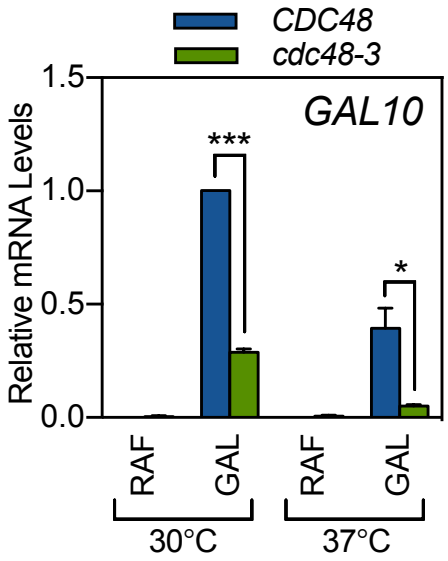

Figure 34. *GAL10* transcript levels decrease in response to Cdc48 disruption at both 30°C and 37°C. (A) *CDC48* (RHY2455) and *cdc48-3* (RHY2457) yeast were grown to log phase at 30°C in raffinose (RAF) media and then shifted to 37°C—or maintained at 30°C—for one hour as indicated. Strains were then treated with 2% galactose (GAL), or water (RAF), for 1.5 hours, at which time RNA was collected and *GAL10* mRNA levels quantified by RT-qPCR. Relative mRNA levels for *GAL10* were normalized to the *CDC48* strain treated with GAL at 30°C. n=3. Error bars represent SEM. (* significant at $p<0.05$, *** significant at $p<0.001$)

Discussion

In order to determine whether the Cdc48 complex facilitated the loss of Gcn4 from promoters following proteasome inhibition, I disrupted the Cdc48 complex with the *cdc48-3* allele and found that disruption of the Cdc48 complex was sufficient to rescue both DNA binding of Gcn4 and Gcn4 target gene transcript levels following proteasome inhibition. I also found through co-immunoprecipitation that Cdc48 physically associated with Gcn4. In the Spent/Stuck model, proteasome inhibition blocks transcription of target genes through inactive transcriptional activators being “stuck” on promoters. However, the results in this Chapter support a new model in which proteasome inhibition prevents target gene transcription via loss of Gcn4 from chromatin through a Cdc48-dependent mechanism (Figure 35).

Effects of the Cdc48 complex on proteasome-dependent Gcn4 levels at the UAS of Gcn4 target genes

There are multiple examples in which Cdc48 prevents chromatin localization including the LexA-VP16 ubiquitin fusion, the transcriptional repressor mat-alpha, and the RNA pol II subunit Rpb1 (Ndoja et al., 2014; Verma et al., 2011; Wilcox and Laney, 2009). The most straight-forward explanation for the rescue of Gcn4 on chromatin through Cdc48 disruption is that Cdc48 functions directly through interaction with Gcn4 to remove it from chromatin. Based on this mechanism, I would predict that Gcn4 bound to chromatin following proteasome inhibition and during Cdc48 disruption is in a highly ubiquitylated state. A beneficial experiment to challenge this model would be to determine the ubiquitylation status of chromatin-bound Gcn4 following proteasome inhibition and Cdc48 disruption.

Effects of the Cdc48 complex on proteasome-dependent Gcn4 target gene transcript levels

Rescuing Gcn4 levels at chromatin following proteasome inhibition through Cdc48 disruption corresponded to an increase in target gene transcript levels. These data support a new model for Gcn4 target gene transcription in which removal of Gcn4 from chromatin during transcription is not essential for continued cycles of transcription. This is in contrast to the Spent/Stuck model in which removal of Gcn4 was necessary due to the transition of Gcn4 from an active to an inactive

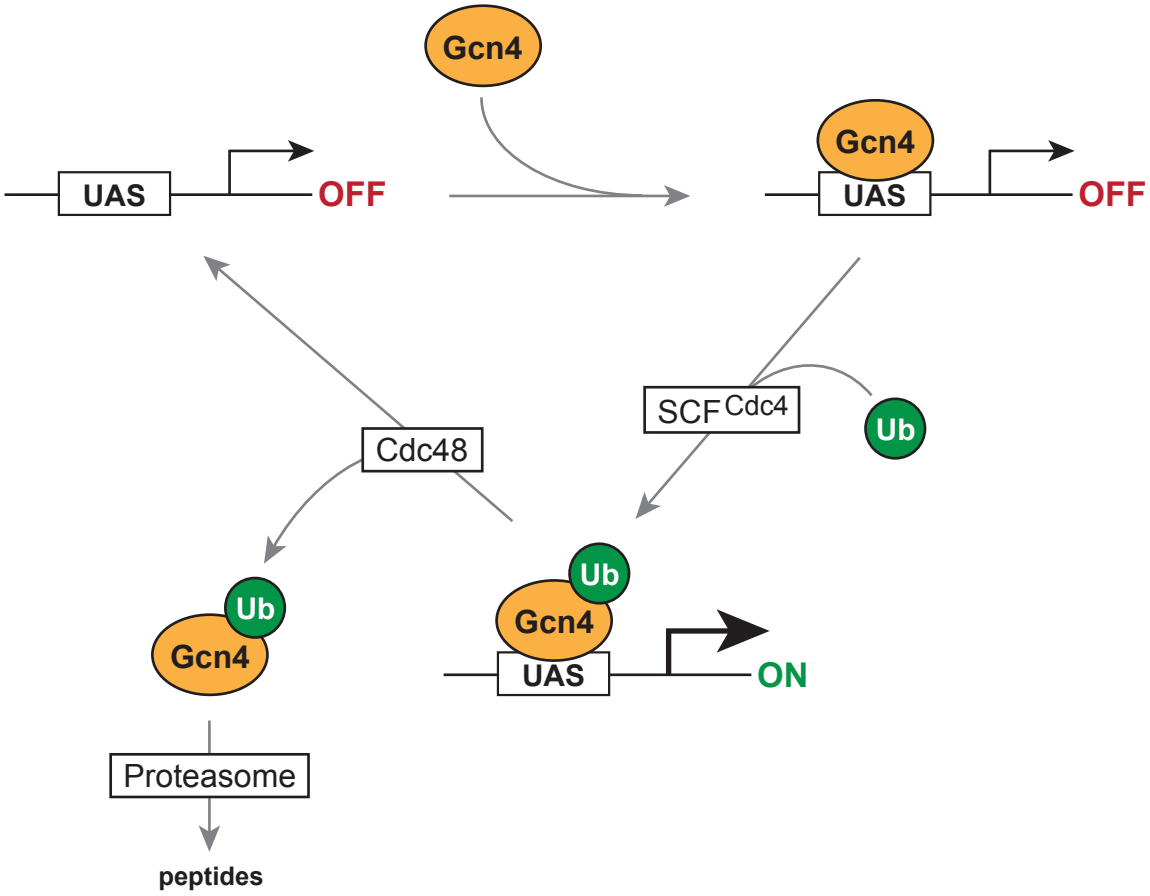

Figure 35. Revised model for Gcn4-mediated transcription. In this model, unmodified Gcn4 binds its cognate UAS element but the resulting complex is inactive for gene activation (OFF). Ubiquitylation of Gcn4 by the SCFCdc4 complex converts Gcn4 into a state that is competent for gene activation (ON) but at the same time renders it a substrate for a Cdc48-containing complex. Cdc48 mediates stripping of Gcn4–Ub from DNA, allowing Gcn4 to be destroyed by the 26S proteasome. Although not shown in the figure, it is possible that Gcn4 could be deubiquitylated after extraction (recycled) and not destroyed. It is also possible that Gcn4 could be ubiquitylated before it encounters DNA, in which case the model still predicts that it would be stripped from promoters in a Cdc48-dependent manner.

state. Interestingly, Cdc48 disruption increased target gene transcript levels even in the absence of proteasome inhibition. This demonstrates that the role of Cdc48 in Gcn4 target gene transcription does not occur exclusively during proteasome inhibition but also during normal Gcn4 function.

Gcn4 interacts with Cdc48

Co-immunoprecipitation of Cdc48 and Gcn4 shows that these two proteins physically interact with one another. However, several questions remain regarding the interaction between these two proteins. One important question is whether Cdc48 and Gcn4 interact at chromatin as co-immunoprecipitation does not distinguish between chromatin-bound proteins. This question can be addressed through a double-ChIP experiment to determine whether Cdc48 and Gcn4 co-localize at the UAS of Gcn4 target genes. Another question that remains is what, if any, co-adapters function in the recognition of Gcn4 by Cdc48. In this study, a single, non-essential adapter protein did not confer proteasome resistant transcription of *ARG1*. However, previous work has shown that adapter proteins can have redundant function. Additionally, the Cdc48 adapter proteins Npl4 and Ufd1 are essential proteins required for cell viability so testing these cofactors will require conditional disruption through temperature sensitive alleles. A more straightforward method for determining which adapter proteins function in recognition of Gcn4 is through immunoprecipitation of Gcn4 following proteasome inhibition followed by western blotting using antibodies against the characterized adapter proteins. This technique has been used previously and could, at least, narrow down the Ubx proteins that could be screened.

Effects of Cdc48 complex disruption on GAL10 transcript levels

Previous work demonstrates that Cdc48 disruption triggers a decrease in Gal4 levels at the UAS of *GAL10* which is in agreement with the decrease in *GAL10* transcript levels following Cdc48 disruption in this study (Bonizec et al., 2014). However, the loss of Gal4 on chromatin is in contrast to the effect on Gcn4 levels which were unaffected following Cdc48 disruption. These results show that Cdc48 does not play a single, common role for in transcription of Gal4 and Gcn4 target genes. However, these data do not exclude the possibility that Cdc48 may function at

multiple steps during *GAL10* transcription including a step upstream of Gal4 binding whose disruption would overshadow accumulation of Gal4 on chromatin following Cdc48 disruption.

If Cdc48 functions in extraction of Gal4 from chromatin, the Cdc48 complex would fill an important gap that has arisen in the literature. It has been demonstrated by both our group and others that Gal4 requires the proteasome for transcription of Gal4 target genes (Geng and Tansey, 2012; Lipford et al., 2005). However, ChIP of the proteasome at the *GAL10* gene shows surprisingly low levels at the Gal4 UAS (Geng and Tansey, 2012). The Cdc48 complex would reconcile these data by providing an intermediary between ubiquitylated Gal4 and the proteasome.

CHAPTER VII

DISCUSSION

In this thesis, I present my studies in which I challenged a new model for transcriptional activation by Gcn4, referred to as the “Spent/Stuck” model, in order to mechanistically explain the requirement for the ubiquitin-proteasome machinery for Gcn4 function. In this model, Gcn4 stimulates transcription by binding chromatin and recruiting the transcriptional machinery (Figure 3). Following the first few rounds of transcription, Gcn4 is phosphorylated to mark Gcn4 as “spent”. Because inactive Gcn4 remains bound to recognition sequences (“stuck”), the UPS is required for the removal of Gcn4 to allow for subsequent rounds of transcription.

I first disrupted the ubiquitylation machinery that targets Gcn4. Following disruption of the E2 enzyme Cdc34 or the Skp1 subunit of the SCF complex, target gene transcript levels decreased. Target gene transcript levels also decreased when Cdc34 was excluded from the nucleus. Furthermore, disruption of the F-box protein Cdc4 resulted in a decrease in transcript levels while having no effect on the levels of Gcn4 bound to recognition sequences at representative target genes. However, proteasome inhibition resulted in a loss of representative target gene transcript levels while also decreasing the levels of Gcn4 found at recognition sequences. Sensitivity of Gcn4 function did not occur due to phosphorylation by Srb10 and Pho85, as preventing Cdk-dependent Gcn4 phosphorylation did not rescue transcription following proteasome inhibition. The loss of Gcn4 did not correspond to a loss of Gcn4 protein as cells retained Gcn4 following proteasome inhibition, although in a ubiquitylated state. Gcn4 also remained localized to the nucleus following proteasome inhibition. Loss of Gcn4 from chromatin does not appear to be due to nucleosome accumulation in promoters as the Gcn4 recognition sequences of *ARG1* and *HIS4* are depleted of nucleosomes following proteasome inhibition. Gcn4 also does not appear to occur due to the arginine repression complex. Instead, the loss of Gcn4 from chromatin following proteasome inhibition occurs through Cdc48 which associates with Gcn4. Disruption of the Cdc48 complex rescues both Gcn4 binding of recognition sequences and target gene transcript levels following proteasome inhibition.

The data presented support a new model in which the ubiquitylation machinery is required for transcriptional activation by Gcn4 (Figure 35). In this model, ubiquitylation by SCF^{Cdc4} is required for multiple steps: one that positively regulates transcription following Gcn4 binding chromatin and one that negatively regulates transcription by stimulating removal from chromatin by Cdc48. These opposing effects of ubiquitylation on transcriptional activation may provide a method of tight, self-limiting regulation of transcriptional output following stimulation of transcription. By interacting with the Cdc48 complex, ubiquitylated Gcn4 is either unable to stably associate with chromatin or is stripped from chromatin immediately after associating and before transcription can begin.

The new model for transcriptional regulation by Gcn4 ubiquitylation is similar to the "licensing" (Salghetti et al., 2001) and "ubiquitin-clock" models (Wu et al., 2007). In these models, ubiquitylation controls transcriptional activator function by limiting the lifespan of the activator. When ubiquitin chains reach the threshold for recognition by the proteasome, the activator is degraded, thereby limiting the function. In contrast, the new model presented here suggests that recognition by the Cdc48 complex—not proteolysis—is the critical step for controlling activator function.

Role of ubiquitylation in transcription of Gcn4 target genes

One way that Gcn4 ubiquitylation may stimulate transcription is by controlling protein-protein interactions between the Gcn4 activation domain and transcriptional machinery. Like Gcn4, the SREBP transcriptional activator requires its ubiquitylation machinery to stimulate transcription. Furthermore, like Gcn4, SREBP ubiquitylation is stimulated by phosphorylation. Nuclear magnetic resonance (NMR) studies examining the SREBP activation domain found that ubiquitin can bind non-covalently to the activation domain (Raiola et al., 2013). Ubiquitin contains a hydrophobic patch made up of the residues L8, I44, and V70 at the surface of ubiquitin which is essential for its cellular functions in yeast (Sloper-Mould et al., 2001). Interestingly, the Gcn4 activation domain

contains seven clusters of hydrophobic residues that are essential for transcriptional activation (Jackson et al., 1996). Therefore, ubiquitin may bind one of the hydrophobic patches of the Gcn4 activation domain. This interaction may cover one or more regions of hydrophobicity in order to control recognition by proteins that could negatively affect transcription. It could also promote protein-protein interactions by conferring a region of structure in the activation domain. Although the activation domain alone is inherently unstructured, small regions of the activation domain confer a structure when bound to interacting partners. This has been demonstrated in structural studies of the interface between the central activation domain of Gcn4 and the Gal11 subunit of the Mediator complex (Brzovic et al., 2011; Jedidi et al., 2010; Warfield et al., 2014). A ubiquitin modification could also facilitate transcription in and of itself by adding an additional region of interaction to the activation domain to recruit transcriptional machinery. This could explain how a single ubiquitin modification is sufficient for transcription as mono-ubiquitylated 3T2S-Gcn4 is capable of stimulating transcription.

Work from the Manley laboratory demonstrates that Gcn4 is also modified by the small ubiquitin-like modifier (SUMO) protein when Gcn4 is at chromatin (Rosonina et al., 2012). As opposed to ubiquitylation, Gcn4 SUMOylation is not required for Gcn4 target gene transcription as a non-SUMOylatable mutant of Gcn4 can stimulate transcription. In contrast to ubiquitylation, SUMOylation acts only as a negative regulator of transcription by stimulating phosphorylation by Srb10 to signal Gcn4 ubiquitylation. However, this work does not examine the effects of the proteasome in this process of SUMO-dependent regulation, thereby leaving open the possibility that the Cdc48 complex may function in the process of SUMO-dependent removal of Gcn4 from chromatin similarly to the model for ubiquitylation and Cdc48.

Gal4 and Gcn4 are both phosphorylated by Srb10 which stimulates ubiquitylation and ubiquitylation is necessary for proper function of both Gal4 and Gcn4 (Chi et al., 2001; Sadowski et al., 1991). However, ubiquitylation appears to facilitate transcription stimulated by Gal4 and Gcn4 through two different mechanisms. In the case of Gal4, ubiquitylation is necessary for proper mRNA processing by affecting recruitment of mRNA processing machinery to the promoter (Muratani et al., 2005). In contrast, Gcn4 ubiquitylation is necessary for mRNA production. This

does not exclude the possibility that Gcn4 ubiquitylation may also facilitate the recruitment of mRNA processing enzymes but that the phenotype associated with this loss is masked by a step further upstream in which ubiquitylation enable mRNA synthesis. Therefore, Gcn4 appears to require ubiquitylation at step in transcription further upstream than that required by Gal4.

Role of the proteasome in transcription of Gcn4 target genes

The fact that transcription of Gcn4 target genes occurs during proteasome inhibition in the absence of Cdc48 demonstrates that the proteasome *per se* is not required for Gcn4 function. Instead, the proteasome may function indirectly to facilitate Gcn4 transcription by keeping ubiquitylated Gcn4 protein levels low relative to non-ubiquitylated Gcn4 protein levels. By controlling this equilibrium, the proteasome will ensure that Cdc48 does not remove Gcn4 from chromatin until after transcription is stimulated. Therefore, inhibition of the proteasome disrupts this equilibrium and promotes the interaction between Gcn4 and Cdc48. Proteasome inhibition may further shift this equilibrium by inhibiting synthesis of new Gcn4 proteins. Another way the proteasome may affect Gcn4 activity is through ubiquitin chain editing. The E4 enzyme Hul5 and the deubiquitinase Ubp6 both associate with the 19S proteasome and both have been shown to affect Gcn4 turnover (Crosas et al., 2006; Hanna et al., 2006; Leggett et al., 2002). Therefore, extension and cleavage of ubiquitin chains could occur through enzymes docked to the 19S proteasome.

The proteasome is also required for the cyclical binding of ERα to chromatin during transcription. This is proposed to occur through interactions between ubiquitylated ERα and the nuclear matrix as ERα mobility decreases in the nucleus during proteasome inhibition and ERα can interact with the HET nuclear matrix protein (Oesterreich et al., 2000; Reid et al., 2003). However, future studies are required to conclusively determine how proteasome inhibition triggers the loss of ERα from chromatin. In contrast to Gcn4, proteasome inhibition causes an increase in Gal4 levels detected on chromatin (Lipford et al., 2005). This difference in effects of proteasome inhibition may be due to different roles of Cdc48 during transcriptional activation. If ubiquitylated Gal4 is

removed from chromatin independently of Cdc48, perhaps directly by the proteasome, Gal4 would remain on chromatin during proteasome inhibition.

Role of Cdc48 in transcription of Gcn4 target genes

The role of Cdc48 in controlling Gcn4 activity is similar to work published by the Yao laboratory in which fusion of ubiquitin to the LexA-VP16 transcriptional activator inhibited interaction with chromatin, and thus transcription of target genes, through the Cdc48 complex (Ndoja et al., 2014). The effects of Cdc48 on chromatin binding of Gcn4 is also similar to work from the Laney laboratory in which ubiquitylation of the alpha-2 transcriptional repressor stimulated removal from chromatin through the Cdc48 complex (Wilcox and Laney, 2009). In light of these studies along with the study presented here, future work examining the role of the UPS during transcriptional activation should not overlook the potential role of the Cdc48 complex in the process.

The decrease in Gcn4 target gene transcript levels in the *3T2S-GCN4* strain following proteasome inhibition is in agreement with my updated model of the role Cdc48 plays in regulating transcriptional activation by Gcn4. Work from the Yao laboratory demonstrated that a single ubiquitin modification is sufficient to stimulate interaction with Cdc48 and removal of a transcription factor from chromatin (Ndoja et al., 2014). Considering their work along with my work demonstrating that 3T2S-Gcn4 is mono-ubiquitylated following proteasome inhibition, transcription of Gcn4 target genes following proteasome inhibition may also occur through the loss of 3T2S-Gcn4 from chromatin through the single ubiquitin modification.

Future directions

To conclusively determine whether Gcn4 ubiquitylation is required for Gcn4 function, a non-ubiquitylatable cis-mutant of Gcn4 is required in order to minimize any potential secondary effects created by disruption of the UPS. Although I attempted to generate this mutant (K0-Gcn4), I was unable to experimentally utilize it as blocking ubiquitylation required mutation of all twenty-three lysine residues which inhibited the detection of K0-Gcn4 on chromatin by ChIP. These lysine residues were dispersed throughout the Gcn4 protein sequence including the DNA binding domain. An alternative to such a dramatic mutant would be a modified version of the 3T2S-Gcn4 mutant in which the site of monoubiquitylation is blocked. By reducing the number of potential ubiquitin modifications, mass-spectrometry could be used to identify this target residue. Ubiquitylation of this mutant could also be rescued by adding the ubiquitin coding sequence to the N-terminus, similarly to what has been previously done with LexA-VP16. A non-ubiquitylatable mutant would also provide a valuable tool for work examining the role of Cdc48 in regulating Gcn4. Cdc48 canonically recognizes substrates through ubiquitylation. Therefore, if loss of Gcn4 from chromatin occurs through Cdc48 recognition of ubiquitylated Gcn4, a non-ubiquitylatable mutant of Gcn4 should remain bound to chromatin despite proteasome inhibition.

Another tool that would provide insight into the role of the UPS during transcription is a mini-chromosome system driven by a Gcn4 target gene promoter. If Gcn4 ubiquitylation is required to recruit an essential cofactor for transcription, mini-chromosome purification coupled with mass-spectrometry during disruption of ubiquitylation could identify changes in proteins found at the promoter. Gcn4 mini-chromosome purification coupled with western-blotting would also provide more insight as to the levels of Gcn4 on chromatin following proteasome inhibition. This method would minimize potential artifacts created by protein-crosslinking such as masking of epitopes.

REFERENCES

Aberle, H., Bauer, A., Stappert, J., Kispert, A., and Kemler, R. (1997). beta-catenin is a target for the ubiquitin-proteasome pathway. EMBO J *16*, 3797-3804.

Adams, C.C., and Workman, J.L. (1993). Nucleosome displacement in transcription. Cell *72*, 305-308.

Beck, T., and Hall, M.N. (1999). The TOR signalling pathway controls nuclear localization of nutrient-regulated transcription factors. Nature *402*, 689-692.

Bengoechea-Alonso, M.T., and Ericsson, J. (2009). A phosphorylation cascade controls the degradation of active SREBP1. J Biol Chem *284*, 5885-5895.

Bengoechea-Alonso, M.T., Punga, T., and Ericsson, J. (2005). Hyperphosphorylation regulates the activity of SREBP1 during mitosis. Proc Natl Acad Sci U S A *102*, 11681-11686.

Blondel, M., Galan, J.M., Chi, Y., Lafourcade, C., Longaretti, C., Deshaies, R.J., and Peter, M. (2000). Nuclear-specific degradation of Far1 is controlled by the localization of the F-box protein Cdc4. EMBO J *19*, 6085-6097.

Bloom, J., and Cross, F.R. (2007). Multiple levels of cyclin specificity in cell-cycle control. Nat Rev Mol Cell Biol *8*, 149-160.

Bonizec, M., Herissant, L., Pokrzywa, W., Geng, F., Wenzel, S., Howard, G.C., Rodriguez, P., Krause, S., Tansey, W.P., Hoppe, T.*, et al.* (2014). The ubiquitin-selective chaperone Cdc48/p97 associates with Ubx3 to modulate monoubiquitylation of histone H2B. Nucleic Acids Res *42*, 10975-10986.

Brzovic, P.S., Heikaus, C.C., Kisselev, L., Vernon, R., Herbig, E., Pacheco, D., Warfield, L., Littlefield, P., Baker, D., Klevit, R.E.*, et al.* (2011). The acidic transcription activator Gcn4 binds the mediator subunit Gal11/Med15 using a simple protein interface forming a fuzzy complex. Mol Cell *44*, 942-953.

Chi, Y., Huddleston, M.J., Zhang, X., Young, R.A., Annan, R.S., Carr, S.A., and Deshaies, R.J. (2001). Negative regulation of Gcn4 and Msn2 transcription factors by Srb10 cyclin-dependent kinase. Genes Dev *15*, 1078-1092.

Collins, G.A., Gomez, T.A., Deshaies, R.J., and Tansey, W.P. (2010). Combined chemical and genetic approach to inhibit proteolysis by the proteasome. Yeast *27*, 965-974.

Collins, G.A., Lipford, J.R., Deshaies, R.J., and Tansey, W.P. (2009). Gal4 turnover and transcription activation. Nature *461*, E7; discussion E8.

Conaway, R.C., and Conaway, J.W. (2011). Origins and activity of the Mediator complex. Semin Cell Dev Biol *22*, 729-734.

Crisucci, E.M., and Arndt, K.M. (2012). Paf1 restricts Gcn4 occupancy and antisense transcription at the *ARG1* promoter. Mol Cell Biol *32*, 1150-1163.

Crosas, B., Hanna, J., Kirkpatrick, D.S., Zhang, D.P., Tone, Y., Hathaway, N.A., Buecker, C., Leggett, D.S., Schmidt, M., King, R.W.*, et al.* (2006). Ubiquitin chains are remodeled at the proteasome by opposing ubiquitin ligase and deubiquitinating activities. Cell *127*, 1401-1413.

De Vit, M.J., Waddle, J.A., and Johnston, M. (1997). Regulated nuclear translocation of the Mig1 glucose repressor. Mol Biol Cell *8*, 1603-1618.

Devlin, C., Tice-Baldwin, K., Shore, D., and Arndt, K.T. (1991). RAP1 is required for BAS1/BAS2- and GCN4-dependent transcription of the yeast *HIS4* gene. Mol Cell Biol *11*, 3642-3651.

Falco, S.C., and Dumas, K.S. (1985). Genetic analysis of mutants of *Saccharomyces cerevisiae* resistant to the herbicide sulfometuron methyl. Genetics *109*, 21-35.

Finley, D., Ulrich, H.D., Sommer, T., and Kaiser, P. (2012). The ubiquitin-proteasome system of *Saccharomyces cerevisiae*. Genetics *192*, 319-360.

Fleming, J.A., Lightcap, E.S., Sadis, S., Thoroddsen, V., Bulawa, C.E., and Blackman, R.K. (2002). Complementary whole-genome technologies reveal the cellular response to proteasome inhibition by PS-341. Proc Natl Acad Sci U S A *99*, 1461-1466.

Franz, A., Ackermann, L., and Hoppe, T. (2016). Ring of Change: CDC48/p97 Drives Protein Dynamics at Chromatin. Front Genet *7*, 73.

Fredrickson, E.K., Rosenbaum, J.C., Locke, M.N., Milac, T.I., and Gardner, R.G. (2011). Exposed hydrophobicity is a key determinant of nuclear quality control degradation. Mol Biol Cell *22*, 2384-2395.

Geng, F., and Tansey, W.P. (2012). Similar temporal and spatial recruitment of native 19S and 20S proteasome subunits to transcriptionally active chromatin. Proc Natl Acad Sci U S A *109*, 6060-6065.

Geng, F., Wenzel, S., and Tansey, W.P. (2012). Ubiquitin and proteasomes in transcription. Annu Rev Biochem *81*, 177-201.

Gietz, R.D., and Schiestl, R.H. (2007). High-efficiency yeast transformation using the LiAc/SS carrier DNA/PEG method. Nat Protoc *2*, 31-34.

Goebl, M.G., Goetsch, L., and Byers, B. (1994). The Ubc3 (Cdc34) ubiquitin-conjugating enzyme is ubiquitinated and phosphorylated in vivo. Mol Cell Biol *14*, 3022-3029.

Goldstein, A.L., and McCusker, J.H. (1999). Three new dominant drug resistance cassettes for gene disruption in Saccharomyces cerevisiae. Yeast *15*, 1541-1553.

Govind, C.K., Qiu, H., Ginsburg, D.S., Ruan, C., Hofmeyer, K., Hu, C., Swaminathan, V., Workman, J.L., Li, B., and Hinnebusch, A.G. (2010). Phosphorylated Pol II CTD recruits multiple HDACs, including Rpd3C(S), for methylation-dependent deacetylation of ORF nucleosomes. Mol Cell *39*, 234-246.

Hahn, S., and Young, E.T. (2011). Transcriptional regulation in *Saccharomyces cerevisiae*: transcription factor regulation and function, mechanisms of initiation, and roles of activators and coactivators. Genetics *189*, 705-736.

Hanna, J., Hathaway, N.A., Tone, Y., Crosas, B., Elsasser, S., Kirkpatrick, D.S., Leggett, D.S., Gygi, S.P., King, R.W., and Finley, D. (2006). Deubiquitinating enzyme Ubp6 functions noncatalytically to delay proteasomal degradation. Cell *127*, 99-111.

Haruki, H., Nishikawa, J., and Laemmli, U.K. (2008). The anchor-away technique: rapid, conditional establishment of yeast mutant phenotypes. Mol Cell *31*, 925-932.

Heinemeyer, W., Fischer, M., Krimmer, T., Stachon, U., and Wolf, D.H. (1997). The active sites of the eukaryotic 20 S proteasome and their involvement in subunit precursor processing. J Biol Chem *272*, 25200-25209.

Hinnebusch, A.G. (1984). Evidence for translational regulation of the activator of general amino acid control in yeast. Proc Natl Acad Sci U S A *81*, 6442-6446.

Hoppe, T., Matuschewski, K., Rape, M., Schlenker, S., Ulrich, H.D., and Jentsch, S. (2000). Activation of a membrane-bound transcription factor by regulated ubiquitin/proteasome-dependent processing. Cell *102*, 577-586.

Howard, G.C., Collins, G.A., and Tansey, W.P. (2012). Letter to the editor. Yeast *29*, 93-94.

Jackson, B.M., Drysdale, C.M., Natarajan, K., and Hinnebusch, A.G. (1996). Identification of seven hydrophobic clusters in GCN4 making redundant contributions to transcriptional activation. Mol Cell Biol *16*, 5557-5571.

Jaenicke, L.A., von Eyss, B., Carstensen, A., Wolf, E., Xu, W., Greifenberg, A.K., Geyer, M., Eilers, M., and Popov, N. (2016). Ubiquitin-Dependent Turnover of MYC Antagonizes MYC/PAF1C Complex Accumulation to Drive Transcriptional Elongation. Mol Cell *61*, 54-67.

Janke, C., Magiera, M.M., Rathfelder, N., Taxis, C., Reber, S., Maekawa, H., Moreno-Borchart, A., Doenges, G., Schwob, E., Schiebel, E.*, et al.* (2004). A versatile toolbox for PCR-based tagging of yeast genes: new fluorescent proteins, more markers and promoter substitution cassettes. Yeast *21*, 947-962.

Jedidi, I., Zhang, F., Qiu, H., Stahl, S.J., Palmer, I., Kaufman, J.D., Nadaud, P.S., Mukherjee, S., Wingfield, P.T., Jaroniec, C.P.*, et al.* (2010). Activator Gcn4 employs multiple segments of Med15/Gal11, including the KIX domain, to recruit mediator to target genes in vivo. The Journal of biological chemistry *285*, 2438-2455.

Jentsch, S., and Rumpf, S. (2007). Cdc48 (p97): a "molecular gearbox" in the ubiquitin pathway? Trends in Biochemical Sciences *32*, 6-11.

Kaffman, A., Rank, N.M., O'Neill, E.M., Huang, L.S., and O'Shea, E.K. (1998). The receptor Msn5 exports the phosphorylated transcription factor Pho4 out of the nucleus. Nature *396*, 482-486.

Kim, S.Y., Herbst, A., Tworkowski, K.A., Salghetti, S.E., and Tansey, W.P. (2003). Skp2 regulates Myc protein stability and activity. Molecular Cell *11*, 1177-1188.

Knop, M., Siegers, K., Pereira, G., Zachariae, W., Winsor, B., Nasmyth, K., and Schiebel, E. (1999). Epitope tagging of yeast genes using a PCR-based strategy: more tags and improved practical routines. Yeast *15*, 963-972.

Komeili, A., and O'Shea, E.K. (1999). Roles of phosphorylation sites in regulating activity of the transcription factor Pho4. Science *284*, 977-980.

Kornitzer, D., Raboy, B., Kulka, R.G., and Fink, G.R. (1994). Regulated degradation of the transcription factor Gcn4. The EMBO Journal *13*, 6021-6030.

Laney, J.D., and Hochstrasser, M. (2003). Ubiquitin-dependent degradation of the yeast Mat(alpha)2 repressor enables a switch in developmental state. Genes Dev *17*, 2259-2270.

Lee, C.K., Shibata, Y., Rao, B., Strahl, B.D., and Lieb, J.D. (2004). Evidence for nucleosome depletion at active regulatory regions genome-wide. Nature genetics *36*, 900-905.

Lee, D.H., and Goldberg, A.L. (1998). Proteasome inhibitors cause induction of heat shock proteins and trehalose, which together confer thermotolerance in *Saccharomyces cerevisiae*. Mol Cell Biol *18*, 30-38.

Lee, T.I., and Young, R.A. (2013). Transcriptional regulation and its misregulation in disease. Cell *152*, 1237-1251.

Lee, W., Tillo, D., Bray, N., Morse, R.H., Davis, R.W., Hughes, T.R., and Nislow, C. (2007). A high-resolution atlas of nucleosome occupancy in yeast. Nature Genetics *39*, 1235-1244.

Leggett, D.S., Hanna, J., Borodovsky, A., Crosas, B., Schmidt, M., Baker, R.T., Walz, T., Ploegh, H., and Finley, D. (2002). Multiple associated proteins regulate proteasome structure and function. Mol Cell *10*, 495-507.

Li, M., Brooks, C.L., Wu-Baer, F., Chen, D., Baer, R., and Gu, W. (2003). Mono- versus polyubiquitination: differential control of p53 fate by Mdm2. Science *302*, 1972-1975.

Lipford, J.R., Smith, G.T., Chi, Y., and Deshaies, R.J. (2005). A putative stimulatory role for activator turnover in gene expression. Nature *438*, 113-116.

Liu, C., Apodaca, J., Davis, L.E., and Rao, H. (2007). Proteasome inhibition in wild-type yeast *Saccharomyces cerevisiae* cells. Biotechniques *42*, 158, 160, 162.

Lonard, D.M., Nawaz, Z., Smith, C.L., and O'Malley, B.W. (2000). The 26S proteasome is required for estrogen receptor-alpha and coactivator turnover and for efficient estrogen receptor-alpha transactivation. Mol Cell *5*, 939-948.

Lord, C.L., Timney, B.L., Rout, M.P., and Wente, S.R. (2015). Altering nuclear pore complex function impacts longevity and mitochondrial function in *S. cerevisiae*. J Cell Biol *208*, 729-744.

Mavrakis, K.J., Andrew, R.L., Lee, K.L., Petropoulou, C., Dixon, J.E., Navaratnam, N., Norris, D.P., and Episkopou, V. (2007). Arkadia enhances Nodal/TGF-beta signaling by coupling phospho-Smad2/3 activity and turnover. PLoS Biol *5*, e67.

Meimoun, A., Holtzman, T., Weissman, Z., McBride, H.J., Stillman, D.J., Fink, G.R., and Kornitzer, D. (2000). Degradation of the transcription factor Gcn4 requires the kinase Pho85 and the SCF(CDC4) ubiquitin-ligase complex. Mol Biol Cell *11*, 915-927.

Messenguy, F., and Dubois, E. (2003). Role of MADS box proteins and their cofactors in combinatorial control of gene expression and cell development. Gene *316*, 1-21.

Molinari, E., Gilman, M., and Natesan, S. (1999). Proteasome-mediated degradation of transcriptional activators correlates with activation domain potency in vivo. EMBO J *18*, 6439-6447.

Muratani, M., Kung, C., Shokat, K.M., and Tansey, W.P. (2005). The F box protein Dsg1/Mdm30 is a transcriptional coactivator that stimulates Gal4 turnover and cotranscriptional mRNA processing. Cell *120*, 887-899.

Nawaz, Z., Lonard, D.M., Smith, C.L., Lev-Lehman, E., Tsai, S.Y., Tsai, M.J., and O'Malley, B.W. (1999). The Angelman syndrome-associated protein, E6-AP, is a coactivator for the nuclear hormone receptor superfamily. Mol Cell Biol *19*, 1182-1189.

Ndoja, A., Cohen, R.E., and Yao, T. (2014). Ubiquitin signals proteolysis-independent stripping of transcription factors. Mol Cell *53*, 893-903.

Oesterreich, S., Zhang, Q., Hopp, T., Fuqua, S.A., Michaelis, M., Zhao, H.H., Davie, J.R., Osborne, C.K., and Lee, A.V. (2000). Tamoxifen-bound estrogen receptor (ER) strongly interacts with the nuclear matrix protein HET/SAF-B, a novel inhibitor of ER-mediated transactivation. Mol Endocrinol *14*, 369-381.

Orlicky, S., Tang, X., Willems, A., Tyers, M., and Sicheri, F. (2003). Structural basis for phosphodependent substrate selection and orientation by the SCFCdc4 ubiquitin ligase. Cell *112*, 243-256.

Palombella, V.J., Rando, O.J., Goldberg, A.L., and Maniatis, T. (1994). The ubiquitin-proteasome pathway is required for processing the NF-kappa B1 precursor protein and the activation of NF-kappa B. Cell *78*, 773-785.

Patton, E.E., Willems, A.R., Sa, D., Kuras, L., Thomas, D., Craig, K.L., and Tyers, M. (1998). Cdc53 is a scaffold protein for multiple Cdc34/Skp1/F-box proteincomplexes that regulate cell division and methionine biosynthesis in yeast. Genes Dev *12*, 692-705.

Polakis, P. (2000). Wnt signaling and cancer. Genes Dev *14*, 1837-1851.

Punga, T., Bengoechea-Alonso, M.T., and Ericsson, J. (2006). Phosphorylation and ubiquitination of the transcription factor sterol regulatory element-binding protein-1 in response to DNA binding. J Biol Chem *281*, 25278-25286.

Raiola, L., Lussier-Price, M., Gagnon, D., Lafrance-Vanasse, J., Mascle, X., Arseneault, G., Legault, P., Archambault, J., and Omichinski, J.G. (2013). Structural characterization of a noncovalent complex between ubiquitin and the transactivation domain of the erythroid-specific factor EKLF. Structure *21*, 2014-2024.

Rape, M., Hoppe, T., Gorr, I., Kalocay, M., Richly, H., and Jentsch, S. (2001). Mobilization of processed, membrane-tethered SPT23 transcription factor by CDC48(UFD1/NPL4), a ubiquitin-selective chaperone. Cell *107*, 667-677.

Ravid, T., and Hochstrasser, M. (2008). Diversity of degradation signals in the ubiquitin-proteasome system. Nat Rev Mol Cell Biol *9*, 679-690.

Reid, G., Hubner, M.R., Metivier, R., Brand, H., Denger, S., Manu, D., Beaudouin, J., Ellenberg, J., and Gannon, F. (2003). Cyclic, proteasome-mediated turnover of unliganded and liganded ERalpha on responsive promoters is an integral feature of estrogen signaling. Mol Cell *11*, 695-707.

Richardson, P.G., Mitsiades, C., Hideshima, T., and Anderson, K.C. (2006). Bortezomib: proteasome inhibition as an effective anticancer therapy. Annu Rev Med *57*, 33-47.

Rodriguez-Navarro, S. (2009). Insights into SAGA function during gene expression. EMBO Rep *10*, 843-850.

Rosonina, E., Duncan, S.M., and Manley, J.L. (2012). Sumoylation of transcription factor Gcn4 facilitates its Srb10-mediated clearance from promoters in yeast. Genes Dev *26*, 350-355.

Sadowski, I., Niedbala, D., Wood, K., and Ptashne, M. (1991). GAL4 is phosphorylated as a consequence of transcriptional activation. Proc Natl Acad Sci U S A *88*, 10510-10514.

Saji, S., Okumura, N., Eguchi, H., Nakashima, S., Suzuki, A., Toi, M., Nozawa, Y., Saji, S., and Hayashi, S. (2001). MDM2 enhances the function of estrogen receptor alpha in human breast cancer cells. Biochem Biophys Res Commun *281*, 259-265.

Salghetti, S.E., Caudy, A.A., Chenoweth, J.G., and Tansey, W.P. (2001). Regulation of transcriptional activation domain function by ubiquitin. Science *293*, 1651-1653.

Salghetti, S.E., Muratani, M., Wijnen, H., Futcher, B., and Tansey, W.P. (2000). Functional overlap of sequences that activate transcription and signal ubiquitin-mediated proteolysis. Proc Natl Acad Sci U S A *97*, 3118-3123.

Sato, B.K., and Hampton, R.Y. (2006). Yeast Derlin Dfm1 interacts with Cdc48 and functions in ER homeostasis. Yeast *23*, 1053-1064.

Sheff, M.A., and Thorn, K.S. (2004). Optimized cassettes for fluorescent protein tagging in *Saccharomyces cerevisiae*. Yeast *21*, 661-670.

Shuai, K., Stark, G.R., Kerr, I.M., and Darnell, J.E., Jr. (1993). A single phosphotyrosine residue of Stat91 required for gene activation by interferon-gamma. Science *261*, 1744-1746.

Sikorski, R.S., and Hieter, P. (1989). A system of shuttle vectors and yeast host strains designed for efficient manipulation of DNA in *Saccharomyces cerevisiae*. Genetics *122*, 19-27.

Sloper-Mould, K.E., Jemc, J.C., Pickart, C.M., and Hicke, L. (2001). Distinct functional surface regions on ubiquitin. J Biol Chem *276*, 30483-30489.

Sundqvist, A., and Ericsson, J. (2003). Transcription-dependent degradation controls the stability of the SREBP family of transcription factors. Proc Natl Acad Sci U S A *100*, 13833-13838.

Teves, S.S., Weber, C.M., and Henikoff, S. (2014). Transcribing through the nucleosome. Trends Biochem Sci *39*, 577-586.

van der Horst, A., de Vries-Smits, A.M., Brenkman, A.B., van Triest, M.H., van den Broek, N., Colland, F., Maurice, M.M., and Burgering, B.M. (2006). FOXO4 transcriptional activity is regulated by monoubiquitination and USP7/HAUSP. Nat Cell Biol *8*, 1064-1073.

Verma, R., Oania, R., Fang, R., Smith, G.T., and Deshaies, R.J. (2011). Cdc48/p97 mediates UV-dependent turnover of RNA Pol II. Molecular Cell *41*, 82-92.

von der Lehr, N., Johansson, S., Wu, S., Bahram, F., Castell, A., Cetinkaya, C., Hydbring, P., Weidung, I., Nakayama, K., Nakayama, K.I.*, et al.* (2003). The F-box protein Skp2 participates in c-Myc proteosomal degradation and acts as a cofactor for c-Myc-regulated transcription. Mol Cell *11*, 1189-1200.

Warfield, L., Tuttle, L.M., Pacheco, D., Klevit, R.E., and Hahn, S. (2014). A sequence-specific transcription activator motif and powerful synthetic variants that bind Mediator using a fuzzy protein interface. Proc Natl Acad Sci U S A *111*, E3506-3513.

Wenta, N., Strauss, H., Meyer, S., and Vinkemeier, U. (2008). Tyrosine phosphorylation regulates the partitioning of STAT1 between different dimer conformations. Proc Natl Acad Sci U S A *105*, 9238-9243.

Wilcox, A.J., and Laney, J.D. (2009). A ubiquitin-selective AAA-ATPase mediates transcriptional switching by remodelling a repressor-promoter DNA complex. Nat Cell Biol *11*, 1481-1486.

Willems, A.R., Lanker, S., Patton, E.E., Craig, K.L., Nason, T.F., Mathias, N., Kobayashi, R., Wittenberg, C., and Tyers, M. (1996). Cdc53 targets phosphorylated G1 cyclins for degradation by the ubiquitin proteolytic pathway. Cell *86*, 453-463.

Workman, J.L. (2006). Nucleosome displacement in transcription. Genes Dev *20*, 2009-2017.

Wu, R.C., Feng, Q., Lonard, D.M., and O'Malley, B.W. (2007). SRC-3 coactivator functional lifetime is regulated by a phospho-dependent ubiquitin time clock. Cell *129*, 1125-1140.

Yaglom, J., Linskens, M.H., Sadis, S., Rubin, D.M., Futcher, B., and Finley, D. (1995). p34Cdc28-mediated control of Cln3 cyclin degradation. Mol Cell Biol *15*, 731-741.

Yarragudi, A., Miyake, T., Li, R., and Morse, R.H. (2004). Comparison of ABF1 and RAP1 in chromatin opening and transactivator potentiation in the budding yeast *Saccharomyces cerevisiae*. Mol Cell Biol *24*, 9152-9164.

Yu, L., and Morse, R.H. (1999). Chromatin opening and transactivator potentiation by RAP1 in Saccharomyces cerevisiae. Mol Cell Biol *19*, 5279-5288.

Zhang, F., Gaur, N.A., Hasek, J., Kim, S.J., Qiu, H., Swanson, M.J., and Hinnebusch, A.G. (2008). Disrupting vesicular trafficking at the endosome attenuates transcriptional activation by Gcn4. Mol Cell Biol *28*, 6796-6818.